UNIVERSITA' DEGLI STUDI DI PADOVA

Department of Engineering Sciences and Mathematics

Wood and Bionanocomposites

Dipartimento di Ingegneria Industriale DII

Corso di Laurea Magistrale in Ingegneria dei Materiali

Nanocellulose-based hydrogels from wood for wound healing

Relatore

Prof. Andrea Bagno

Correlatore

Prof. Kristiina Oksman

Mattia Diamanti 1191098

Anno Accademico 2019/2020

Ai miei genitori e mia sorella che mi sostengono

con il loro affetto incondizionato.

A Sonia che ha sempre creduto in me.

A me stesso che ha vinto anche questa sfida.

Acknowledgments

At the end of this work, as the last step that concludes my university career, I would like to thank you.

First of all, I thank Professor Andrea Bagno, supervisor of this thesis, for the great availability and courtesy shown to me, and for all the help he gave me during the drafting.

I would like to express my special thanks of gratitude to my supervisor Linn Berglund and Prof. Kristiina Oksman who gave me the golden opportunity to carry out this wonderful project on the topic of nanocellulose. Thank you for introducing me to the world of research and for allowing me to learn many new things. I am truly grateful to you.

Special thanks go to Simon Jonasson who has given me countless suggestions and ideas to develop this thesis. Also, I want to warmly thank my colleagues from the University of Luleå: Bony, Farida, Gejo, Luísa, Mitul, Oisik and Paula. Thanks for every word you have spent with me.

A special thanks to Enrico, who accompanied me from the first day of university. Thank you for every lesson, for every exam, for every challenge won and above all thank you for making the experience in Sweden the best of my life. Second but not least, thanks to Elia, companion of laughter, of lunches to talk about formulas and numbers but also a companion always available for any clarification. Thanks Enrico and Elia, you were like two older brothers. I will never forget when you came by surprise to the European Skating Championships in Innsbruck, Austria.

Thanks to Alice for putting up with and supporting me over the past two years. Thanks also to my other classmates Margherita, Nicolò, Silvia and Viola. Thanks for all the coffees we shared at Illy.

A huge thanks to my parents Mariano and Milena, who helped me in this growth path. Thank you because even if you are not perfect, you are the best parents in the world.

Thanks to my sister Sofia, who, even if she never shows me how much she cares about me, is always ready in time of need. Thanks to Sonia, the person I love and who motivates me every day.

Thanks to my study and party friends Alberto, Andrea, Diego M., Diego F., Marco M., Marco R., Thomas, Riccardo, Wladi, Umberto, Simone, Luca and Jonathan. May this be the first of a thousand other satisfactions together.

Thanks to my team, who have seen me grow up since I was a child. Thank you because through dedication and commitment, to teach me through victories and defeats that you have to give your best every day if you want to achieve great goals. Thanks for every yardstick done together

Thanks to the people I met during my experience in Sweden. Thank you for showing me your love every day. Thank you for every Sunday barbecue, for every Monday carbonara and every Tuesday tacos. Thanks Andrea, Antonio, Riccardo, Verdiana, Martina, Giulia, Justus, Elodie, Tom, Marco, Adrian, Merve, Alessandro, Thore, Nacho, Ruben, Alfredo, Leon. You were my second family.

Finally, I want to thank every person who contributed even with a small gesture to this journey together. Thanks.

December 2020. Padova

Mattia Diamanti

Ringraziamenti

Alla fine di questo lavoro, come ultima tappa che conclude il mio percorso universitario, vorrei fare alcuni ringraziamenti.

Ringrazio innanzitutto il professor Andrea Bagno, relatore di questa tesi, per la grande disponibilità e cortesia dimostratami, e per tutto l'aiuto che mi ha dato durante la stesura.

Vorrei esprimere il mio speciale ringraziamento di gratitudine al mio supervisore Linn Berglund e alla Prof.Kristiina Oksman che mi hanno dato l'opportunità d'oro di realizzare questo meraviglioso progetto sul tema della nanocellulosa. Grazie per avermi introdotto nel mondo della Ricerca e di avermi dato la possibilità di imparare molte cose nuove. Vi sono veramente grato.

Un ringraziamento speciale va a Simon Jonasson che mi ha dato innumerevoli suggerimenti e idee per sviluppare questa tesi. Inoltre, voglio ringraziare calorosamente i miei colleghi dell'Università di Luleå: Bony, Farida, Gejo, Luísa, Mitul, Oisik e Paula. Grazie per ogni parola spesa con me.

Un ringraziamento particolare ad Enrico, che mi ha accompagnato fin dal primo giorno di università. Grazie per ogni lezione, per ogni esame, per ogni sfida vinta e soprattutto grazie per aver reso l'esperienza in Svezia la migliore della mia vita. Secondo ma non ultimo, grazie ad Elia, compagno di risate, di pranzi a parlare di formule e numeri ma anche compagno sempre a disposizione per qualsiasi chiarimento. Grazie Enrico ed Elia, siete stati come due fratelli maggiori. Non dimenticherò mai quando siete venuti a sorpresa ai campionati europei di pattinaggio a Innsbruck, in Austria.

Grazie ad Alice per avermi sopportato e supportato negli ultimi due anni. Grazie anche agli altri miei compagni di corso Margherita, Nicolò, Silvia e Viola. Grazie per tutti i caffè che abbiamo condiviso all'Illy.

Un enorme grazie ai miei genitori Mariano e Milena, che mi hanno aiutato in questo percorso di crescita. Grazie perché anche se non siete perfetti, siete i migliori genitori del mondo.

Grazie a mia sorella Sofia, che anche se non mi dimostra mai quanto ci tiene a me, è sempre pronta nel momento del bisogno. Grazie a Sonia, la persona che amo e che mi motiva ogni giorno.

Grazie ai miei amici di studio e di festa Alberto, Andrea, Diego M., Diego F., Marco M., Marco R., Thomas, Riccardo, Wladi, Umberto, Simone, Luca e Jonathan. Che questo sia la prima di mille altre soddisfazioni insieme.

Grazie alla mia squadra, che mi ha visto crescere sin da bambino. Grazie perché ha saputo attraverso dedizione e impegno, ad insegnarmi attraverso vittorie e sconfitte che bisogna dare il massimo ogni giorno se vuole raggiungere dei grandi obiettivi. Grazie per ogni metro fatto insieme.

Grazie alle persone che ho incontrato durante la mia esperienza in Svezia. Grazie per avermi mostrato il vostro affetto ogni giorno. Grazie per ogni grigliata della domenica, per ogni carbonara del lunedì e per ogni tacos del martedì. Grazie Andrea, Antonio, Riccardo, Verdiana, Martina, Giulia, Justus, Elodie, Tom, Marco, Adrian, Merve, Alessandro, Thore, Nacho, Ruben, Alfredo, Leon. Siete stati la mia seconda famiglia.

Infine, voglio ringraziare ogni persona che ha contribuito anche con un piccolo gesto a questo viaggio insieme. Grazie.

December 2020. Padova

Mattia Diamanti

Abstract

Any person has experienced minor skin injuries at least once in the life that has required the use of a patch. These lesions usually heal spontaneously and rapidly, without paying too much attention to them. Conversely, if lesions are of greater importance such as burns, acute wounds or ulcers, they can assume clinical relevance and the application of a patch cannot be enough. The wound dressings that are applied to such wounds are specific for each of the different phases in the wound healing process and need to be regularly changed. A dressing is therefore required, which does not require multiple procedures and minimizes healing duration.

Cellulose has been used since ancient times for wound healing in the form of leaves or herbs or, more recently, incorporated into modern dressings. The forestry industry has recently focused on the use of cellulose as a dressing material in the medical field since traditional applications of cellulose (e.g., paper industry) underwent a significant decrease in demand along with technological advancements. Wound dressings based on the use of nanocellulose as major constituent, have the potential to replace current materials because they possess the characteristics of an ideal dressing.

Nanocellulose is a natural material able to form a sort of network that can entrap a large amount of water. Water is necessary to maintain the wound as hot and humid as possible: these are the optimal conditions for a rapid and safe recovery (Boateng *et al.* 2008). Many studies have shown that nanocellulosic materials are able to shorten the healing duration, whatever the degree of its extension is (Lin & Dufresne *et al.* 2014, Jorfi & Foster *et al.* 2015). However, this may not be true for all nanocellulose-based materials, as they may have different characteristics. These characteristics substantially depend on the processes to produce and treat nanocellulose.

This thesis project investigated characteristics and properties of wood-derived nanocellulose as a wound healing dressing being a cheap and renewable material. In particular, in the first part of the project, the attention was focused on identifying the best chemical and mechanical treatment to be carried out on wood to obtain hydrogels. In the central part, the hydrogels produced by two different techniques were compared: filtration under vacuum (Vacuum Filtration) and evaporation of the solvent (Solvent Casting). In this section, physical and mechanical properties of the hydrogels have

been evaluated. In the third and last part, the interest was focused on comparing the hydrogels produced with a commercially available hydrogel that is already used in the medical field.

The patch to be replaced is composed of bacterial cellulose, a particular form of cellulose produced by bacteria that differs from that of vegetable origin. Bacterial cellulose is made up of nano-sized fibers, called nano fibrils, which aggregate forming micro fibrils: these latter can form a three-dimensional structure. Like all kinds of cellulose, bacterial cellulose is biodegradable, intrinsically safe, with excellent mechanical properties, hydrophilic with excellent liquid absorption capacity, and not allergenic. All these features imply that bacterial cellulose can be used in many fields, and particularly in the medical field. Anyway, bacterial cellulose presents poor reproducibility on ~~a~~ large scale: this affects the production time and, consequently, the cost-effectiveness of the overall process for hydrogels production.

This master's thesis is the initial part of a five-year project (*Healix*), which includes the University of Luleå (where the work was carried out), the Universities of Linköping and Örebro, and a company dealing with the production of materials for wound dressing.

Sommario

Qualsiasi persona ha subito almeno una volta nella vita una piccola ferita che ha richiesto l'uso di una medicazione come il cerotto. Queste lesioni solitamente guariscono da sole ed in breve tempo senza richiedere troppa attenzione. Se invece si tratta di lesioni di maggiore importanza come ustioni, ferite acute o ulcere, è necessario l'utilizzo di molta più attenzione e l'applicazione del solo cerotto non è sufficiente. Le medicazioni che vengono applicate a tali ferite sono specifiche per le diverse fasi della guarigione e devono essere cambiate regolarmente. Viene dunque richiesta una medicazione per la quale non siano necessarie molteplici sostituzioni e che riduca al minimo i tempi di guarigione.

La cellulosa è stata usata fin dai tempi antichi come medicazione per le ferite sotto forma di foglie o erbe o, come negli ultimi tempi, incorporata all'interno di medicazioni moderne. Di recente l'industria forestale ha puntato fortemente sull'uso della cellulosa come materiale da medicazione nel campo medico in quanto, con l'avanzare della tecnologia, le altre applicazioni della cellulosa (per esempio, nell'industria cartaria) potrebbero riscuotere interesse decrescente. Le medicazioni per ferite basate sull'utilizzo della nanocellulosa come maggior costituente, hanno il potenziale per rimpiazzare gli attuali materiali utilizzati perché possiedono tutte le caratteristiche di una medicazione ideale.

La nanocellulosa è un materiale naturale, che è in grado di formare una sorta di network con cui può intrappolare una grande quantità d'acqua. L'acqua è necessaria per mantenere una ferita il più possibile calda e umida, ovvero nelle condizioni ottimali per una rapida e sicura guarigione (Boateng *et al.* 2008). Molti studi hanno evidenziato come i materiali nanocellulosici siano in grado di abbreviare i tempi di guarigione di una ferita, qualsiasi sia la sua estensione (Lin & Dufresne *et al*. 2014, Jorfi & Foster *et al*. 2015). Questo potrebbe però non essere vero per tutti i materiali basati sulla nanocellulosa, in quanto essi possono possedere caratteristiche diverse. Queste caratteristiche dipendono sostanzialmente dai processi di produzione e trattamento della nanocellulosa.

In questo progetto di tesi sono state studiate le caratteristiche e le proprietà della nanocellullosa derivata dal legno come medicazione per la guarigione delle ferite essendo un materiale economico e rinnovabile. In modo particolare, nella prima parte del progetto, si è concentrata l'attenzione

nell'individualizzazione del miglior trattamento chimico e meccanico da effettuare sul legno per ottenere hydrogels per la medicazione di ferite. Nella parte centrale sono stati confrontati gli hydrogels prodotti mediante due tecniche differenti: filtrazione sotto vuoto (Vacuum Filtration) ed evaporazione del solvente (Solvent Casting). In questa sezione sono state valutate le proprietà fisiche e meccaniche degli hydrogels prodotti. Nella terza ed ultima parte si è focalizzato l'interesse nel comparare gli hydrogels prodotti con una tipologia di hydrogels già presenti nel mercato ed utilizzati nel campo della medicazione.

Il cerotto che si vuole sostituire è composto da cellulosa batterica, una particolare forma di cellulosa prodotta da batteri che si differenzia da quella di origine vegetale. La cellulosa batterica è formata da fibre di dimensioni nanometriche, chiamate nano-fibrille, che possono aggregarsi formando delle microfibrille che, a loro volta, possono formare una struttura tridimensionale. Come tutti i tipi di cellulosa, anche quella prodotta dai batteri è biodegradabile, intrinsecamente sicura, con proprietà meccaniche ottime, idrofilica con eccellenti capacità di assorbimento dei liquidi e non è allergenica. Tutte queste proprietà fanno sì che questa cellulosa venga usata in molti campi industriali e, come in questo caso, anche in campo medico. La cellulosa batterica presenta però scarsa riproducibilità nella produzione su larga scala di hydrogels per la medicazione di ferite: ciò determina lunghi tempi di produzione e costi elevati.

Questa tesi magistrale è la parte inziale di un progetto ben più ampio (*Healix*), dalla durata di cinque anni, che comprende l'Università di Luleå (presso la quale è stato svolto il lavoro), le Università di Linköping e Örebro, e una azienda che si occupa della produzione di materiali per medicazione di ferite.

Summary

Chapter 1

Overview on nanocellulose

1.1 Introduction

In recent years, there has been an increased attention toward environmental protection that has led the industry to focus on the development and production of environmentally sustainable materials. Great importance has been given to bio-based plant materials that are composed of cellulose, hemicellulose and lignin (Miao *et al.* 2014, Mtibe *et al.* 2015). They present excellent characteristics such as biodegradability, renewability and biocompatibility and, for these reasons, these materials have received great consideration.

Cellulose is the most abundant polymer on Earth (Brigham *et al*. 2018). It can be found in plants, some marine animals, algae and furthermore they are produced by specific bacteria. Cellulose is characterized for its renewable origin, high abundance, non-toxicity, and a hierarchical structure from which cellulose-based objects with dimensions in the nanoscale can be isolated (Klemm *et al.* 2011). Cellulose nanomaterials are materials essentially composed of cellulose in a size range from 1 to 100 nanometers. Materials with internal or surface cellulose structure in the nanoscale are also included (Safenano *et al*. 2020). On 18th of October 2011, the European Commission adopted the following definition of a nanomaterial:

"A natural material, random or product containing particles, in an untied state or as an aggregate or as an agglomerate and where, for 50% or more of the particles in the distribution of numerical quantities, one or more external dimensions are in the range of size 1 nm – 100 nm. In specific cases and where justified by concerns for the environment, health, safety or competitiveness, the distribution threshold of the 50% numerical quantities can be replaced by a threshold between 1 and 50%." (European commission *et al*. 2019).

This definition refers to both nanocrystals (CNC) and microfibrillated cellulose (CNF). The acronym CNC indicates the nanocrystalline cellulose, which is presented in the form of a rod and is characterized by high rigidity. This is due to the fact that CNCs have a high degree of crystallinity ranging from 54% to 88% (Filson *et al*. 2009). The length of cellulose nanocrystals varies from 50 to 500 nanometers, while their diameter is between 3 and 50 nm. Unlike CNCs, cellulose nanofibrils (CNF), also called nanofibrillated cellulose, are made up of significant amorphous regions, with long, soft chains ranging from 10 to 500 nanometers in diameter and micrometer-scale lengths that often result in network-like structures. Another type of nanocellulose that falls within this definition is the bacterial cellulose, indicated by BC. The nanofibrils are not derived from plant sources but are synthesized and secreted by the *Gluconoacetobacter xylinus* family (Klemm *et al*. 2011). Bacterial nanocellulose is produced by the growth of bacteria for a few days in a liquid culture medium containing glucose, phosphorus, carbon and nitrogen (Iguchi *et al*. 2000).

Nanocellulose can be obtained by two different approaches: bottom up and top down. The production of CNF is a procedure that converts the large-scale unit into the small unit. In this case mechanically induced destructuring strategy is mainly applied: it involves grinding, high pressure homogenization and chemical-enzymatic treatment. As opposed to the production of CNF, bacterial cellulose is obtained by a process of construction from tiny unit to small unit. This nanocellulose, herein termed bacterial cellulose (BC), is pure cellulose without the presence of hemicellulose, lignin and pectin (Iguchi *et al*. 2000). From here we can see the first substantial difference between bacterial cellulose and nanofibrillated cellulose. The processes for the production of the two different kinds of nanocellulose are diametrically opposite. With regards to BC, it is possible to obtain 3D structures starting from units of the scale of ångström; to obtain CNF, one has to start from macroscopic units and produce 3D structures with additional operations such vacuum filtration or solvent casting. **Figure 1.1** schematizes the two approaches to obtain nanocellulose.

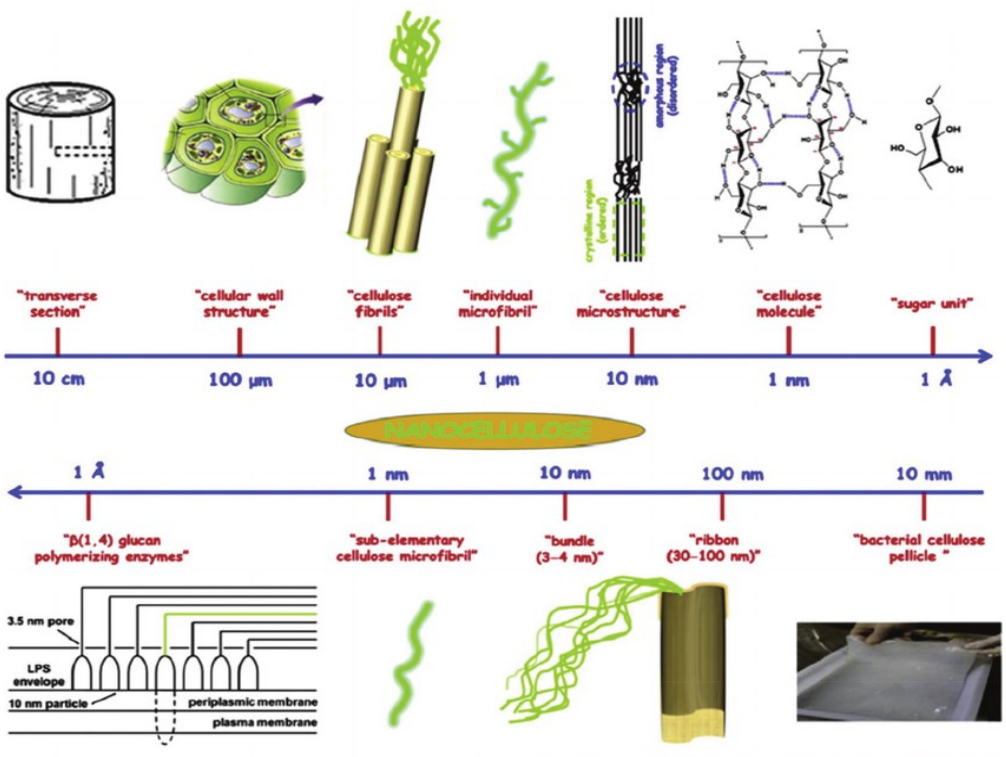

Figure 1.1 Schematic illustration of the two different approaches to obtain nanocellulose: top down and bottom up.

In recent years, particular attention has been paid to exploit the nanoscale potential in various applications and industrial sectors. As highlighted by the data extracted from the *Science Direct* database in **Figure 1.2**, there has been an exponential increase in the number of articles published per year on nanocellulose since 2007. In this data collection, it should be noted that the value belonging to the year 2021 refers to the publications that are being published.

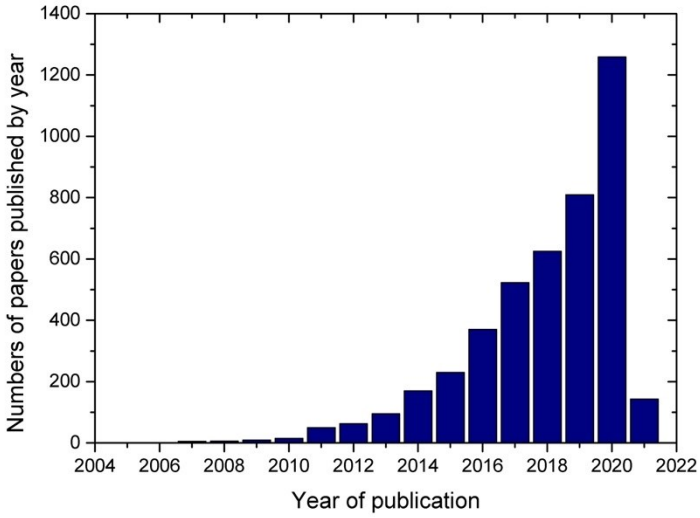

Figure 1.2 Trend of publications on nanocellulose from 2007 until the first days of March 2020 (Science Direct).

Among the countries with the highest number of articles published the year, China (860), USA (668), Sweden (473) and Finland (390) stand out (**Figure 1.3**).

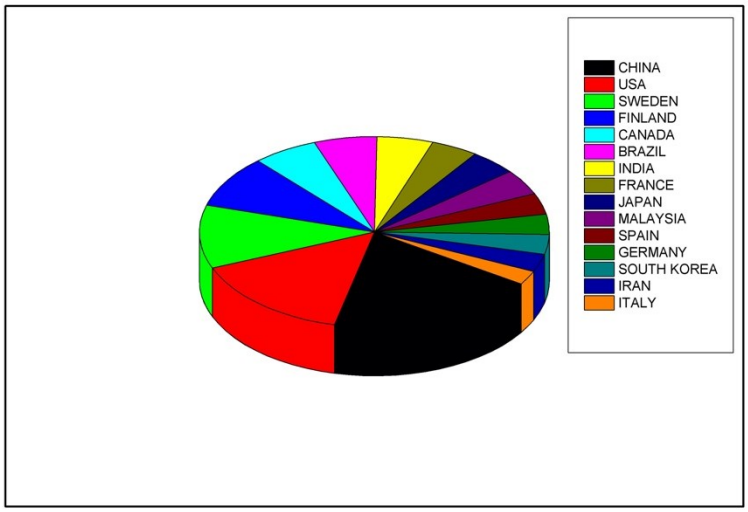

Figure 1.3 Number of articles on nanocellulose by country from 2007 until the first days of March 2020 (Science Direct).

In the global market, the nanocellulose market is approximately 35 million metric tons / year (Bilek *et al*. 2014). Currently, cotton and wood are the main sources for cellulose extraction. Separation of the cellulose into nanocellulose has received increased attention from research and industries. Thanks to its interesting nanoscale properties, its low production cost and its biodegradability, ~~the~~ nanocellulose has enjoyed great success in various applications of different industrial sectors. Nanocellulose can be used in various fields in our life, such as biomedical products, nanocomposite materials, textiles and so on. The excellent barrier properties and the biocompatibility of the nanocellulose are exploited for the production of polymeric films for the packaging of food, fruits and vegetables (Mondal *et al*. 2017).

In the biomedical field, the nanocellulose, appropriately extracted and treated, can be used in tissue engineering as reinforcing phase in the production of hydrogels. These latter are exploited for the construction of scaffolds with high mechanical properties, structural stability, excellent compatibility and a porous architecture capable of supporting cell growth (Mondal *et al*. 2017). Possible applications are cartilage reconstruction, drug delivery devices, sensors, contact lenses, artificial skin and cardiovascular prostheses. Nanocellulose-based bio-inks have also been proposed for 2D and 3D molding of human prostheses such as ear and meniscus. Thanks to its high-water content (95%), high purity and mechanical stability, the nanocellulose has been used for the production of masks and moisturizers (Kaith *et al*. 2011). As above mentioned, nanocellulose is a natural material that can form a network in which water can be retained and this help to maintain the wound moist (Boateng *et al*. 2008). Some studies (Ning *et al*. 2014, Mehdi *et al*. 2015) have been carried out on dressings for wounds based on nanocellulose and it has been shown that these materials have great potential, as they are able to reduce healing times. This topic will be discussed with more detail in the next chapter.

The nanocellulose has an important feature with regard to the possibility of chemical functionalization: the high surface area and the abundance of hydroxyl groups allow nanocellulose being used for surface modification. In fact, it is possible to create specifically modified nanomaterials according to the intended application. The modifications on cellulose nanofibers occur mainly at the level of the hydroxyl group *(-CH_2OH)* and the aim of this functionalization is to modify the hydrophobicity of the surface, improving its compatibility and dispersibility in

specific solvents. For these reasons, nanocellulose is a material that can be used for many applications, and in particular in the field of wound dressing.

1.2 Background

The most common natural polymers on earth are polysaccharides including starch, pectin, glycogen, cellulose and chitin. They are polymeric carbohydrate molecules formed by long chains of repeated monosaccharide units with general formula $(C_6H_{10}O_5)_n$ (where *n* is typically between 40 and 3000) which is based on glucose monomers linked by glycosidic bonds. They can appear in an extremely linear form or even in a branched form. Polysaccharides such as cellulose have a linear shape while others, such as glycogen, are branched. These polysaccharides seem to have a very well defined and promising path thanks to the characteristics of biodegradability and compatibility with living tissues.

Around the year 1840, Anselme Payen, a French chemist, discovered cellulose for the first time by extracting and isolating it from various plant tissues. **Figure 1.4** shows the typical structure of cellulose from plants, which can be obtained from wood, cotton and other plant fibers.

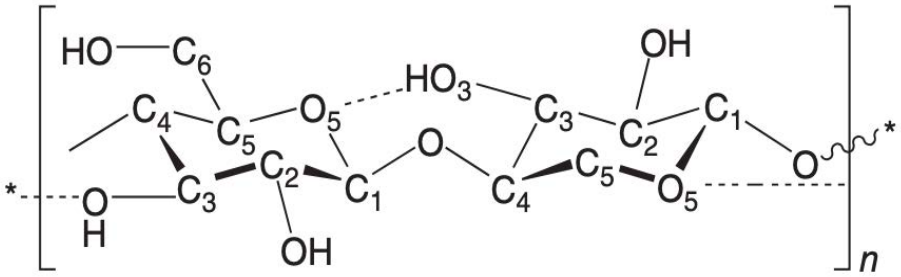

Figure 1.4 Single cellulose chain repeating unit, showing the directionality of the 1–4 linkage and internal hydrogen bonds (dotted line).

First and most traditional source of cellulose is its extraction from plants and their wastes. The biomaterial obtained in this way contains also hemicellulose and lignin. The cellulose, hemicellulose and lignin content in plant fibers vary depending on the plant species, origin, quality and environmental conditions (Liu *et al*. 2018).

The vegetable fibers have a tubular structure from 1 to 50 mm long, with a diameter of around 10-50 μm consisting of a central channel, called lumen, and a cell wall (**Figure 1.5**). The lumen is

responsible for the transport of water and nutrients and has a diameter of 25 µm when the fiber is considered cylindrical; in most cases, it is reduced to a thin segment of 5 µm due to the mechanical stresses that the fiber undergoes (Thangaraju *et al*. 2016).

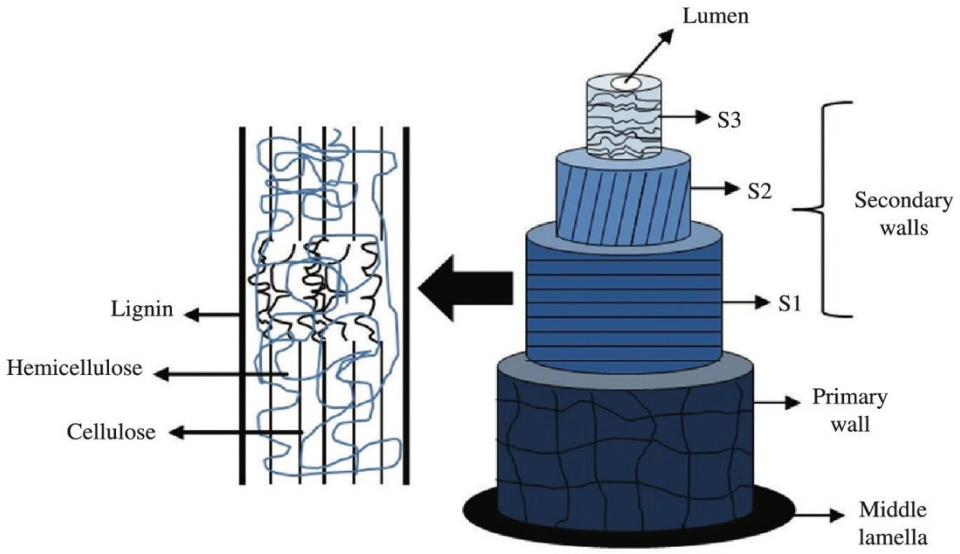

Figure 1.5 Physical structure of plant fibers (Benini *et al*. 2015).

With the biological death of the cells, the remaining structure coincides with the cell wall of variable thickness, between 1 and 5 µm depending on the plant species and consists of two coaxial layers called primary and secondary walls wrapped by the middle lamella (Belgacem *et al*. 2016). The primary wall is a very thin layer, between 30 and 1000 nm thick, which settles during cell growth and envelops the internal wall like an epidermis: it is divided into three layers called the S1 external secondary wall, the intermediate secondary wall S2, and internal secondary wall S3 (Benini *et al*. 2015). The intermediate S2 secondary wall is the thickest and it is responsible for the mechanical properties of the fiber. The layers differ from each other in structure and chemical composition. They consist of semi-crystalline oriented cellulose microfibrils immersed in a hemicellulose and lignin matrix of variable composition (Kaith *et al*. 2011). The fibrils are made up of 30-100 extended chain cellulose molecules and confer mechanical resistance to the fibers (Kaith *et al*. 2011); they constitute the major phase of reinforcement of trees, plants, some marine creatures (tunicates), algae and bacteria (some bacteria secret cellulose fibrils creating an external structure).

Plant fibers are made up of three main components: cellulose, hemicellulose and lignin. This is why they are also referred to as cellulosic or lignocellulosic fibers. Other components in smaller amounts are pectin, waxes and water-soluble substances. The chemical composition and structural conformation of the lignocellulosic fibers vary considerably according to the species and the age of the plant and according to the climatic conditions and the soil.

Cellulose is the most abundant renewable polymer on earth and the main component of vegetable fibers. Cellulose is a linear homopolysaccharide with a flat ribbon-like conformation, whose repeating unit, cellobiose $(C_6H_{10}O_5)_2O$, is given by condensation of two anhydroglucose rings, therefore it is also called anhydrocellobiose (Gurunathan *et al*. 2015) (**Figure 1.6**).

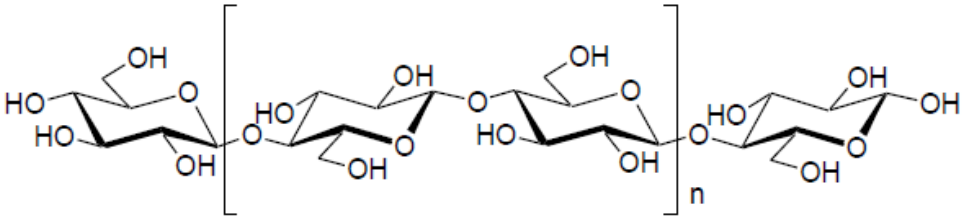

Figure 1.6 Structure of cellulose.

Anhydroglucose rings are joined together by covalent bonds between oxygen and the C1 of a glucose ring and the C4 of the adjacent ring (1 → 4 bond), called β 1-4 glucosidic bonds (Bras *et al*. 2010; Martini *et al*. 2011). The hydrogen atom intrachained between the hydroxyl groups and the oxygen atoms of the adjacent molecules stabilizes the bond, giving a linear configuration to the cellulose chain. Each anhydroglucose unit has six carbon atoms with three hydroxyl groups (on the C2, C3 and C6 atoms) giving a high degree of functionality to the cellulose molecule and hydrophilic properties. The ability of hydroxyl groups to form strong hydrogen bonds is responsible for directing the crystalline packing of cellulose and its final properties. During biosynthesis, Van der Waals forces and intermolecular hydrogen bonds between hydroxyl groups and oxygen atoms of adjacent molecules promote the stacking of the different cellulose chains, giving rise to high-packing index of crystalline regions called fibrils, which further aggregate forming the microfibrils, interspersed with amorphous regions with a low-packing index. The inter and intramolecular hydrogen bonds make cellulose a stable polymer and give the fibrils a high axial stiffness. The degree of crystallinity of cellulose strongly depends on the source from which it is extracted and on the isolation method. Wood, cotton, linen, ramie, sisal and banana have a high degree of

crystallinity (65-70%), which increases in the progressive elimination of the other components during the treatment of the fibers (Kaith *et al*. 2011). The degree of polymerization (DP) is expressed by the number of anhydroglucose units per chain and it will therefore be equal to double of the repetitive units of the cellulose molecule. Like the degree of crystallinity, the DP also varies according to the species of the plant which the cellulose belongs to and the method of extraction: in cellulose from wood, for example, it is equal to 10,000 while in cotton it is between 15,000 and 20,000. (Bras *et al*. 2010; Belgacem *et al*. 2016). During the cellulose purification processes, the DP varies considerably, being reduced by an order of magnitude compared to its initial value (Bras *et al*. 2010). The decomposition temperature of cellulose is equal to 250-300 ° C (Carrino *et al*. 2011).

Hemicellulose is the second most abundant organic material in nature after cellulose. Its structure (**Figure 1.7**) is more complex than cellulose, differing from the latter for the branched chain and for the presence of more sugars in addition to 1,4 β-D-glucopyranose. Furthermore, the DP of hemicellulose is 10 to 100 folds lower than that of cellulose (Gurunathan *et al*. 2015). Although hemicellulose is not covalently linked to cellulose, it is difficult to separate it from cellulose.

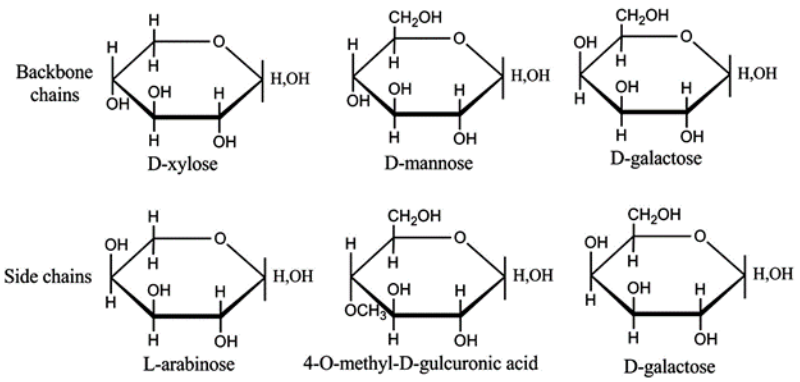

Figure 1.7 Structure of the different sugars from which the hemicellulose is formed.

Lignin is a highly cross-linked molecular complex with an amorphous structure that plays the role of binding agent between the individual cells of the fiber and the fibrils making up the cell wall. It consists of aromatic units of phenylpropane that form strong intramolecular bonds giving the cellular structure of the fiber rigidity and considerable resistance to compression. Lignin fills the voids of the cell wall by interposing between pectin, cellulose and hemicellulose, forming partially covalent bonds with the latter. The mechanical properties of lignin are lower than those of cellulose.

Pectin is responsible for the luster, feel and flexibility of the fibers. Furthermore, it has the function of keeping the fibers joint in bundles, thus acting together with the hemicellulose as a cementing agent. It represents a complex group of heteropolysaccharides called glycosaminoglycans and is present in greater concentration in the primary cell wall and in the middle lamella of the fiber. Pectin is soluble in water only after partial neutralization with alkaline or ammonium hydroxide (Kaith *et al*. 2011).

Finally, waxes determine the characteristic softness to the touch of the fibers and decrease the friction between them. They consist of different types of alcohols soluble in both water and acids (Kaith *et al*. 2011).

Cellulose can therefore be obtained from a large variety of sources such as plants, animals and bacteria. As already highlighted, size and properties of the cellulose depend on the source from which it is extracted.

The nanocellulose maintains the original properties of cellulose in terms of biocompatibility, non-toxicity and biodegradability, but it has greater crystallinity, larger surface area, higher mechanical properties and greater active energy sites, attracting considerable scientific and technological interest. A further advantage of nanocellulose is that it allows producing transparent films having a diameter equal to one tenth of the length of the light, finding application in pharmaceutical, biomedical, electronic, textile and packaging sectors (Arcot J. *et al.* 2016). As for the plant resource, wood, rice husk, sisal, hemp, flax, kenaf, and coconut husk are some of the materials considered for the extraction of cellulose and nanocellulose (Abrahama *et al*. 2013). Wood is the most used material for the extraction of cellulose and nanocellulose thanks to its abundance in nature. It is a natural composite material with a hierarchical architecture composed of cellulose, hemicellulose, pectin and lignin. It has a porous anisotropic structure and is characterized by low density and high toughness, flexibility and rigidity (Terenzi *et al*. 2015). **Figure 1.8** schematically depicts the hierarchical structure of wood fibrils and microfibrils.

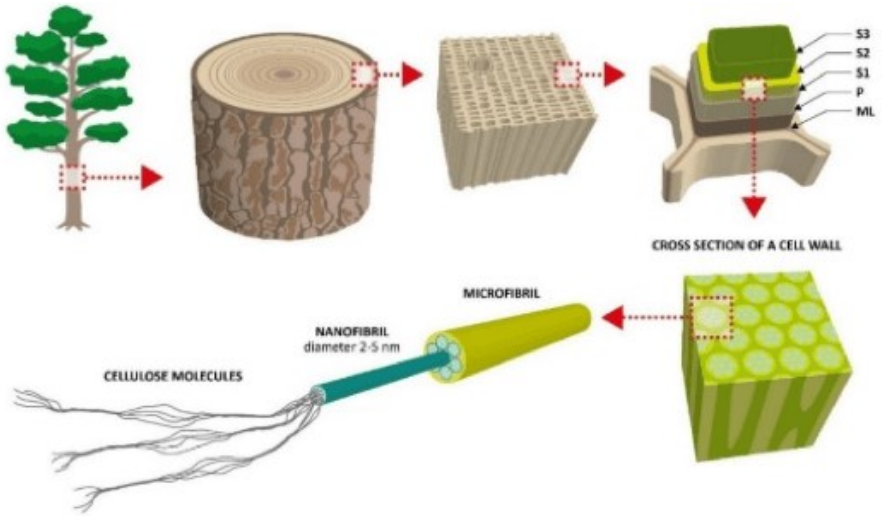

Figure 1.8 Wood hierarchical structure: from tree to nanocellulose.

The isolation of cellulose particles from plant fibers generally takes place in two stages and should comply with three basic requirements (Hamid SBA, 2014):

1) avoiding the breakdown of the cellulosic structure and the loss of cellulose, hemicellulose and lignin;
2) having a reasonable cost;
3) minimizing use and production of toxic or harmful substances for the environment;

The first stage consists in a pre-treatment of purification and homogenization of the material from which the cellulose is extracted, in order to partially remove components such as hemicellulose and lignin and in order to make it more reactive for subsequent treatments. The main difficulty in this initial phase is due to the resistance of the cell wall of the fiber to deconstruction because of the strong crystalline character of the cellulose immersed in the lignin and hemicellulose matrix (Hamid *et al.* 2014). On the other hand, the second stage operates the separation of the microfibrils and crystalline regions from the purified cellulosic material and allows the actual cellulosic material to be obtained in nanometric size or not, depending on the technique used. There are basically three possible approaches to separate cellulose: chemical, mechanical and enzymatic. The most used methods involve a mechanical or chemical process that can also be used in combination (Martini *et al.* 2011). Before actual isolation, pre-treatments can be performed. The goal of the pre-treatment is to make the cellulosic material as homogeneous as possible by breaking down the lignocellulosic complex and solubilizing components such as lignin, hemicellulose, waxes and oils that cover the outer surface of the cell wall of the fiber. It generally consists of two stages: delignification (pulping) and bleaching. (Belgacem *et al.* 2016).

Cellulose and nanocellulose can be extracted also from tunicates. They are marine invertebrates, members of the subphylum Tunicata. In this area, research has paid more attention to one class in particular, the class of *sea squirts* (*Ascidiacea*), which are a species of marine invertebrate filter feeders. Cellulose from tunicates is produced from the outer fabric. This kind of cellulose is called a tunic and a type of cellulose with a higher degree of purity, called tunicin, can be extracted from it.

Finally, cellulose can derive from algae. Cellulose fibers can be extracted from green filamentous algae such as Cladophora, Chaetomorpha, Microdyction, Rhizoclonium and members of

Siphonocladales (Nicolai *et al.* 1997). Their strong rheological properties and robustness makes them suitable materials for food packaging, wound dressings and pharmaceutical applications. Despite all the advantages, CNF extraction from algal sources is lower compared to plants and bacterial sources. The crystalline form of cellulose deriving from algae extraction differs according to the algae used.

Last but not least, cellulose can be obtained from some bacteria. As already mentioned, the process to obtain this cellulose is essentially the opposite of that used for extraction from plants, algae or animals. Bacterial cellulose (BC) was discovered in 1886 when A. J. Brown published the first article in which a gelatinous mat was produced by synthesis from acetic fermentation (Brown *et al.* 1887). Amongst the cellulose-forming bacteria, Acetobacter strains (also called Gluconacetobacter) are especially suitable for the production of cellulose. They are aerobic bacteria and appear as ellipsoidal rods, slightly bent or straight (Klemm *et al.* 2005). These bacteria are capable of producing easily isolable extracellular cellulose. During the synthetic process, glucose chains are produced inside bacterial cells and are subsequently extruded through tiny pores on cell membrane. These glucose chains then combine, forming nano-sized fibers that further aggregate into ribbons that can reach 100 nm in width. These microfibers in turn generate a web-like mesh structure with many gaps between the fibers. Well separated BC nanofibers create an expanded surface and highly porous matrix. In **Figure 1.9** we can easily see the formation of this network by the bacteria.

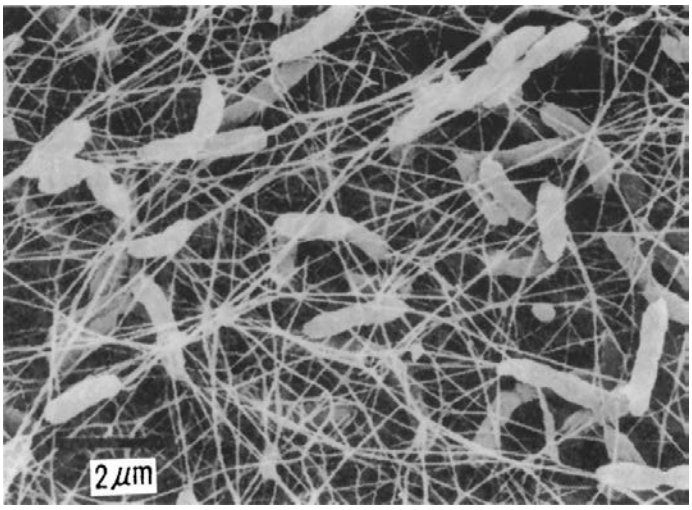

Figure 1.9 A scanning electron micrograph of freeze-dried surface of bacterial cellulose gel (Iguchi *et al.* 2000).

Cellulose production from bacterial cultures in laboratory is an interesting, attractive and competitive technique to get pure cellulose. Thickness, shape and microstructure are directly controlled by some independent parameters such as substrate, growing conditions, additional additives and bacterial strains. As discussed above, in plants cellulose coexists with lignin and other polysaccharides such as hemicellulose. Achieving pure cellulose is not easy and cheap because it is necessary to use chemical and mechanical treatments, sometimes alone and sometimes combined. Especially for products used in biological and medical fields, purification takes a considerable importance. Contrarily to vegetable cellulose, bacterial cellulose is a biopolymer characterized by high purity and a high DP values ranging between 2000 and 8000. It has unique properties and sometimes superior to that of vegetable cellulose. Among these properties, the most important are crystallinity (with ranges between 60 and 90%) (Czaja *et al.* 2004), high capacity to absorb water with values that can reach three to four thousand folds its own weight, and very high tensile resistance. Bacterial cellulose is getting a good response regarding the field of modern medicine and biomedical applications, in which it has not been possible to use vegetable cellulose. This is due to its high purity and very good biological affinity. Among other advantages, there are some disadvantages to consider. First of all, the high costs due to sterilization and the high costs of the substrates (sugar). It is estimated that the price of bacterial cellulose is one hundred times higher than that of vegetable origin. Moreover, another major drawback is the lack of large-scale production capacity. In addition, the process that leads to the synthesis of BC has reduced volumetric yields and an extremely long production time. Finally, the process for obtaining bacterial cellulose involves a large amount of caustic residual water used for washing the BC film.

Chapter 2

Hydrogels for wound healing

2.1 Introduction

Wound healing is a very dynamic and complex process that specifically requires an adequate environment to go to completion. As technology advances, many products have been designed and developed for treating different kinds of wounds, carefully looking at the various steps of the healing process. Gauze, plasters, natural or synthetic bandages and cotton wool are some of the traditional products used in the medical field as primary and / or secondary dressings to protect the wound from contamination. Gauze made from woven and non-woven fibers of cotton and polyester offer good protection against bacterial infections. Some gauze pads are used as a sponge to absorb fluids and exudates from the wound. These traditional dressings require frequent changes to protect against maceration of healthy tissues. When gauze dressings are considered, these are less convenient since excessive wound drainage makes them moist and adhering to the wound: thus, their removal can be painful. Because these traditional dressings are unable to provide a moist wound environment, they have been replaced by modern and more advanced dressings. Unlike traditional dressings, modern dressings have been developed to facilitate the healing process of a wound rather than just covering it. These dressings are designed to protect the wound from dehydration and thereby promote healing. There are numerous products on the market for any kind of wound. Modern wound dressings are generally based on synthetic polymers and are classified as passive, interactive and bioactive products. Passive products are non-occlusive, such as gauze and tulle dressings, used to cover the wound to restore the function of the tissue underneath. Interactive dressings are semi-occlusive or occlusive, available in the forms of films, foam, hydrogel and hydrocolloids. These dressings act as a barrier against penetration of bacteria into the wound bed. This category includes semi-permeable film dressings, semi-permeable foam dressings, hydrocolloid dressing, alginate dressing and hydrogels dressing. In this work, the focus is on hydrogels as wound dressing.

In this chapter we will briefly illustrate the wound healing process and then we will describe in detail the hydrogels used in wound dressing and all their characteristics.

2.2 Wound healing process

A wound is defined as damage or destruction of normal anatomical structures and their functions. They can range from a simple lesion of the epithelial integrity of the skin to a deep lesion that involves subcutaneous tissues with damage to other anatomical structures: tendons, muscles, vessels, nerves. The wounds can have an accidental, intentional etiology or they can be the result of a pathology. Regardless of the cause, the injury damages the tissue and destroys the local biological environment. Wound healing is a dynamic and complex process involving a large array of molecules and cellular events. Through the release of plasma with coagulation and platelet aggregation, re-epithelialization and remodeling of the damaged tissue, the body tries to restore the integrity and functionality of the injured tissue. Healing of skin wounds is a multi-stage phenomenon that begins rapidly after injury and involves the cells present in the site and the cells that migrate from different areas of the body (keratinocytes, endothelial cells, fibroblasts, and inflammatory cells), the extracellular matrix and many soluble mediators. This process involves inflammation mediators and growth factors that affect cell-cell and cell-extracellular matrix interactions. The set of these processes controls cell proliferation, migration and differentiation, re-epithelialization, angiogenesis and remodeling. A wound can be declared healed when the affected tissue has returned to "normal" anatomical structure and function within a reasonable time (*restitutio ad integrum*). Local and systemic factors can alter the normal healing process causing the wound to become chronic (Velnar *et al.* 2009).

The wound healing process occurs in all tissues and organs of the body. It is a complex phenomenon that involves and coordinates immunological and biological systems. Although the wound healing process is continuous, it has been arbitrarily divided into four phases in order to understand the physiological processes that take place at the injury site and surrounding tissues: coagulation and hemostasis, inflammation, proliferation, tissue remodeling.

Coagulation and hemostasis

Immediately after the formation of the wound, coagulation and hemostasis take place at the site of the injury. The immediate goal of these events is to prevent bleeding. A second, longer-term goal is to provide a temporary matrix for infiltrating cells for the later stages of the healing process. Hemostasis is the arrest of bleeding and constitutes the response to vascular injury. A dynamic balance between coagulation and fibrinolysis regulates hemostasis. Furthermore, neuronal reflex mechanisms and the secretion of vasoconstrictor factors mediate vasoconstriction in the affected site, reducing bleeding. Along with the hemostatic events, the coagulation cascade is activated. As blood flows to the wound site, blood components (e.g., platelets) come into contact with collagen and other components of the extracellular matrix. This leads to platelets activation/aggregation and activation of coagulation factors to form the platelet plug. The platelet plug not only plays a hemostatic role but also provides a temporary matrix for cell migration in the next phase and as a reserve of growth factors required during the healing process. The platelet plug is eventually stabilized by fibrin, which is the final product of the hemocoagulative cascade: the blood clot is then formed.

Inflammatory phase

Inflammation is the protective response aimed at the elimination of cell/tissue debris and possible pathogens from the injury site and the initiation of the reparative process. Clinically, the signs of inflammation are redness, swelling, heat, pain, functional alteration of the inflamed area. Manifestations of the alterations occurring after an injury are vasodilation, increased vascular permeability with the passage of fluids from the vascular bed to the injured tissue (edema), leukocyte infiltration in the lesion area. The inflammatory phase begins with the infiltration of neutrophils into the wound site, the first cells to be recruited. Neutrophils begin to be attracted to the wound site 24-36 hours after injury by various chemoattractants, products of bacterial origin, complement components, prostaglandins and thromboxanes from the arachidonic acid cascade. Chemical or physical stimuli activate cellular phospholipases and allow the release of arachidonic acid. The metabolites of arachidonic acid also initiate the complement cascade. The complement system is activated by eicosanoids and proteolytic enzymes that make up the inflammatory exudate, releasing chemotactic factors and increasing vascular permeability. It is therefore involved in the defense of the organism. Neutrophils migrate out of the vessels to the damaged tissue, a process

known as diapedesis. Neutrophils adhere to the endothelial cells at the level of the capillaries surrounding the wound and roll along the surface of the endothelium, evacuating the bloodstream. The release of neutrophils from the vessels allows them to reach the site of the lesion and engulf pathogenic microorganisms and tissue structures damaged. Once their function is over, neutrophils are phagocytosed by macrophages (Petri *et al.* 2006).

Late inflammatory phase

48-72 h after the injury, macrophages appear on the wound site to continue the phagocytosis process. These cells were originally blood monocytes produced in the bone marrow. Monocytes migrate from the circulation into tissues and turn into macrophages. Macrophages are activated by cytokines, bacterial toxins and ECM proteins and are attracted to the wound site by chemotactic agents such as coagulation factors, complement components, cytokines, chemokines and collagen degradation products. In turn, macrophages release other inflammatory mediators by activating keratinocytes, fibroblasts and endothelial cells. The last cells to enter the wound site are lymphocytes, attracted 72 hours after the injury. Thus, in addition to the defense function, inflammatory cells are also an important source of growth factors and cytokines that trigger the proliferative phase of the healing process (Velnar *et al.* 2009).

Proliferative phase

It begins three days after the injury and lasts for the next two weeks. It is characterized by the migration of fibroblasts and by the deposition of the new extracellular matrix, which replaces the temporary one composed of fibrin and fibronectin. Thus, a new tissue called “granular tissue” is deposited: it is characterized by the massive presence of capillaries. In this phase, different processes are observed: migration of fibroblasts, synthesis of collagen, angiogenesis and formation of granulation tissue, re-epithelialization.

Wounds can be classified according to various criteria one of which is the healing time. Based on time, the wounds can be divided into:

- **acute wounds**: these are wounds that heal by themselves following the normal wound healing pathway and leading to complete anatomical and functional recovery of the

affected part. The healing time can vary from 5-10 days up to thirty days. It involves only the soft tissues and is caused by minor or short-lived traumatic events;

- **chronic wounds**: these are wounds that do not follow the normal healing process. This process is incomplete or disturbed by various factors such as infections, tissue hypoxia, necrosis, excess of inflammatory cytokines. The continuous state of inflammation of the wound creates a cascade of responses that perpetrate the state of non-healing.

Other wound classification criteria include etiology (bruises, abrasions, lacerations, cuts, burns), the development of contamination (aseptic wounds, contaminated wounds, septic wounds), morphological characteristics

2.3 Wound healing dressing

After an exemplary description of the wound healing process, in this section we will discuss the optimal characteristics that a dressing must possess. Furthermore, attention will be focused on the properties of the hydrogels used as ~~a~~ wound dressing and the reason why they are widely exploited in this field.

A good wound dressing must have the following characteristics:

- it must be able to remove necrotic tissue and foreign material thus helping leukocytes to shorten the inflammatory phase;
- it must be able to maintain a humid and warm environment, trying to keep the temperature as constant as possible;
- it must be biocompatible (non-cytotoxic at least);
- it must be able to absorb blood and ensure adequate gas exchange (low oxygen levels stimulate angiogenesis while other levels promote epithelialization and fibroblasts growth);
- it must act as a barrier to take bacteria away and thus prevent infection;
- it must give minimal adherence to the wound, seek isolation from the external environment but avoid removing healthy cells together with the dressing;
- it should have a low cost and do not require frequent changes.

In the introduction, it has been said that hydrogels are part of modern dressings. Hydrogels are insoluble and hydrophilic materials mainly consisting of polymers (synthetic or natural such as nanocellulose). They consist of cross-linked polymers and more than 95% water, which is confined into the polymer network. They are able to absorb large amounts of water, effectively helping the granulation tissues and the epithelium in a humid environment. The soft elastic property of the hydrogels allows an easy application and removal after wound healing completion without any damage. In **Figure 2.1** it is possible to see how these hydrogels can be easily removed after healing completion, without causing further damage or injury. Furthermore, hydrogels reduce the temperature of skin wounds thus producing a soothing and refreshing effect. A study (Jorfi *et al.* 2015) found that hydrogel dressings are suitable for all the four stages of the healing process. The disadvantages that have been highlighted regarding hydrogels are the production of bad smells due to the accumulation of exudate that leads to maceration and bacterial proliferation. Furthermore, the low mechanical resistance makes their manipulation difficult. In this research, we tried to increase the mechanical properties of these hydrogels in order to make their application easy.

Figure 2.1 A burn wound before applying a hydrogel as dressing (left) and after its removal (right).

Hydrogels, and other gels in general, can be loaded with compounds (e.g. drugs) or be composites in which other materials are mixed into the polymer network (Boateng *et al.* 2008). These dressings are best suited for tissue-free wounds, wounds with high amounts of exudate, and chronic wounds. **Figure 2.2** schematically illustrates the process of absorption of exudate by the hydrogel in contact with a wound.

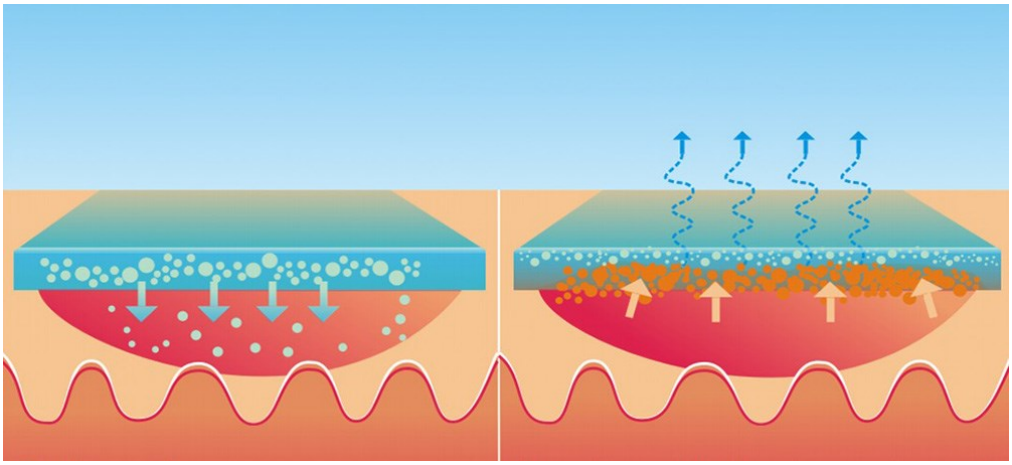

Figure 2.2 Illustration of how a hydrogel keeps wounds optimally moist (left) and how it absorbs excess exudate, preventing necrosis and bacterial colonization (right)

We have seen that hydrogels have numerous advantages over traditional dressings. Briefly, they:

- decrease dehydration and cell death. Neutrophils and fibroblasts, necessary for wound healing, cannot survive in a dry environment;
- increase angiogenesis;
- dry wounds decrease the supply of blood and nutrients. This results in the formation of a barrier and in decreasing epithelialization. For this reason, a dressing of this kind guarantees the maintenance of a humid environment with a consequent increase in re-epithelialization;
- the material is transparent and allows easy monitoring of the state of the wound;
- they are flexible and have good moldability. This allows them to adhere to any type of body surface, even the most difficult ones like the face is. **Figure 2.3** shows the ability to adapt to any part of the body.

Figure 2.3 Illustration of some applications of hydrogel as wound dressing.

2.4 Swelling of hydrogel: water diffusion into hydrogels

The ability to display a measurable change in volume in response to external stimuli is a fundamental property of hydrogels (Lee and Park *et al.*1996). Some hydrogels show a change in volume by swelling, while others show transitions between the sol gel phases (Brannon-Peppas e Peppas *et al.* 1991).

Many factors affect the ability to absorb water. For example, the crosslinking degree can influences the area allowed for diffusion through the network and consequently the ability to absorb water also varies (**Figure 2.4**).

This water capacity is represented by the equilibrium swelling ratio (**Equation 2.1**), where $M_{hydrated}$ is the mass of the fully inflated hydrogel (in equilibrium with aqueous medium) and $M_{dehydrated}$ is the mass in the dry state.

$$Swelling\ Ratio = \frac{M_{hydrated} - M_{dehydrated}}{M_{dehydrated}} \tag{2.1}$$

Hydrogels can have ionic or neutral side groups attached to their backbone, and both groups influence water uptake (Peppas *et al.* 2000). The Flory-Rehner theory helps to describe swelling of neutral hydrogels (Peppas *et al.* 2000). Briefly, a neutral hydrogel experiences a thermodynamic force of mixing and a contractive force that become balanced once a hydrogel reaches its equilibrium swelling state (Peppas *et al.* 2000). The theory was modified by Peppas and Merrill to account for hydrogels synthesized in water (Peppas *et al.* 2000). Anionic and cationic hydrogels have an additional force exerted on their networks due to their ability to form ionic interactions (Peppas *et al.* 2000).

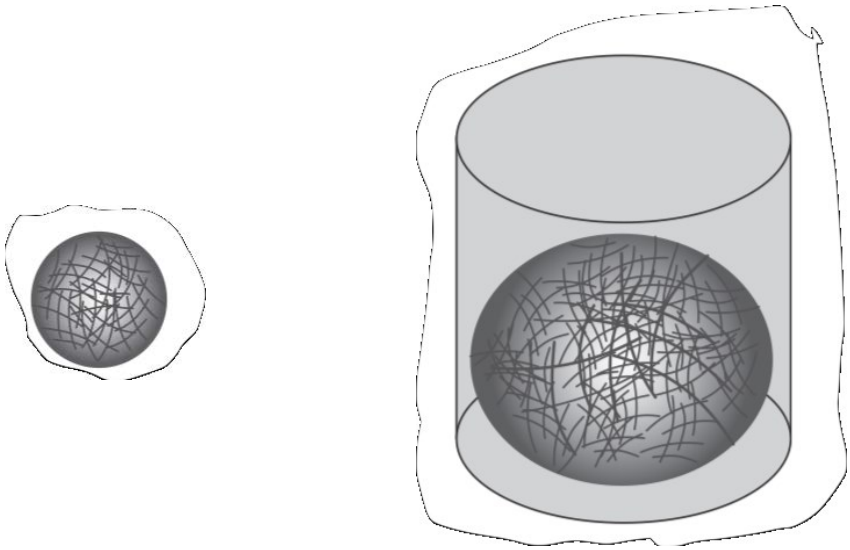

Figure 2.4 Dehydrated (on the left) and swollen (on the right) hydrogels as the result of water absorption.

Chapter 3

Difference between pulp and wood CNF

3.1 Introduction

Thanks to all its excellent properties, nanocellulose is an optimal material to be used in the medical field, especially for wound dressings. The purpose of this thesis work is to search for an innovative and biodegradable material capable of replacing bacterial cellulose in the field of wound dressing patches. To accelerate the healing process and promote re-epithelialization, it is necessary to resort to the use of innovative and no longer traditional dressings. It has been seen how hydrogels are excellent candidates as they can absorb a large amount of water, effectively keeping the wound environment moist and creating the optimal conditions for rapid healing.

We previously said that some chemical or mechanical treatments are required for the extraction of nanocellulose based on the intended result. It has also been said that the extracted cellulose is not pure as the one derived from bacteria, but it contains byproducts such as hemicellulose, lignin and pectin. To obtain pure cellulose, different approaches are required that include different treatments to isolate the nanocellulose. Depending on the treatments performed, we can obtain the "pulp" or the nanocellulose. The characteristics of these two types of nanocellulose will be studied and compared in terms of water absorption and mechanical properties. This is the first step to identify the hydrogel that guarantees an excellent compromise between swelling and tensile strength. The hydrogels were prepared by vacuum filtration and were subsequently subjected to characterization.

3.2 Chemical and mechanical treatments

To replace an existing material, it is necessary to find another one, which has to possess identical or superior chemical and mechanical properties and whose cost is adequate with respect to the intended application. The cost is strictly influenced by mechanical treatments because they require large energy consumption. The first part of the work aims at finding the best combination of mechanical and chemical treatments to extract and isolate the nanocellulose so that it has excellent properties at a low cost.

Starting from wood as a primary source, it is possible to carry out pre-treatments on it. The goal of the pre-treatment is to make the cellulosic material as homogeneous as possible by breaking up the lignocellulosic complex and solubilizing components such as lignin, hemicellulose, waxes and oils that cover the outer surface of the cell wall of the fiber. It generally consists of two stages: pulping and bleaching (Belgacem *et al.* 2016). There are several methods for obtaining the delignification of plant fibers that can be used alone or in combination with other treatments to obtain a greater effect. Alkaline treatment is the most commonly used as a pre-treatment and can occur in the presence of NaOH (Abdillahi *et al.* 2010), KOH (Alvarez *et al*. 2013), $Ca(OH)_2$, hydrazine or ammonium hydroxide, under mechanical agitation. Depending on the severity of the process, more or less high times and concentrations of the reagents can be obtained. This mechanism induces the saponification of the intermolecular ester bond that binds hemicellulose to lignin, increasing the porosity of the material and thus favoring subsequent depolymerization. The ester group is replaced by a nucleophilic acyl in the presence of an alkaline salt to form a carboxylic salt and an alcohol. The alkaline reagent has the function of a swelling agent, that is, a swelling of the cellulose, promoting an increase in the internal surface area. This treatment avoids the degradation of cellulose and its transformation into glucose, thanks to the presence of lignin that makes it inaccessible to the reagent. It should also maximize the amount of cellulose obtainable for the synthesis of nanocellulose. Subsequent treatments allow the removal of the remaining lignin and the separation of cellulose (Hamid *et al.* 2014).

Following delignification, the bleaching or whitening treatment involves a further removal of the lignin content through a treatment with hydrochloric substances such as sodium hypochlorite (NaOCl), sodium chlorite ($NaClO_2$) in concentrations ranging from 1 to 5%. In addition to lignin removal, this treatment induces a reduction in the diameter of the fibers and an improvement of

some properties such as crystallinity, elastic modulus, aspect ratio and surface area. Despite the good results obtained with this treatment, which has been widely studied and used, this process is not very eco-sustainable; in this regard there are less efficient but more eco-friendly alternatives that use ozone or hydrogen peroxide (Belgacem *et al.* 2016). After the pre-treatments, we move directly to the actual treatments. They can be of chemical or mechanical type. The most commonly performed chemical treatment is acid hydrolysis. The nanocellulose obtained from this process is highly dependent on various factors such as the origin of the natural source, type and concentration of the acid, reaction time and hydrolysis temperature. Currently, acid hydrolysis is the most effective process for the production of nanocellulose, it requires low energy consumption but is incompatible from the environmental point of view, with additional costs related to the treatment of the acid solutions.

Another widely used chemical treatment is carboxylation through TEMPO. The oxidation by TEMPO is an interesting alternative to isolate the nanocellulose as it does not require high concentrations of acid such as those used in acid hydrolysis or high energies as in the case of the steam explosion process and mechanical treatments (Arcot *et al*., 2016). The basic principle of the TEMPO / NaBr / NaClO treatment is the oxidation of cellulose fibers through the nitrosonium ion ($^{+}N \equiv O$) generated in situ through the reaction of the TEMPO radical with the oxidizing species (**Figure 3.1**, **Figure 3.2**). The primary alcoholic group of cellulose is converted into an aldehyde, which is further oxidized and transformed into a carboxylic group. Through this process, the depolymerization of cellulose is obtained, to which two phenomena are associated: the elimination of the β phase due to the presence of aldehyde groups under alkaline conditions and the cleavage of the anhydroglucose unit due to the presence of hydroxyl radicals formed with further lateral reactions (Belgacem *et al.* 2016). After the oxidation mediated through TIME, some unconverted aldehyde groups may remain, which induce yellowing of the cellulose nanofibers during subsequent drying in the oven (Belgacem *et al.* 2016). This process can also be used as a pre-treatment to make subsequent mechanical treatment more effective.

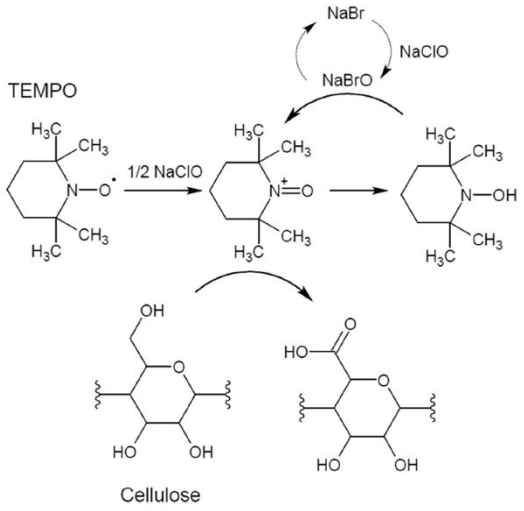

Figure 3.1 TEMPO oxidation of cellulose (Arcot J. *et al*. 2016).

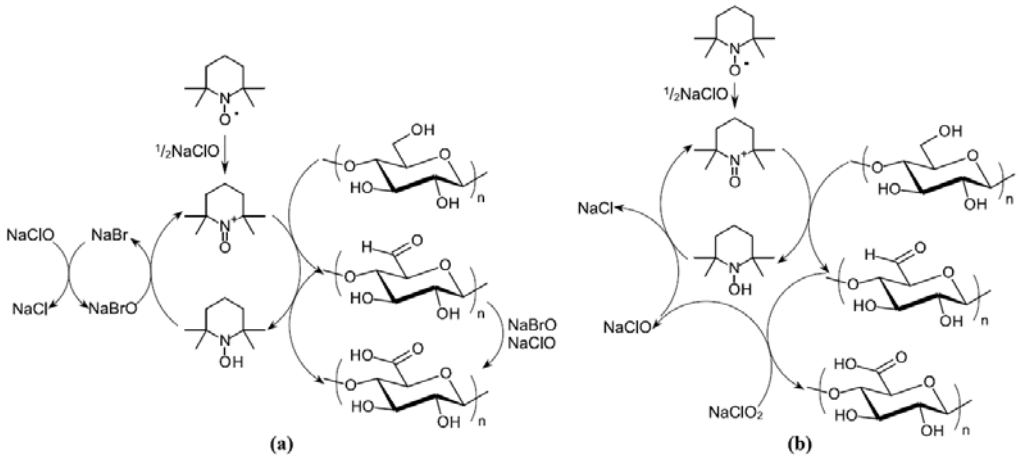

Figure 3.2 Schematic diagram of the selective regio-oxidation of the primary alcohol groups of cellulose through (a) TIME / NaBr / NaClO in water at basic pH and (b) TIME / NaClO / $NaClO_2$ in water at neutral or slightly acidic pH (Belgacem *et al*. 2016).

The mechanical processes involve several steps through which the cellulose fibers are shredded, exploiting high shear stresses to produce a transverse cleavage along the longitudinal axis of the microfibrillar structure of the cellulose. It is possible to obtain the delamination of the nanofibrils by overcoming the energy of the interfibrillar hydrogen bond. To avoid the reformation of the interfibrillar hydrogen bond and therefore the coalescence of the newly separated fibrils, the mechanical methods are generally carried out in aqueous media at low concentrations of cellulose ($< 5\% \, wt.$). The resulting cellulose particles show lower mechanical properties with a reduction in the degree of polymerization, crystallinity and aspect ratio (Belgacem, Bras *et al.* 2016). After a

mechanical treatment, filtration takes place to remove the cellulose fractions that have not been defibrillated. The fibers can be further subjected to a chemical method in order to remove the amorphous fraction or functionalize its surface (Martini A. *et al.* 2011).

The most used and effective mechanical methods are high pressure homogenization, refining and grinding. In this work, high pressure homogenization (HPO) was used.

The high-pressure homogenization is carried out through the use of a homogenizer (**Figure 3.3 a**) or a microfluidifier. In the case of the homogenizer, a slurry with a low cellulose concentration ($< 2\% \, wt.$) is passed through a thin gap between the homogenizer valve and an impact ring (**Figure 3.3 b**), subjecting the fibers to shear and impact forces that allow fibrillation. The main limitation of this technique is the high energy consumption, reaching up to $70 \frac{MWh}{t}$, which can however be reduced by making pre-treatments to $2 \frac{MWh}{t}$. Another disadvantage is due to the clogging of the machine in the case of very long fibers.

(a) (b)

Figure 3.3 (a) Homogenizer (LM10, Microfluidics USA) (b) Schematic representation of the homogenizer operation.

3.3 Pulp and wood CNF

After briefly explaining the characteristics of the treatments used, we now want to focus our attention on how the "pulp" and CNF are obtained. First, we started with a soft wood which has undergone a process of reduction in size in order to increase the surface area. This wood, after being reduced to powder, underwent a bleaching combined with an alkali treatment. This was subsequently treated with a TEMPO chemical treatment for 72 hours at 60 ° C, thus obtaining the so-called "pre-treated pulp". Finally, the treated celluloses were diluted prior to being disintegrated in a high shear fluid homogenizer at 1000 bar. To better understand the process, refer to **Figure 3.4**.

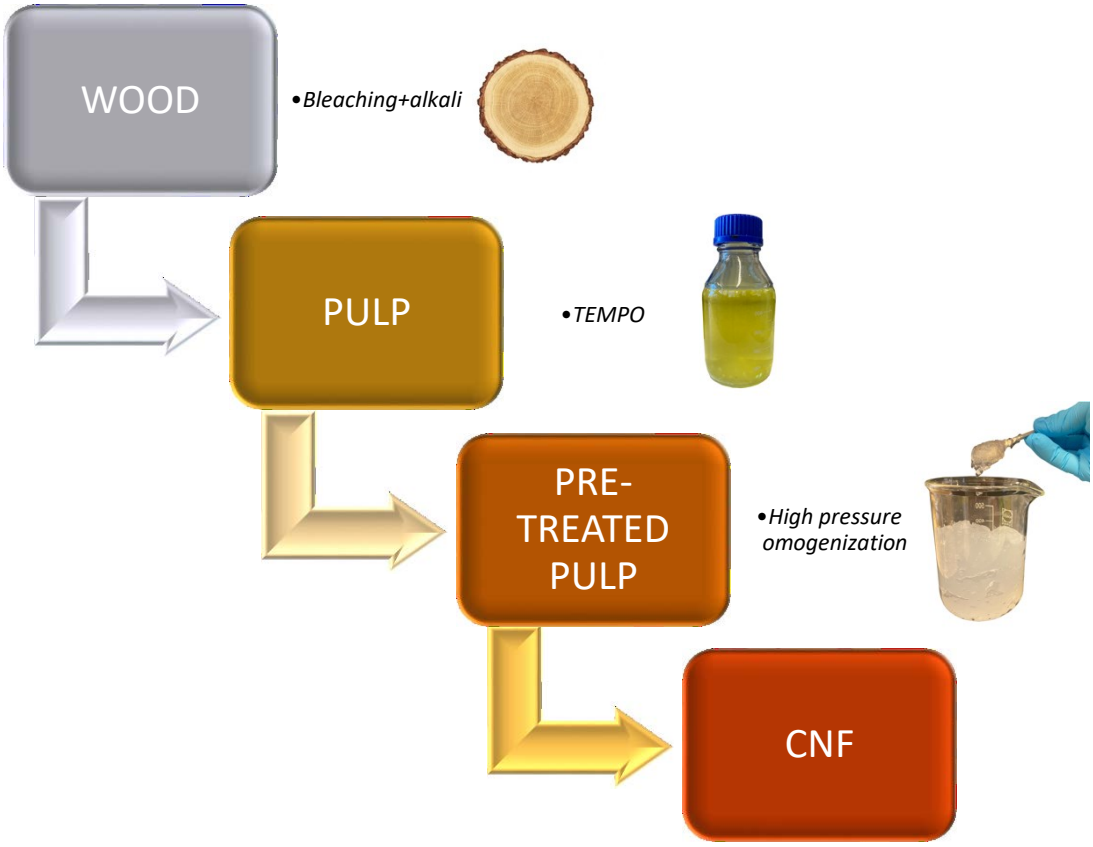

Figure 3.4 Illustration of how to obtain pulp and nanocellulose from wood.

Figure 3.5 shows the materials obtained after each single treatment starting from grinded wood up to nanofibrillated cellulose.

Wood powder *Pulp* *Pre-treated pulp* *Cellulose nanofibrillated*

Figure 3.5 Illustration of the material obtained after each treatment.

The resulting pulp was evaluated from the point of view of chemical composition and the results obtained are shown in **Table 3.1**.

	Cellulose (%wt.)	*Hemicellulose (%wt.)*	*Lignin (%wt.)*	*Inorganics (%wt.)*
PULP CNF	95.6	3.5	0.4	0.5

Table 3.1 Chemical composition of the pulp.

3.3.1 AFM characterization

AFM (*Veeco MultiMode scanning probe, Santa Barbara, USA*) was used in tapping mode to determine morphology and dimensions of the nanofibers. Antimony doped silicon cantilevers (*NCHV-A, Bruker*) were used with a spring constant of $42\,\frac{N}{m}$ and a nominal tip radius of 8 nm. Height responses (z-axis) were solely used for height-determination of the CNFs in order to avoid misleading dimensions due to tip broadening effects (x–y axes). Samples were prepared by depositing a drop of $0.0015\ \%wt$. Obtained micrographs were analyzed in the open-source software *Gwyddion* (Nečas and Klapetek *et al.* 2012). The micrographs were presented after image corrections comprising of mean plane subtraction and polynomial background removal.

AFM is a common technique for studying nanofibers morphology. The AFM height images of nanofibers from pulp are shown in **Figure 3.6.** From these images it is possible to see how the length of these nanofibers is quite short. This is mainly due to the fact that these nanofibers have not been subjected to the fibrillation process by means of high-pressure homogenization. It is very easy to estimate the length of these nanofibers as it is very easy to identify their extremities even if there are entanglements, albeit in limited quantities.

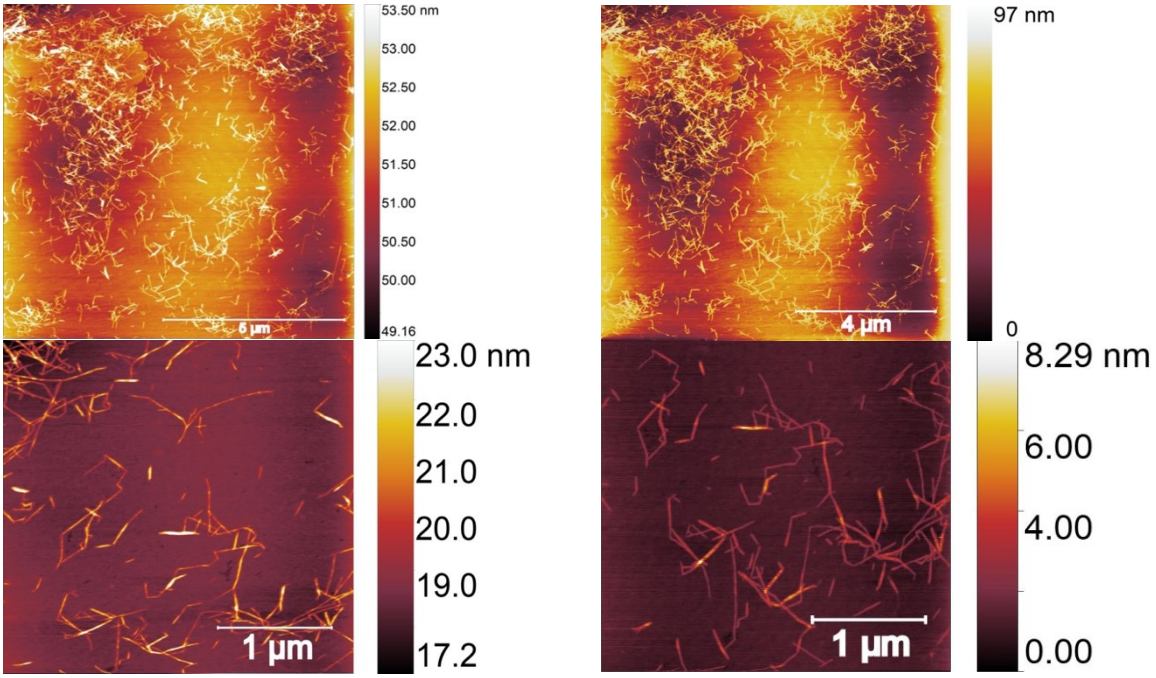

Figure 3.6 AFM images of pulp CNF.

The morphological analysis of the nanofibers was also performed for the nanocellulose obtained after mechanical HPO treatment. The images obtained are presented in **Figure 3.7**. It is evident that this mechanical treatment leads to the formation of a large quantity of entanglements and it is difficult to identify the extremities of a single nanofiber. In this case, the length of the CNF nanofibers is undoubtedly higher than the pulp nanofibers and this is clearly visible from the AFM images. This leads to a greater number of entanglements as previously highlighted with a consequent increase in viscosity. With the same concentration of the two samples, the difference

in viscosity was visually observed: the pulp sample appeared as a homogeneous solution with a density similar to water, while the CNF sample was very similar to a gelatinous compound.

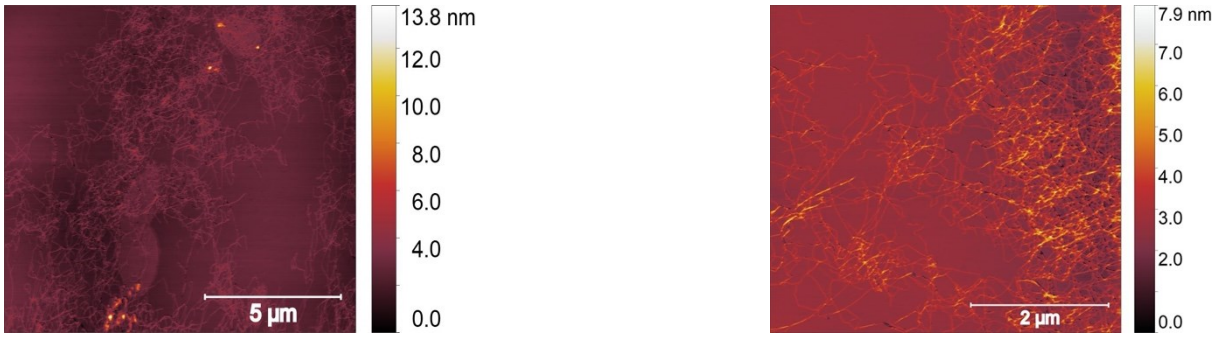

Figure 3.7 AFM images of wood CNF.

With AFM analysis it is possible to measure nanofibers height. The results obtained are represented in **Figure 3.8**: from this image it appears that fibrillation reduces the size of the nanofibers.

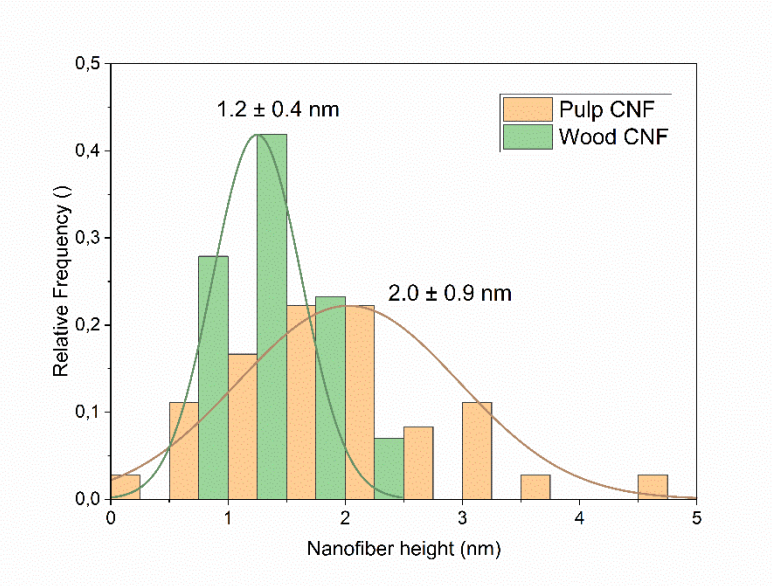

Figure 3.8 Size distribution of pulp and nanofibrillated cellulose.

Table 3.2 summarizes the treatments performed on the two samples together with the dimensions obtained by AFM analysis.

	Sample code	*Pre-treatment*	*Width (nm)*
PULP	PULP CNF	Alkali, bleaching	2.0 (0.9)
CELLULOSE NANOFIBRILLATED	WOOD CNF	Alkali, bleaching, TEMPO	1.2 (0.4)

Table 3.2 Summary of treatments and dimensions of different nanofibers. Standard deviations are shown in parentheses.

3.3.2 Tensile test

After the morphological characterization of the nanofibers, we now discuss the influence of fibrillation on hydrogels properties. These hydrogels have been prepared by the vacuum filtration method and the detailed procedure can be found in **Appendix A1**. These hydrogels were tested by uniaxial tensile test. The samples were obtained by using a pre-mold in order to get samples of identical shape: a rectangle (80 mm x 5.9 mm) with variable thickness. Hydrogels mechanical properties were tested using the *Shimatzu AG-X* (Japan) universal testing machine with a 1 kN load cell. The tests were performed with an extension rate of 2 mm / min and a gauge length of 20 mm.

Theoretically, the mechanical properties are closely related to the morphology of the nanofibers. It can be thought that the mechanical properties are indirect measures of the efficiency of the separation process. The shorter the fibers, the higher their aspect ratio. As a consequence, there are numerous entanglements and contact points that lead to the formation of a strong network. This is influenced by numerous factors that can affect the evaluation of treatments effectiveness; therefore, the results obtained must be interpreted. Another important issue is the presence of lignin and hemicellulose in the CNF pulp. Some studies (Lahtinen *et al.* 2014) have shown how the presence of hemicellulose greatly influences the fibrillation process, increasing its efficiency in a directly proportional way in relation to the amount present. The same thing applies to lignin that, however, has beneficial effects on the network for compression tests, while it negatively affects the stiffness and strength of the network under tensile test, thus lowering the mechanical properties. The hydrogels were tested with a solid content (SC) of 10.5%. SC is the ratio between the mass of the hydrogel in the dry state (m_{dry}) and that of the hydrogel in the wet (m_{wet}) state as expressed by the **Equation 3.2**.

$$SC(\%) = \frac{m_{dry}}{m_{wet}} \times 100$$

(3.2)

It is important to compare the mechanical properties of different hydrogels under the same testing conditions. Given the SC value, we compared two hydrogels with the same grammage in order to evaluate the contribution of the nanofibers to the mechanical resistance. **Figure 3.9** shows the graph of the tensile test performed on the CNF pulp and wood CNF hydrogels.

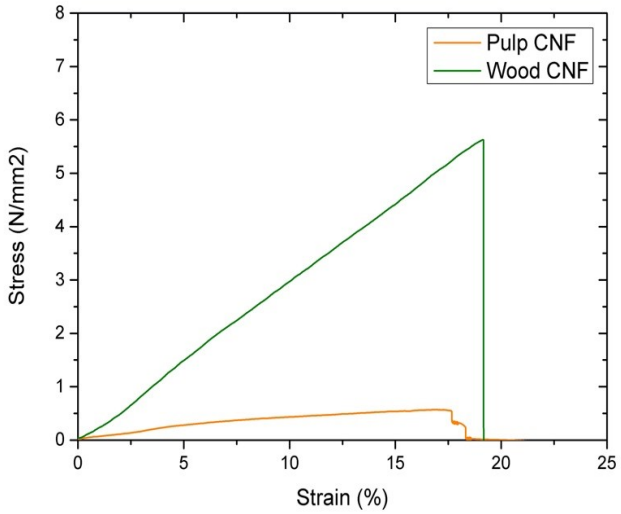

Figure 3.9 Tensile test of pulp and wood CNF.

Table 3.3 shows the grammage, Young's modulus, maximum elongation and ultimate tensile strength (UTS) values.

	Grammage $\left(g/m^2\right)$	*Young's modulus* (MPa)	*Max elongation* $(\%)$	*Ultimate tensile strength* (MPa)
PULP CNF	40.41	4.41 (1.56)	16.94 (4.87)	0.63 (1.29)
WOOD CNF	43.74	30.51 (2.18)	19.17 (1.84)	5.78 (0.77)

Table 3.3 Value of mechanical properties of pulp and wood CNF hydrogel. Standard deviations are shown in parentheses.

Certainly, the mechanical properties of wood CNF hydrogel are superior. During the tests on the CNF pulp, problems were also found due to easy evaporation of the absorbed water, thus

not allowing the achievement of the fixed SC. This is also the explanation for the high standard deviations. The two hydrogels are comparable to each other from the point of view of the maximum elongation, showing almost identical compartments.

The poor mechanical properties of cellulose pulp are essentially due to the presence of hemicellulose. It is known that this polysaccharide has a positive influence on the mechanical properties of the materials as it forms strong hydrogen bonds in the crystalline region of the nanofibers. However, in the presence of humidity, the hemicellulose plasticizes giving rise to a decrease of nanofibers cohesion. In our case, having tested the pulp CNF hydrogel with a content of about 90% by weight of water, it is evident that the values of Young's modulus and UTS are low due to poor cohesion and a weak network.

3.3.3 Swelling capacity

It has already been widely discussed how a nanocellulose-based material can absorb large amounts of water and promote wound healing. We therefore compared the two hydrogels from this point of view and evaluated their characteristics. Furthermore, attention was focused on assessing the efficiency of cellulose fibrillation and isolation and the treatments performed. In this regard, water absorption tests were carried out on the single hydrogel. After vacuum filtration, the hydrogel was allowed drying. Afterwards, the hydrogel was immersed at regular time intervals in a beaker containing distilled water at room temperature. Before checking its weight, excess water was carefully removed on the edges to not include it in the total weight. The test was considered concluded after reaching the plateau (**Figure 3.10**): this indicates that the maximum amount of water within the network is reached.

Three absorption tests were performed in order to have sufficient data to represent the statistical deviation over three replicates for each time point. The hydrogels were then observed for 2880 minutes to physically assess their aesthetic characteristics (**Figure 3.11)**. The surface of the hydrogel from the pulp is irregular and the sample is hard to handle, especially on the corners

that are critical points from which breakage can occurs. On the contrary, wood CNF hydrogel is very flexible and easy to handle with a very regular surface and without defects.

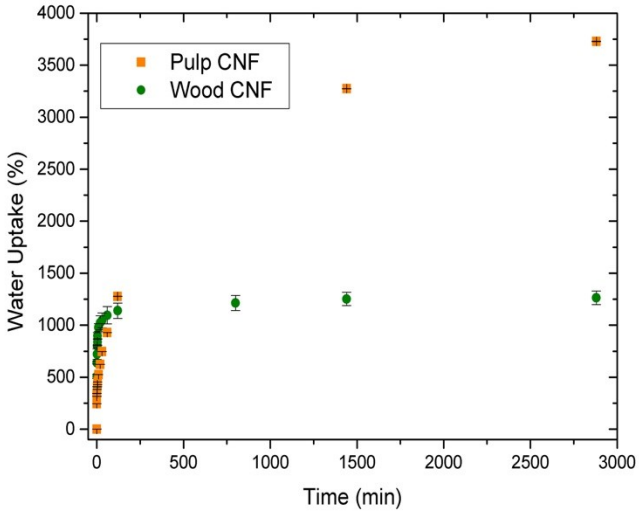

Figure 3.10 Swelling test of pulp and wood CNF.

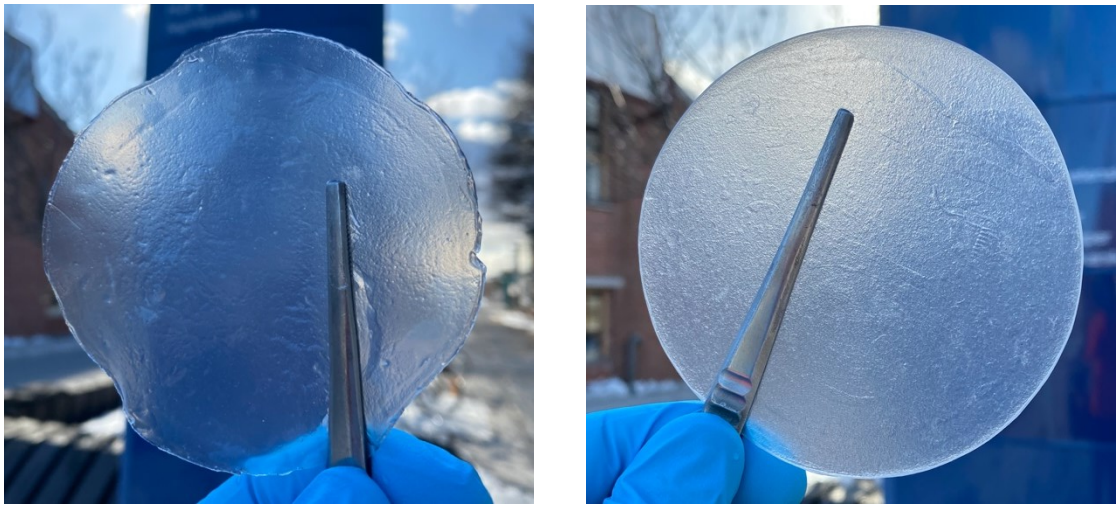

Figure 3.11 Pulp CNF hydrogel (left) and wood CNF hydrogel (right) after 2880 min in water.

The water absorbed by the hydrogel was calculated using **Equation 3.3** where $m_{hydrogel}$ is the mass of the hydrogel at time *t* and m_{dry} is the mass of the hydrogel in the dry state.

$$Water\ Uptake\ (\%) = \frac{m_{hydrogel} - m_{dry}}{m_{dry}} \times 100 \quad (3.3)$$

In addition to the water absorbed by the hydrogel, the solid content was calculated using **Equation 3.2.** The slope of the curve in the first 5 minutes is calculate using function "*slope*" on *Microsoft® Excel®*. Furthermore, the thicknesses of the hydrogels in the dry state (time *t*=0min) and in the state of maximum water absorption (time *t*=2880min) were calculated by using a thickness gauge with a precision of 0.001 mm. The results obtained from the curves are shown in **Table 3.4**.

	Grammage $\left(g/m^2\right)$	*Solid Content* $(\%wt.)$	*Slope WU* $\left(\%/min\right)$	*Thickness dry* (μm)	*Thickness wet* (μm)
PULP CNF	53.16	2.66 (0.44)	57.51 (9.17)	114.37 (2.61)	1078.84 (45.17)
WOOD CNF	54.26	7.41 (1.49)	133.49 (10.99)	80.50 (1.96)	655.37 (27.65)

Table 3.4 Results obtained from the swelling curves. Standard deviations are shown in parentheses.

As can be seen from the swelling curves, the CNF pulp hydrogel does not reach the plateau, but its water content increases linearly with time. This is basically due to the presence of hemicellulose as it is known that it greatly influences water absorption: the greater the amount of hemicellulose, the greater the swelling (Karaaslan *et al.* 2010). Given the same grammage, it can be seen that the slope of the wood CNF hydrogel is slightly greater. This means that initially this hydrogel quickly absorbs water; then it reaches a plateau after 20 minutes. Thickness increase by both hydrogels means that the absorption of water occurs in the direction parallel to the surface (Peppas *et al.* 2000) and not in the orthogonal direction.

3.4 Conclusions

In this chapter the treatments necessary to obtain and isolate cellulose nanofibers have been studied in detail. According to the different chemical or physical treatments, it is possible to obtain nanofibers with different chemical compositions and, consequently, with different mechanical properties. Two different types of differently treated wood-derived nanocellulose were compared. The pulp is the result of the chemical treatment using alkali and bleaching, while the nanofibrillated cellulose is due to the combination of the chemical treatments of alkali, bleaching

and TEMPO combined with the mechanical treatment of fibrillation by means of high-pressure homogenization. The two masterbatches obtained were subjected to AFM characterization, which highlighted how the TIME and the mechanical HPO treatment led to very long fibers with dimensions in the order of nanometers (fibrillated nanocellulose). As for the pulp, short fibers were obtained always in the range of nanometers. We then moved on to the production of the hydrogels through the use of the vacuum filtration technique. The hydrogels obtained were evaluated from the mechanical point of view. It has been found that nanofibers fibrillation leads to the formation of a strong and resistant network with excellent mechanical properties unlike the network formed by the short nanofibers derived from the pulp. Finally, water absorption capacities of the two hydrogels were evaluated. Amazing results have been found for both materials, which absorb more than 1000% of water by weight. The CNF hydrogel pulp showed better swelling behavior. This is undoubtedly due to the presence of hemicellulose and lignin, albeit in small quantities. On the other hand, it has been found that the presence of these two polysaccharides negatively affects the mechanical properties. Although the search for the optimal material for the production of dressing plasters must be based on a material capable of forming a network able to absorb liquids and keeping the wound as moist as possible, the mechanical properties cannot be neglected. Moreover, their weight in the final application has to be also considered. We are looking for a material able to withstand elongation, with a strong network capable of not breaking during the application or removal and, above all, able to adapt perfectly to the wound. It has been noted that both the investigated hydrogels possess this characteristic. Furthermore, both hydrogels are able to undergo several cycles of water absorption / desorption without changing their properties.

In conclusion, the material chosen for the continuation of the present study is the one derived from the fibrillation of the pulp (i.e., wood CNF): even though it requires further treatments that result in higher processing cost, it guarantees an excellent combination of mechanical properties and absorption capacity.

Chapter 4

Different hydrogels production strategies: Vacuum Filtration and Solvent Casting

4.1 Introduction

Hydrogels can be classified into physical or chemical hydrogels based on crosslinking mechanism. In this work the physical crosslinking mechanism was used. Physical bonds include chain entanglement, hydrogen bond, hydrophobic interaction and crystallite formation. These crosslinks may not be permanent, but they are sufficient to create a stable and insoluble 3D structure in an aqueous medium. Furthermore, this physical crosslink generates an irreversible structure. The hydrogel formed with this technique allows obtaining structures capable of absorbing large amounts of water as seen in **Chapter 3** (where attention was focused on studying the best combination of treatments in order to obtain cellulose nanofibers capable of generating hydrogels with high water absorption and good mechanical properties). These hydrogels were obtained using the vacuum filtration method. This method requires many precautions such as the correct leveling of the filter in order to generate flat structures and the correct vacuum degree. Furthermore, by using a paper filter as a filter membrane, considerable difficulties are encountered in removing the hydrogel from it, thus damaging the surface of the lattice and obtaining hydrogels with a grammage different from the theoretical one. Identical hydrogels can be obtained using extremely simple technique, the solvent casting. In this process, an aqueous solution containing the nanofibers is used to create 3D membranes. The theoretical principle underlying this technique is solvent (water) evaporation at room temperature, allowing the formation of a network by the nanofibers. In this case, the degree of physical crosslinking is weak compared to the use of vacuum. On the other hand, this method does not require particular precautions, it is easy to implement and allows obtaining hydrogels of the same grammage as the theoretical one. Despite these advantages, this process has extremely high lead times when compared with the vacuum method. In this project, a

method was sought to allow the production of hydrogels to be used as wound dressings capable of replacing bacterial cellulose. The production of cellulose, which follows the "bottom up" approach, depends on many factors such as culture medium, bacteria used, nitrogen and carbon sources and, more importantly, it requires a very long production time. Both methods allow the production of transparent hydrogels. This is a great feature with respect to the intended application, e.g. wound healing. In this way, it is easy to monitor all the phases of the healing process. **Figure 4.1** shows the two hydrogels obtained with the different methods.

Figure 4.1 Transparency of hydrogels produced by vacuum filtration (left) and solvent casting (right).

Therefore, in this chapter we compare the hydrogels produced by vacuum filtration method (see **Appendix A**) with those produced by the solvent casting technique (see **Appendix B**) in terms of water absorption capacity. The effect of absorption and desorption cycle and the effect of grammage on absorption will be assessed. Last but not least, the mechanical properties of the two hydrogels will be evaluated.

4.2. Tensile test

In this section the mechanical properties of the hydrogels produced by vacuum filtration and solvent casting are investigated. The mechanical properties were compared to check the presence of substantial differences in the network formation. Two hydrogels were compared: the first hydrogel (vacuum filtration) with a grammage of 23.27 $\left({}^{g}/_{m^2}\right)$ and the second (solvent casting) with a grammage of 19.97 $\left({}^{g}/_{m^2}\right)$. Both hydrogels have been tested with the same SC (10.5%) and under the same conditions under which they have to operate in real applications over the skin. Furthermore, we tried to test hydrogels with the same grammage but as already mentioned, vacuum filtration does not assure reproducible products. **Figure 4.2** shows the trend of the uniaxial tensile tests performed on the two samples: it is likely to acknowledge that the hydrogel produced by filtration has a higher elastic modulus. The elongation at break is, albeit slightly, higher for the solvent casting method.

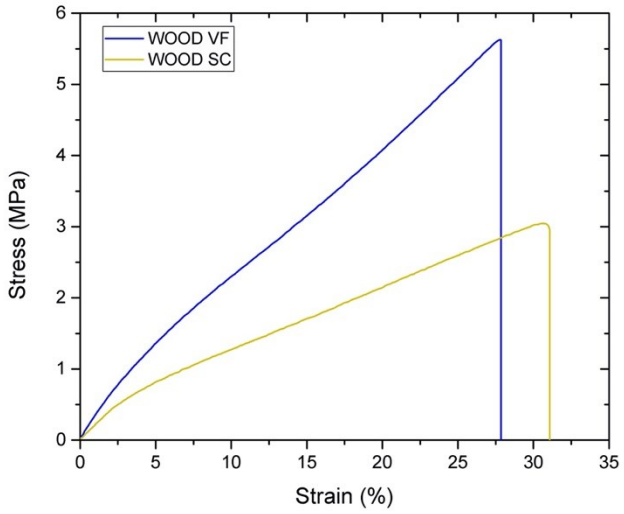

Figure 4.2 Stress vs. strain curves for the investigated hydrogels.

Table 4.1 shows the values of the mechanical properties calculated from the curves in **Figure 4.2**.

	Grammage $\left(g/m^2\right)$	*Young's modulus* (MPa)	*Max elongation* (%)	*Ultimate tensile strength* (MPa)
WOOD VF	23.27	22.75 (3.32)	27.88 (3.84)	5.78 (0.77)
WOOD SC	19.97	16.59 (0.75)	31.11 (1.99)	3.23 (1.13)

Table 4.1 Values of the mechanical properties measured by tensile tests of the investigated hydrogels. Standard deviations are shown in parentheses.

Using vacuum to create a hydrogel has significant influences on the mechanical properties: it is evident that a stronger network is created that resists traction better. On the other hand, by means of the solvent casting method, a network is obtained that shows larger elongation but lower tensile resistance.

In **Figure 4.3** it is possible to see the evolution of the tensile test for the hydrogel obtained by vacuum filtration. It is worthy to notice that the breaking of the sample occurs in the center of the sample.

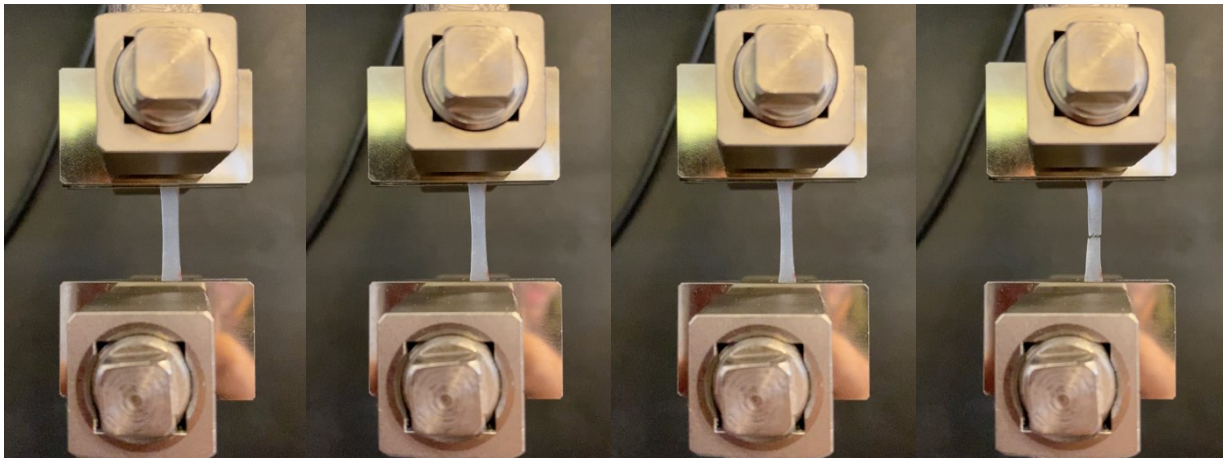

Figure 4.3 Tensile test of vacuum filtration sample.

4.3 Swelling capacity

After evaluating the mechanical properties, water absorption capacity was assessed. Both the methods used are extremely simple and, above all, they can easily be adapted for large-scale productions. Anyway, possible limitations of these methods have to be considered. For this reason, two important factors have been studied: the grammage and the effect of the absorption / desorption cycles.

4.3.1 Effect of grammage

First, we have to specify that the two methods for hydrogels production can result in different grammages. For example, it is very easy to obtain hydrogels with high grammage and thickness with the vacuum filtration method rather than the solvent casting method. For the solvent evaporation method, long times are required to produce hydrogels of large grammage. In addition, there is a practical factor to be considered. In this work PTFE Petri dishes were used. An attempt was made to evaporate the solvent in PE and glass Petri dishes, but it was impossible to remove the hydrogel without damaging the network. In this way, different hydrogels with different grammage were created and analyzed in terms of water absorption. **Table 4.2** and **Table 4.3** show the grammage of the hydrogels obtained by vacuum and solvent casting methods, respectively. Numerous hydrogels were produced using the solvent casting method and the maximum grammage was $20\ \left(^{g}/_{m^2}\right)$. A higher grammage involves the formation of hydrogel in a long time (about 2 weeks for grammage around $30\ \left(^{g}/_{m^2}\right)$), with a weak network and an irregular surface.

	Theoretical grammage $\left(^{g}/_{m^2}\right)$	*Real grammage* $\left(^{g}/_{m^2}\right)$
WOOD VF 10	10	9.91 (0.66)
WOOD VF 20	20	21.02 (0.33)

Table 4.2 Theoretical and real grammage values of hydrogels obtained by vacuum filtration. Standard deviations are shown in parentheses.

	Theoretical grammage $\left(g/m^2\right)$	*Real grammage* $\left(g/m^2\right)$
WOOD SC 10	10	11.16 (0.64)
WOOD SC 20	20	17.14 (1.11)

Table 4.3 Theoretical and real grammage values of hydrogels obtained by solvent casting. Standard deviations are shown in parentheses.

Both methods present a difference between theoretical and real grammage. Thus, hydrogels with similar grammage were compared in order to distinguish liquid absorption characteristics.

Figure 4.4 shows the trend of the absorption curves of the hydrogels obtained by filtration. It can be observed that the hydrogel containing the largest number of nanofibers by weight resulted in low water absorption values. The values obtained for the hydrogel with a low content of nanofibers are almost threefold compared to the one with a greater number of fibers. It can be hypothesized that increasing the grammage, the water absorption value also increases, assuming that the two variables are proportional. Actually, this is not the case. Both hydrogels reach the absorption plateau after about 120 minutes, showing the same behavior, albeit with different values.

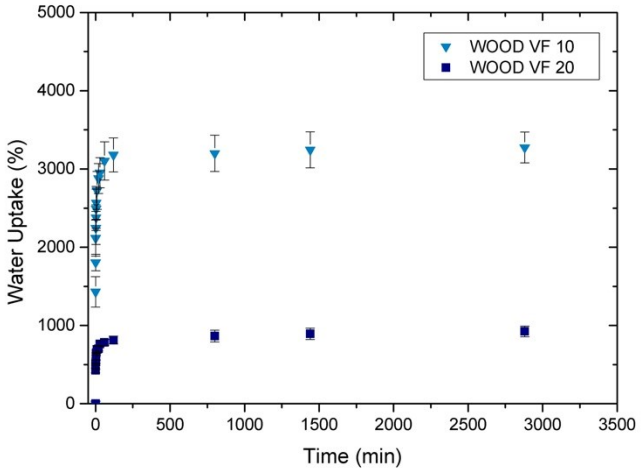

Figure 4.4 Absorption curves for the hydrogels produced with different grammage by vacuum filtration.

The hydrogels produced by solvent casting were also tested in a similar way. The results obtained are shown in **Figure 4.5**. Again, there is a noticeable difference between the two hydrogels. Although they exhibit the same trend as those produced by filtration, higher absorption values have been reached. Once again, the plateau is reached after around 120

minutes, without any further significant increases in water content. When compared, the two methods reveal the same behavior for hydrogels of different grammages. Both methods show how a hydrogel with lower grammage absorbs more water than those with higher grammage.

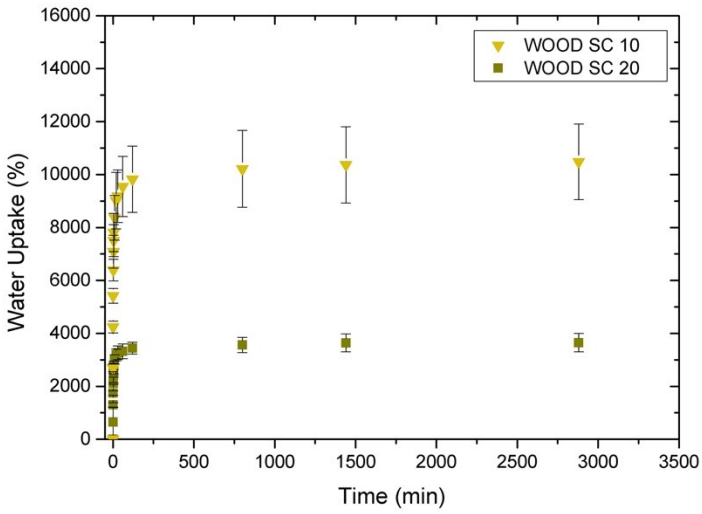

Figure 4.5 Absorption curves for the hydrogels produced with different grammage by solvent casting.

In **Figure 4.6** all four hydrogels are compared. It can be seen how the hydrogels produced by solvent evaporation absorb huge water amounts. Basically, this is due to the fact that vacuum filtration gives rise to a network in the form of nanofibers layers superimposed on each other. These layers, thanks to the force exerted by the vacuum, pack one by one creating intermolecular bonds (mainly hydrogen bonds). In the other case, there is no external force acting to compact layer upon layer and creating reciprocal links, so the network is weakly cross-linked. It can be stated that the vacuum filtration method creates a strongly cross-linked network, while the other one generates a weakly cross-linked lattice.

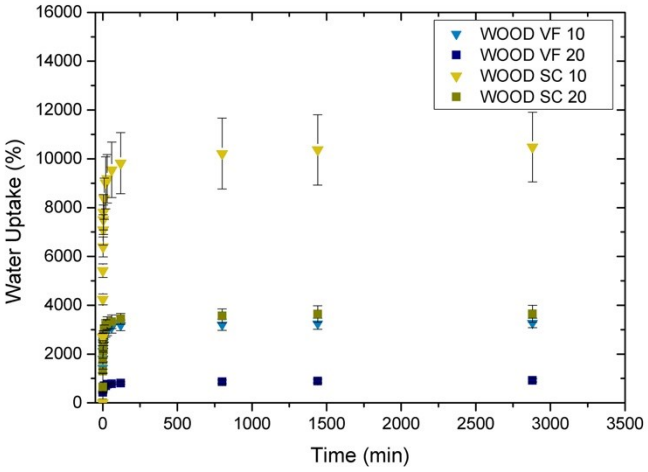

Figure 4.6 Absorption curves for the hydrogels produced with different grammage by vacuum filtration and solvent casting.

It was therefore said that hydrogels are made by superimposing layers of nanofibers one over the other. In **Chapter 5** some SEM images will be presented to prove it. These layers incorporate water inside, increasing the initial porosity. Here, we have measured the thickness of the four hydrogels in the dry state and in the state of maximum absorption (*2880 min* in water) using a thickness gauge (**Table 4.4**).

	Thickness dry (μm)	*Thickness wet* (μm)
WOOD VF 10	17.33 (4.97)	152.83 (12.64)
WOOD VF 20	27.46 (7.44)	136.71 (6.98)
WOOD SC 10	13.24 (0.84)	974.12 (56.47)
WOOD SC 20	17.52 (2.65)	603.80 (69.05)

Table 4.4 Thickness of the hydrogels obtained by vacuum filtration and solvent casting at different grammage. Standard deviations are shown in parentheses.

It has to be noticed that in the dry state, the hydrogels with higher grammage have a greater thickness. These results are in agreement with the hypothesis of constancy of the volume (being of the same size, by increasing nanofibers concentration the thickness increases). *WOOD VF 10* and *WOOD SC 10* both have higher values than the corresponding hydrogels obtained with the same method but with higher grammage. This outcome is in line with the absorption curve in **Figure 4.6**. It is worthy to highlight that the hydrogels produced by solvent casting show much

higher thickness values in the wet state than the others. As mentioned above, this is due to the weak physical cross-linking that occurs with this method. The slope of the curves was also compared in order to have an idea of the rate of water absorption by the four hydrogels. **Table 4.5** shows these results together with the SC value.

	Slope water uptake $\left(\%/_{min}\right)$	*Solid content* (%)
WOOD VF 10	333.13 (53.54)	2.97 (0.17)
WOOD VF 20	85.63 (8.99)	9.58 (0.58)
WOOD SC 10	1235.35 (146.29)	0.94 (0.63)
WOOD SC 20	447.44 (40.05)	2.82 (0.10)

Table 4.5 Slope water uptake and solid content value of the hydrogels with different grammage obtained by vacuum filtration and solvent casting. Standard deviations are shown in parentheses.

The results confirm the above mentioned assumption. It has to be noted that the absorption rate is higher for the lower grammage hydrogels in both methods. The solid content value also shows the same behavior, reaching excellent values for the WOOD SC 10 hydrogel. When the hydrogels have a low SC, they possess very poor mechanical properties.

4.3.2 Effect of swelling cycles

In this paragraph the results obtained from the water absorption / desorption cycles will be shown. During the normal swelling test, there was a progressive decrease in the amount of water absorbed. We therefore evaluated this behavior comparing the two production methods . In fact, both methods can be used on a large-scale production and the effect of swelling on the hydrogels with different cross-linkage extents is under evaluation. **Figure 4.7** and **Figure 4.8** show the different absorption curves for the different hydrogels with different grammages.

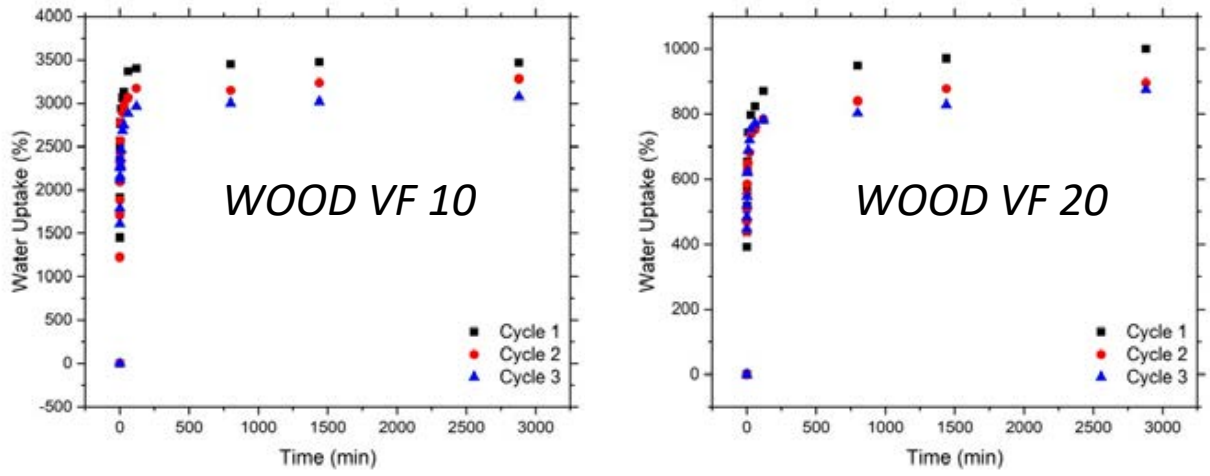

Figure 4.7 Cyclic swelling test for the hydrogels produced with different grammages by vacuum filtration.

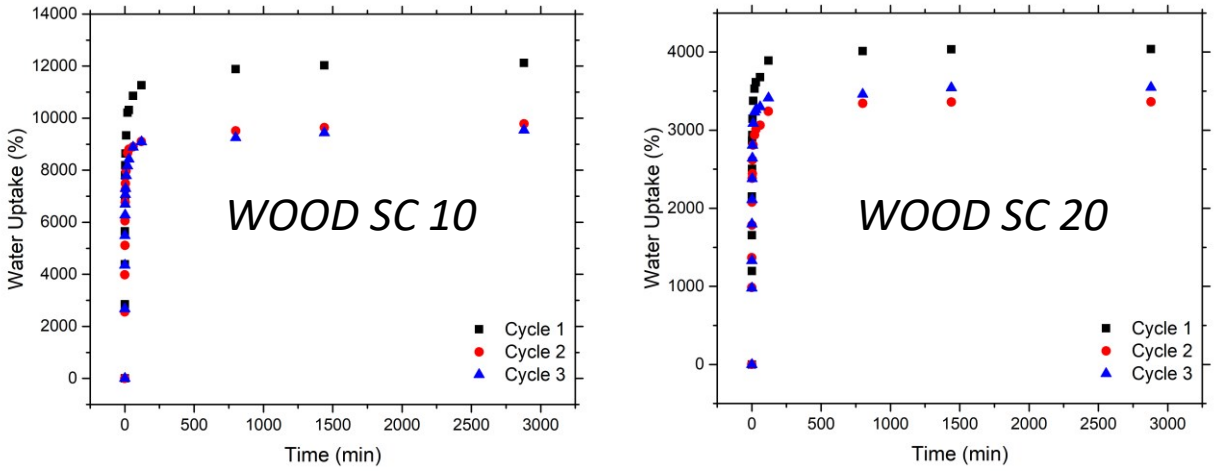

Figure 4.8 Cycle swelling test for the hydrogels produced with different grammages by solvent casting.

Only absorption curves are shown because it was not possible to accurately evaluate desorption curves (the necessary instrumentation was not available). The three absorption cycles are therefore reported even if it should not be forgotten that the first real effective cycle has not been evaluated as part of the hydrogel production (**Appendix A** and **Appendix B**). The difference in maximum absorption between the first and third cycle is slight. In the third cycle, the absorption does not show a drastic decrease of absorbed water.

It is evident that both methods show the same behavior during cyclic swelling. As cycles increase, water absorption decreases. This may be due to the fact that for these materials,

although they retain good shape-memory properties, the layers change slightly during the cycles, decreasing the porosity and consequently the absorption capacity. To better understand the physical structure of the hydrogels under investigation, the cross section of a hydrogel after immersion in water for 1440 minutes is shown in **Figure 4.9**. It is likely to see the presence of numerous layers superimposed on each other. Furthermore, the presence of porosity between these layers due to water absorption is evident.

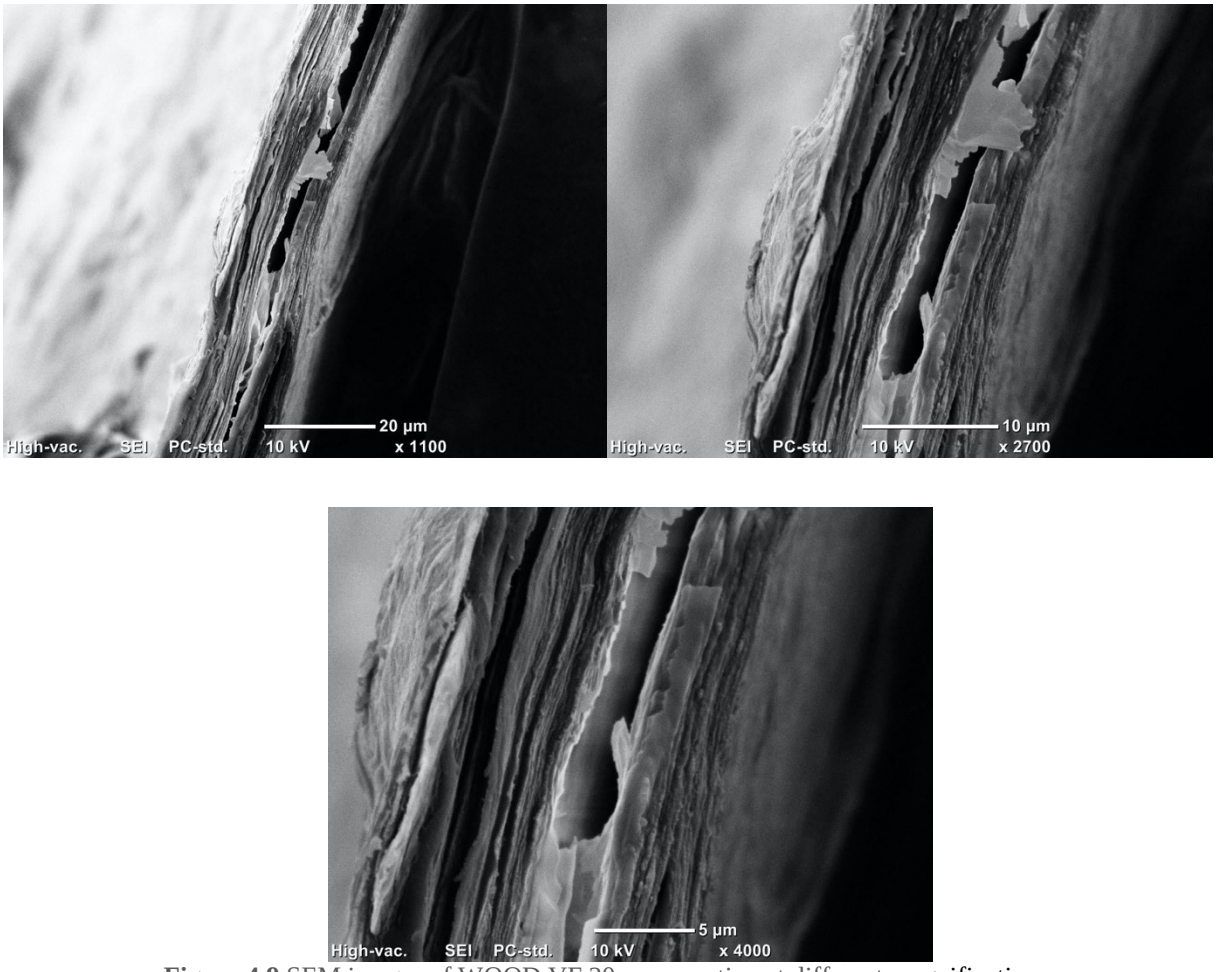

Figure 4.9 SEM images of WOOD VF 20 cross section at different magnifications.

4.4 Conclusions

Given the best combination of chemical and mechanical treatments, we moved on to evaluate the efficiency of two hydrogel production methods: a simpler one, based on solvent evaporation creating a network of cellulose nanofibers, and a second method, using vacuum filtration also creating a nanofibers network.

Both methods are easy to implement and allow obtaining a network based on the cross-linkage of layers superimposed on each other. This cross-linking is physical. We have seen how the two methods give rise to more or less strong cross-links. If vacuum is used, a strong network is created with good mechanical properties even if water absorption is limited due to the strong packing of the layers. On the contrary, the solvent casting method showed a remarkable water absorption due to the low packing of the layers. This is mainly due to not using any external force, other than gravity, to pack the layers. With this method, the properties are slightly lower than those obtained with hydrogels produced by the filtration method. The elongation value obtained with the solvent casting method should not be underestimated: it was higher than that obtained by using vacuum. The solvent casting method has a limitation in the production of high values grammage. Two different grammages were then evaluated for each method, reaching the maximum grammage with solvent casting, that is $20\,{}^{g}/_{m^2}$. Hydrogels produced with a low nanofibers concentration per surface showed much higher water absorption values than those characterized by a high nanofibers concentration by the same production method. If we compare the two low-grammage hydrogels, the water absorption for the solvent casting method is far superior. This method achieves very low SC values but the hydrogel network is easily breakable and difficult to model. Finally, no particular differences were highlighted regarding the absorption / desorption cycles. Both methods show a decrease in absorption with increasing cycles. This is due to the change in the morphology of the layers. Nevertheless, both methods produce hydrogels with good shape recovery during the absorption / desorption cycles.

In conclusion, both methods have shown excellent results. The vacuum filtration method generates hydrogels with good mechanical properties and allows obtaining hydrogels with high grammage. On the contrary, the solvent casting method has some limitations in the preparation of high grammage hydrogels. The two methods differ to each other with respect to the time required for

the realization of a hydrogel of the same grammage: for the solvent casting method, 7 days are required against 3 hours for the vacuum method. Both methods can be scaled up, but the productivity of the vacuum filtration is significantly higher. However, it should be noted that caution is required in removing the membrane used as a filter to prevent any damage to the network. On the other hand, the hydrogel obtained by solvent casting can be easily removed from the PTFE Petri dish.

For all these reasons, it is not possible to definitely identify the most effective method for the production of hydrogels intended for wound dressings comparable to a commercial product based on bacterial cellulose.

Further studies and characterizations of the hydrogels produced by vacuum filtration are necessary; the solvent casting method is not discarded yet, but a final decision is postponed to **Chapter 6**.

Chapter 5

Characterizations of hydrogel made by Vacuum Filtration

5.1 Introduction

In the previous chapter we identified the optimal conditions to produce nanocellulose hydrogels, which have to be comparable with bacterial cellulose hydrogels that are currently on the market. Although both hydrogels show excellent features, our attention was focused on their production by vacuum filtration. This method results in hydrogels of variable thickness and variable nanofibers concentration per surface area. In addition, the time required to produce a hydrogel was also considered. On average, the VF method ~~it~~ takes more than 5 hours to get a hydrogel ready to be characterized with different techniques. In particular, we carried out uniaxial tensile tests with hydrogels of different grammage to evaluate its effect on the mechanical properties. Furthermore, *VF* allows producing a hydrogel with the thickness necessary to perform a compression test. Considering the intended application, an absorption test in solution at different pH was carried out. It was evaluated whether these hydrogels were able to respond differently if immersed in solutions with different pH. If so, they may provide indications on the state of wound healing by inserting special detectors. Finally, the mechanism of water absorption by these hydrogels was elucidated by SEM images of their cross section after immersion in water at different time intervals.

5.2 Tensile test

Hydrogels produced by VF were tested by uniaxial tensile test. We evaluated the behavior of these hydrogels depending on their grammage. Table 5.1 shows the grammages used for this characterization. Hydrogels with a theoretical grammage ranging from 10 $^{g}/_{m^2}$ to 120 $^{g}/_{m^2}$ were characterized. These two extremes represent the minimum and the maximum grammages that were obtained with VF, respectively. With this test, we tried to find a correlation between the mechanical properties and the effect of the number of fibers per surface unit. The hydrogels were tested under the same conditions with a solid content of 10.5%.

	Theoretical grammage $\left(^{g}/_{m^2}\right)$	*Real grammage* $\left(^{g}/_{m^2}\right)$
WOOD VF 10	10	6.91 (0.66)
WOOD VF 20	20	21.02 (0.33)
WOOD VF 30	30	27.63 (0.79)
WOOD VF 50	50	52.73 (1.49)
WOOD VF 60	60	58.81 (3.47)
WOOD VF 80	80	78.58 (0.95)
WOOD VF 120	120	117.46 (3.47)

Table 5.1 Theoretical and real grammage values of hydrogels obtained by vacuum filtration. Standard deviations are in parentheses.

Theoretical and real values slightly differ. This difference is due to the method used for sample preparation. Using paper filters, part of the network that was created during filtration remained attached to the filter, consequently affecting the real grammage. Polymeric membranes were also tested, even if the results were identical. For hydrogels with a grammage higher than 50 $^{g}/_{m^2}$, removal from the filter was much easier. For the other hydrogels, it was necessary to pay attention and leave them in water for a longer time before removing the filter.

Figure 5.1 shows the trends of the tensile tests. It was not possible to test the *WOOD CNF 120* hydrogel because it was too thick. Due to its thickness, it was impossible to tighten the machine's clamps without damaging the sample.

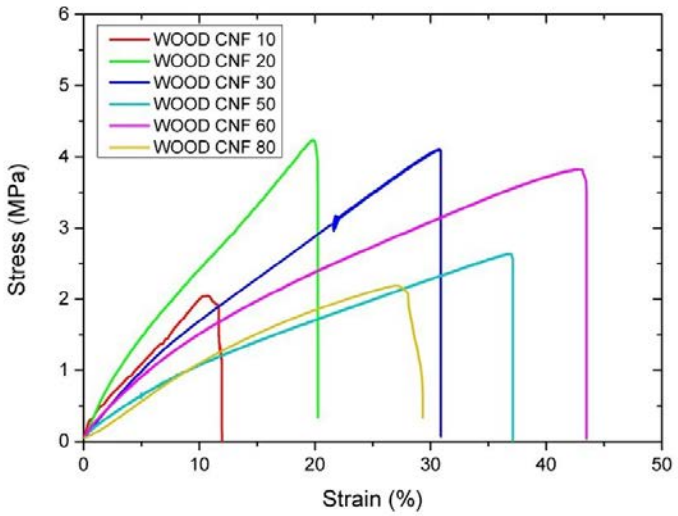

Figure 5.1 Stress vs. strain curves of hydrogels with different grammages.

The mechanical properties of these hydrogels would be expected to be linearly correlated to the number of fibers per unit area. Actually, this is not the case. **Figure 5.2** and **Figure 5.3** show the main mechanical parameters of these hydrogels.

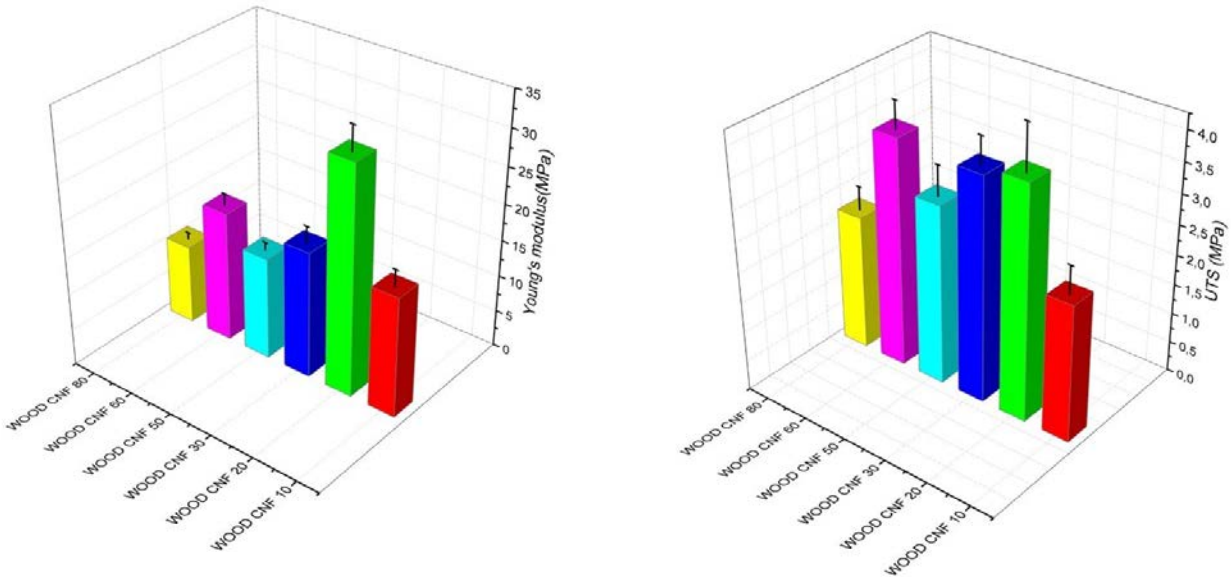

Figure 5.2 Young's modulus (left) and UTS (right) of hydrogels with different grammages.

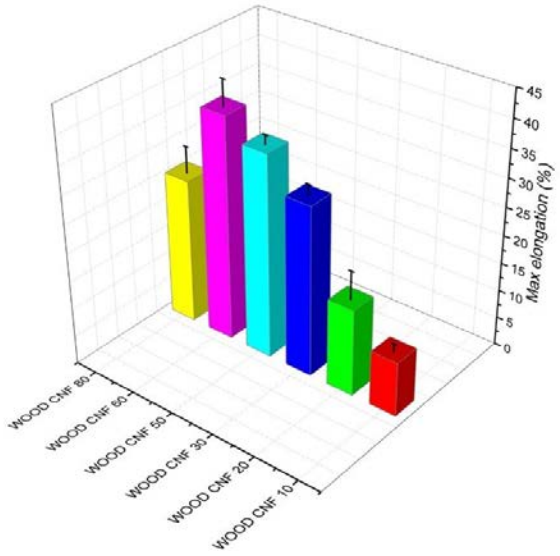

Figure 5.3 Max elongation of hydrogels with different grammages.

The hydrogel with the highest Young's modulus contains 20 grams of fiber per unit area. For the others hydrogels, the Young's modulus values are more or less the same. As for the UTS, the "best" samples reached values close to 4 MPa. Again, no clear correlation between grammage and maximum resistance before breaking is evident. However, this is not the case for the maximum elongation values, which seem proportional to grammage. The only value that differs is that of the *WOOD CNF 80* hydrogel. This may be due to the inaccuracy of the machine due to its high thickness. In general, results were satisfactory, with Young's modulus values ranging from 10 to 30 MPa under testing conditions similar to the operating ones.

5.3 Compression test

A compression test was also performed to further characterize the hydrogels. Also, in this case, we tried to simulate as closer as possible the working conditions of these hydrogels. Only high grammage hydrogels could be tested as they have an adequate thickness. Low grammage hydrogels, such as *WOOD CNF 10*, have a thickness of about 10 microns. It is therefore impossible to carry out compression tests on them. A normal compression test was carried out on the *WOOD CNF 80* sample. For the test, a square-shaped sample with a side of 5.74 mm and a thickness of 1.1

mm was used. The sample was characterized by a solid content of 11.5%. **Figure 5.4** shows the compression curve obtained and **Table 5.2** depicts the mechanical values obtained.

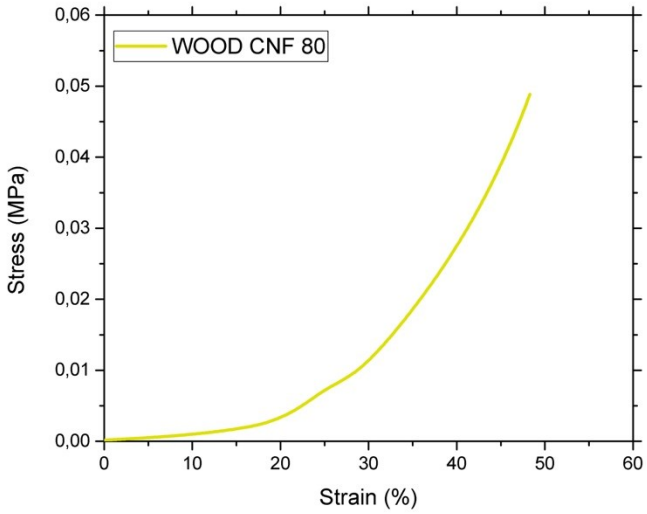

Figure 5.4 Compression curve from WOOD CNF 80.

	Compression modulus (KPa)	*Maximum compression* $(\%)$
WOOD SC 80	10.23 (0.55)	48.28 (2.67)

Table 5.2 Value of mechanical properties from the compression curve. Standard deviations are in parentheses.

With regard to the compression module, the results obtained are not satisfactory. The measured value is in the range of KPa. Viceversa, the maximum compression mean value is very good. Although not excellent, these results do not influence the excellent judgment on these hydrogels as the main properties are obtained from the tensile test. During the application on the wound, these hydrogels undergo mainly a tensile stress; therefore, the properties obtained from the tensile test are of great importance.

5.3.1 Cyclic compression: the effect of swelling

Compression tests were performed not to obtain quantitative data on the hydrogel but to show how swelling can affect the hydrogel network. In particular, we wanted to highlight how these hydrogels are able to recover their performances after compression cycles. To carry out this test, the *WOOD CNF 120* hydrogel was used as it has a high thickness. At first, the cyclic compression test was carried out without immersing the sample in water. The sample was

compressed once, then compressed again after a dwell time of 5 minutes. The sequence was repeated three times, in order to obtain three compression cycles (**Figure 5.5 a**). The second sample, always belonging to the same hydrogel, was subjected to the same test. Only one difference was present: after the compression cycle, instead of leaving the sample in air, it was immersed in water for 5 minutes. Also, in this case three compression cycles took place. The results of this test are shown in **Figure 5.5 b**.

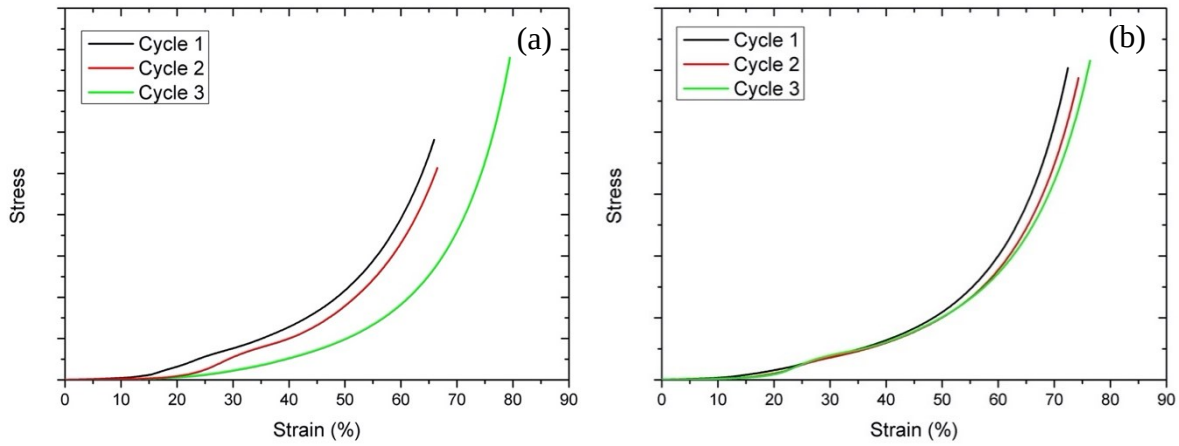

Figure 5.5 (a) Cyclic compression curves without swelling recovery. **(b)** Cyclic compression curves with swelling recovery.

It has to be noted that during the recovery with the swelling in the water, the network recovers the same properties, showing an almost identical behavior during the three cycles. On the other hand, there is a substantial difference in the cycles that do not include the recovery effect. This test gives a qualitative indication on how these hydrogels are able to recover part of their properties: they exhibit the same behavior after cyclic compression just by immersion in water for 5 minutes. Considering their application, it will be possible to apply them to the skin that has suffered an excoriation without changing their characteristics, considering that they can absorb a large amount of liquid thus remaining in a dry state.

5.4 Swelling test

It has been already mentioned that swelling is the characteristic that distinguishes these hydrogels. We want to briefly highlight the behavior of these hydrogels, prepared by the VF if they are immersed in water. In the previous chapter, it has been demonstrated that hydrogels can absorb

large amounts of water, increasing from two to three thousand times their weight. Moreover, in this section we want to evaluate if there is a correlation between the amount of fiber and the amount of water absorbed. Furthermore, the effect of the absorption / desorption cycles on the quantity of absorbed water will be evaluated.

5.4.1 Effect of grammage

These hydrogels are made up of layers superimposed on each other. Theoretically, the greater the number of fibers, the greater the number of layers. An increase in layers should correspond to an increase in the water absorbed by the hydrogels. To assess this issue, the hydrogels in **Table 5.1** were subjected to absorption tests by measuring the amount of water absorbed at regular intervals. The absorption curves are shown in **Figure 5.6**.

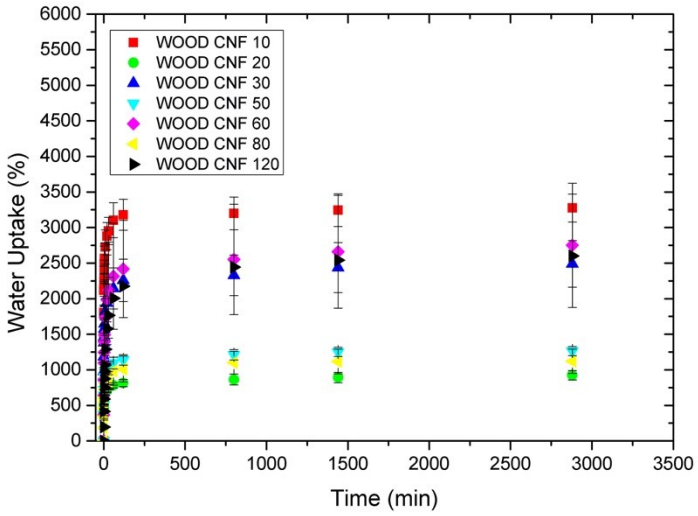

Figure 5.6 Absorption curves for hydrogels produced by vacuum filtration with different grammages.

It is evident that there is no relation between grammage and the quantity of absorbed water. The hydrogel that is able to absorb the largest amount of water is the one that contains the least amount of fiber: this evidence is in disagreement with the previously made hypothesis. To better evaluate the behavior, the solid content reached, and the water absorption speed were calculated for each hydrogel (**Table 5.3**).

	Solid content (%)	*Slope water uptake* $\left(\%/_{min}\right)$
WOOD VF 10	2.97 (0.17)	333.13
WOOD VF 20	9.58 (0.58)	85.62
WOOD VF 30	3.90 (0.48)	243.00
WOOD VF 50	7.41 (0.35)	133.49
WOOD VF 60	3.75 (2.19)	255.35
WOOD VF 80	8.30 (1.09)	117.57
WOOD VF 120	3.85 (3.47)	188.69

Table 5.3 Solid content and slope of the water uptake for the hydrogels. Standard deviations are shown in parentheses.

As for the solid content, it is possible to divide the behavior into two classes: hydrogels that have reached a solid content of around 10% and hydrogels that have reached a solid content of around 3%. The *WOOD CNF 20* hydrogel proved to be the worst both in terms of solid content and water absorption speed. Unlike the previous one, the *WOOD CNF 10* hydrogel exhibits a high absorption rate and reaches a solid content below 3% after being immersed for 2880 min in water (**Figure 5.7**).

Figure 5.7 WOOD CNF 10 during swelling absorption test.

5.4.2 Effect of swelling cycles

After the normal absorption cycle, each hydrogel was subjected to a desorption cycle and subsequently to a new absorption cycle. This test was carried out to evaluate how the absorption properties change with increasing absorption cycles. The behaviors obtained are shown in **Figure 5.8**.

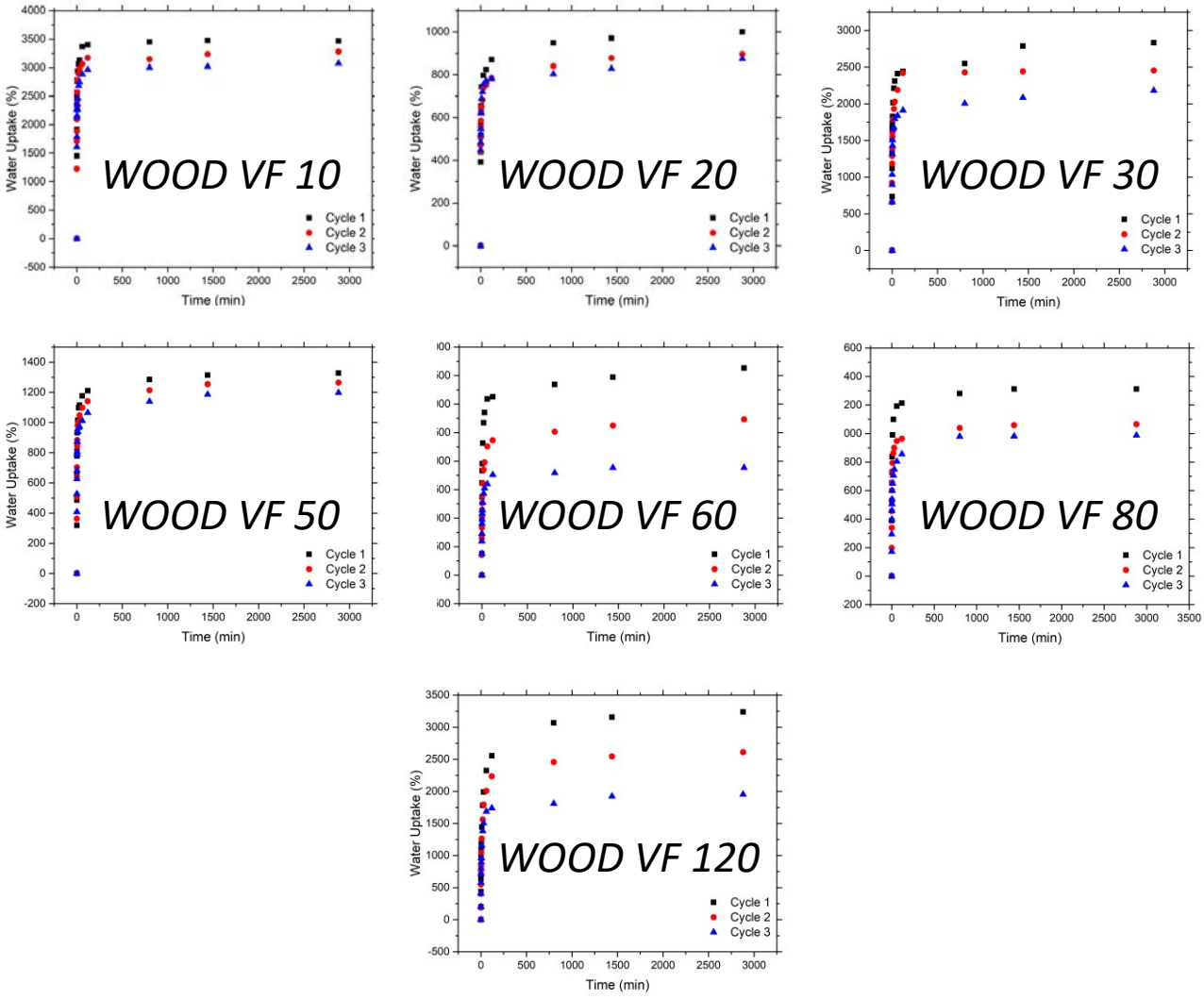

Figure 5.8 Cyclic swelling test for hydrogels produced by vacuum filtration with different grammages.

As already noted in the previous chapter (*4.3.2*), as the number of absorption / desorption cycles increases, the ability to absorb water decreases. A decrease in absorption appears as grammage increases. Probably during the absorption cycle the water evaporates and intermolecular bonds are created (such as hydrogen bond) which facilitate the packing of the network and the

reduction of its porosity. During the next absorption cycle, these intermolecular bonds make it difficult to separate two adjacent layers, thus negatively affecting further water absorption. It can be said that the network during the absorption / desorption cycles is constantly evolving. During these cycles, the physical crosslinking mechanism is more and more strengthened.

5.5 SEM characterization

To better understand how the absorption of these hydrogels occurs, a cross-sectional scan was performed using a scanning electron microscope (SEM). The JEOL JSM-IT300 (Tokyo, Japan) instrument was used to evaluate how water absorption affects the hydrogel network with an acceleration voltage of 15 kV. We used the *WOOD CNF 120* sample for this characterization because it had sufficient thickness to show the variation of the network during absorption. Images of hydrogel cross-sections with lower grammage will also be reported.

It was decided to acquire the SEM images of samples with three different solid content (SC) values. SC values of 20%, 10% and 3% were chosen. **Figure 5.9** shows the absorption curve of the high grammage hydrogel and the time-position in which the different solid content values were reached**.** After reaching the desired solid content, samples were cut and prepared as reported in **Appendix C**.

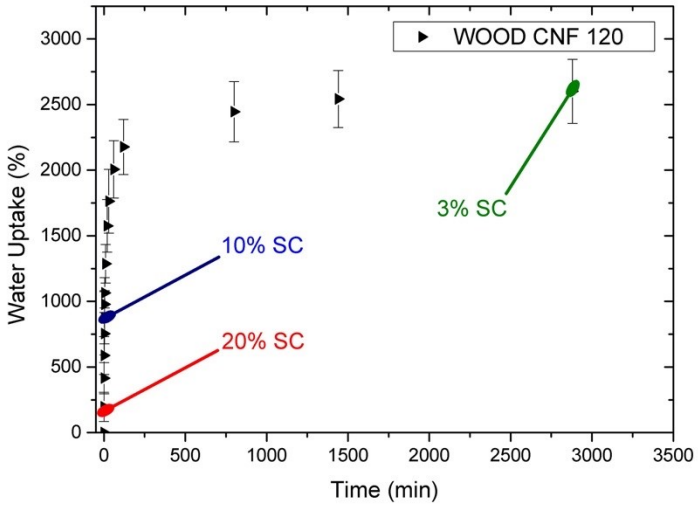

Figure 5.9 Position of the different solid contents in the absorption curve of the WOOD CNF 120 hydrogel.

The samples were analyzed with the SEM at different magnifications. The frames of the cross sections are shown in **Figure 5.10**, **Figure 5.11**, **Figure 5.12** and **Figure 5.13**.

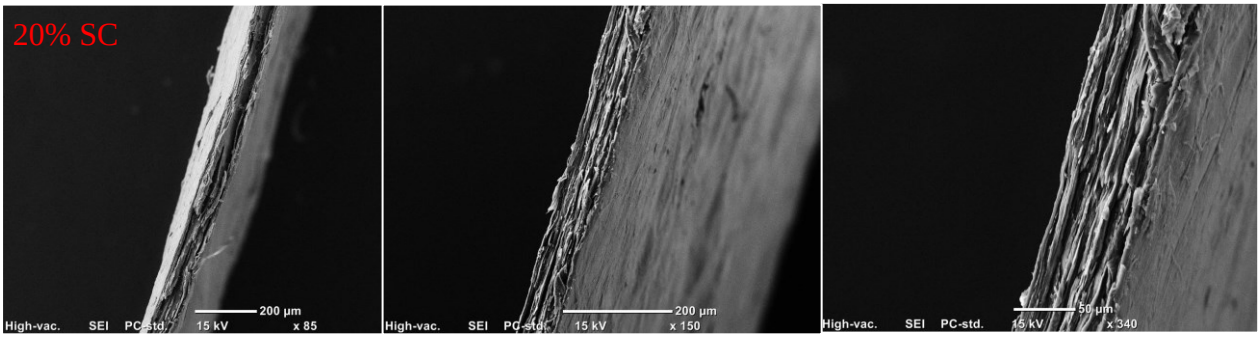

Figure 5.10 SEM frames of the cross section of the hydrogel with 20% solid content.

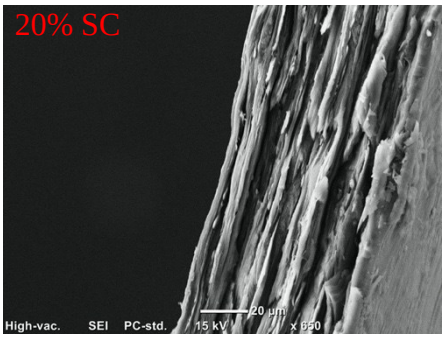

Figure 5.11 SEM frame of the cross section of the hydrogel with 20% solid content at high magnification.

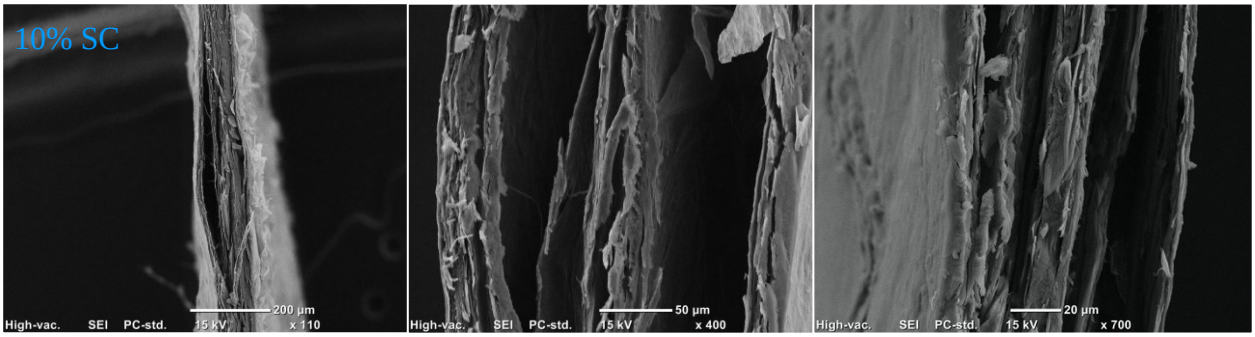

Figure 5.12 SEM frames of the cross section of the hydrogel with 10% solid content.

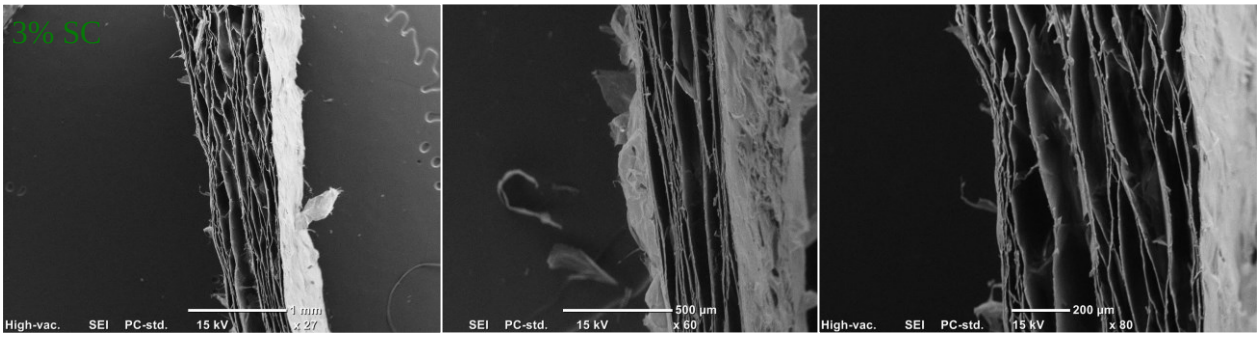

Figure 5.13 SEM frames of the cross section of the hydrogel with 3% solid content.

SEM images show that the hydrogels are composed of layers superimposed on each other. The network, as previously mentioned, is formed thanks to physical cross-linking. The strength of the cross-links can be different depending on the method used to produce the hydrogels. The vacuum, which is required to create these hydrogels, greatly affects the extent of the cross-links. The 20% SC is reached almost immediately after immersing the hydrogel for a few seconds in water. In this situation, from the SEM analysis the layers appear compact: there are few free spaces between the layers even but not excessive. **Figure 5.11** shows a high magnification frame in which the layers are compact. After about one minute of hydrogel immersion in water, 10% SC is reached. The absorbed liquid allows increasing the space among the layers. In this case, the hydrogel thickness increases as a result of water absorption. Referring to the reference scale in **Figure 5.12 (center)**, the porosity is of about 50 micrometers. Comparing the sample with 20% SC with one with 10% SC, there are a change in the network and an increase in porosity. To reach the minimum SC, i.e., 3%, the hydrogel has to be immersed in water for two days. Beyond this time point, the absorbed water is negligible, without variations in the SC: this limit is due to saturation. The porosity increase is marked and visible with a resolution of 1 mm. The structure seems to assume a beehive-like conformation. The layers are superimposed one on the top of the other as it was also highlighted in the previous cases. In this case, contact points between adjacent layers are evident. These are due to the effect of the physical cross-linking. Thus, open pores are formed, interconnected with each other, which facilitate the absorption of water in the direction parallel to the surface. From these images, it was possible to illustrate the physical structure of the network and to confirm that the absorption occurs in a direction orthogonal to the cross-section: indeed, the thickness of the hydrogel increases as the water absorbed increases.

5.6 Swelling test at different pH

Monitoring of severe injuries requires hospitalization once. This can be an inconvenient and expensive option for the patient. There are commercial devices that can monitor the wound healing process. These are based on the detection of pH changes and consequently on the change in concentration of inflammatory proteins, such as C-reactive protein (Pasche *et al*. 2008). Biomedical detection systems capable of performing this monitoring can be integrated into the dressing, especially to supervise skin grafts or ulcer treatments. The measurement can be continuous and performed using non-invasive biosensors. As the biosensor is integrated into the

wound, the measurement can also be carried out remotely. Thus, there is a rapid and effective control of the wound, avoiding the repeated and unnecessary removal of the dressing. In the background, it was said how wound healing goes through three main phases: inflammation, granulation and re-epithelialization. The first phase involves the release of high concentrations of growth factors and other proteins, which lead to the formation of a temporary matrix. In the second phase, there is the secretion of biological components in large quantities. In the third phase, there is the degradation of the provisional matrix and the beginning of the maturation phase. The composition and chemical and physical properties of the wound exudate change substantially along the three phases and are important for the proper healing progress. Several parameters have been identified that can provide information on the wound healing evolution. One of these is the pH of the exudates: it can indicate both the stage of healing and the presence of an infection. The pH of a normal wound during the healing phase is usually between 5.5 and 6.5. For a non-healing wound with inflammation, the pH assumes values greater than 6.5. Finally, the pH of the skin in the ripening phase is generally between 4.2 and 5.6 (Mostafalu *et al.* 2018). Hence, this justifies the application of these hydrogels as an innovative wound dressing. If the hydrogels produced with the nanocellulose extracted and isolated from the wood are able to show variations in absorption in relation to pH variations, then these possess the characteristics to enhance a better healing and monitor the wound. To this purpose, a hydrogel was prepared by the vacuum filtration method. A hydrogel with a grammage of 50 $^{g}/_{m^2}$ was prepared and seven identical samples were obtained by a rectangular cutter ($80mm \times 5.9mm$). Then absorption tests were carried out by varying the dipping solution. The following pH of the solutions were used:

- $pH = 4$
- $pH = 4.6$
- $pH = 5.4$
- $pH = 6.2$
- $pH = 7$
- $pH = 7.6$
- $pH > 8$

The results obtained are illustrated in **Figure 5.14**.

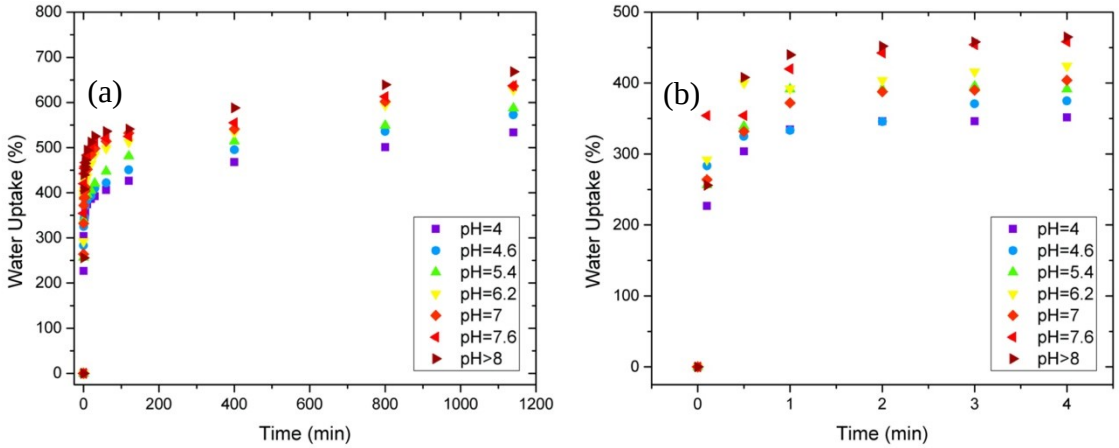

Figure 5.14 Complete absorption curves at different pH values **(a)** and trend of the first 5 minutes **(b).**

A slight variation in absorption can be seen as a function of pH. This confirms the hypothesis that these patches, if properly equipped with a sensor, are able to provide necessary information on the wound healing status. Further evidence can be obtained from the data shown in **Table 5.4**, in which the SC values after 1140 minutes and the absorption speed of the first part of the curve are illustrated.

	Solid content (%)	*Slope water uptake* $\left(\%/_{min}\right)$
pH=4	14.21 (0.96)	39.11 (3.651)
pH=4.6	14.03 (0.11)	40.03 (8.747)
pH=5.4	13.93 (3.47)	44.51 (2.624)
pH=6.2	13.76 (1.34)	48.39 (2.379)
pH=7	13.59 (1.72)	49.89 (5.004)
pH=7.6	13.56 (0.77)	52.80 (0.771)
pH>8	13.02 (0.01)	56.22 (0.016)

Table 5.4 Solid content and slope of the water uptake for the hydrogel at different pH value. Standard deviations are shown in parentheses.

The swelling behavior of the hydrogels is determined by the intrinsic parameters of the nanofibrillated cellulose and by the environmental conditions. After undergoing chemical treatments such as TEMPO, CNF possesses weak carboxylic groups. These functional groups dissociate completely at pH above 8 (Junka *et al*. 2013). During the absorption test, the electrostatic repulsion between the ionic charges ($-COO^-$) changed due to different pH values. At different pH, the dissociation and association of the carboxylic acid was modified. Consequently, this repulsion modification determined the difference in the swelling behavior of the hydrogels in the solutions at different pH.

Thickness is another, more easily measurable, parameter. During the absorption tests in solutions with different pH, thickness values after one hour of immersion were measured (**Figure 5.15**).

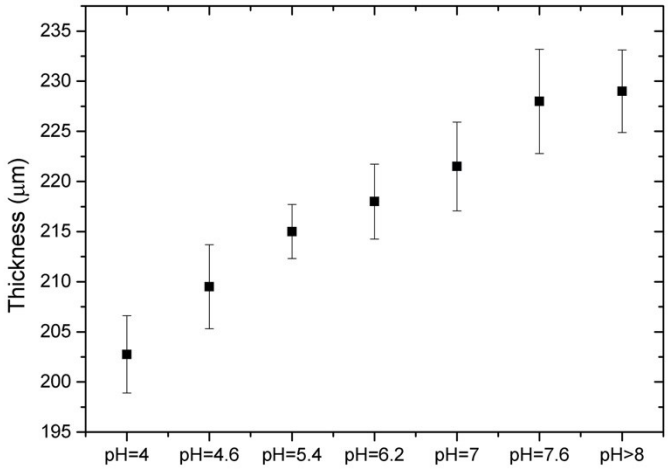

Figure 5.15 Thickness increase due to swelling in solutions with different pH.

It is very clear that the thickness increases as the pH increases. Unlike pH, the thickness is easily measurable and does not require long times.

Such pH-sensitive swelling behavior can result in a promising approach to fine-tune these dressings for the desired biomedical application, for example for the controlled release of bioactive agents or for monitoring wound healing processes.

5.7 Conclusions

In the previous chapters, we optimized the chemical and mechanical treatments to produce nanofibers capable of obtaining a network with good mechanical properties and excellent absorption capacity. Furthermore, the influence of the manufacturing method on mechanical properties and absorption capacity was evaluated. The production by VF is the most promising method, both in terms of production efficiency and mechanical and absorption characteristics. In this chapter, we focalized the study of the hydrogels produced with vacuum filtration. Hydrogels were tested with different quantities of nanofibers per unit area and it was found that there is no relation between the number of fibers and the mechanical properties. Only with regard to the maximum tensile elongation, there is a directly proportional relation with the grammage. High grammage hydrogels were tested to evaluate their compression properties. The results were not satisfactory as a compression modulus in the range of 10 kPa was reached. These results are of little importance when you think about the characteristics that innovative wound dressings might exhibit. The main feature they must possess is the adaptability to the area where they have to be placed and the maintenance of structural integrity under traction. In addition, during the compression tests, we studied whether these hydrogels can maintain their characteristics when loaded. The result was surprising: they can almost completely recover their integrity after immersion in water. It takes only 5 minutes to recover their characteristics. Therefore, these hydrogels can be used more times without any cyclic effect affecting their properties. The liquid-absorbing abilities of these hydrogels at different grammages were also assessed. As for the mechanical properties, there is no relation between the number of fibers and the amount of water absorbed. The hydrogel that showed the highest absorption was the one with the lowest number of fibers, reaching water absorbed values of about 3000% by weight. In this thesis, we want to replace bacterial cellulose hydrogels with hydrogels produced with nanocellulose derived from wood. The commercial bacterial cellulose hydrogels have a very low grammage. The results obtained from wood-derived nanocellulose low-grammage hydrogels are very interesting if we want to compare them with those from bacterial cellulose. This aspect will be discussed in the next chapter. The hydrogels produced during the cyclic swelling tests have shown that the absorption capacity decreases by increasing the absorption / desorption cycles. To better understand the behavior of the hydrogel network during water absorption, SEM images of hydrogles cross-section with different solid content were acquired. As the water absorbed increases, network porosity increases: this

causes the adjacent layers to be distanced from each other and consequently the thickness of the hydrogel increases. The thickness increase due to the water absorption is an intriguing issue: it has been hypothesized that it could produce hydrogels capable of monitoring the healing status of a wound. To this purpose, an absorption test was carried out in solutions with different pH. There was a difference in absorption due to different pH values. In addition to the variation in absorption, the thickness is also different. Therefore, by incorporating biosensors into the hydrogels, it is possible to assess the state of healing of the wound by keeping it constantly monitored without removing the dressing.

In conclusion, we are really satisfied with the results obtained both with regard the mechanical properties and the absorption characteristics, and the different hydrogels behavior in solution. Due to the sum of their features, the hydrogels have the potential to replace the bacterial cellulose-based wound dressings commercial products. In order to check their effectiveness and safety, the hydrogels have to be tested in vitro and in vivo before moving toward an approved commercial product.

Chapter 6

Hydrogels with low grammage: Wood CNF by Vacuum Filtration, Wood CNF by Solvent Casting and Bacterial Cellulose

6.1 Introduction

The main objective of this investigation is the replacement of bacterial cellulose with nanocellulose from wood for wound dressings. Bacterial cellulose has excellent mechanical and liquid absorption properties. It is also biocompatible and environmentally friendly, and it is already marketed as a wound dressing. There are numerous companies, such as *S_2Medical AB©*, which produce patches based on bacterial cellulose. These hydrogels are characterized by low grammage. For this reason, low grammage hydrogels are considered in this chapter. For the comparison, hydrogels produced with the solvent casting method and with the vacuum filtration method were used. With the first method, low grammage hydrogels are easy achievable. On the other hand, the production of hydrogels with a grammage similar to BC produced by vacuum filtration is more problematic. The hydrogels were compared from the point of view of the mechanical properties and absorption capacity. As we have previously seen, these characteristics are necessary to decrease the healing time of a wound. We tested the three hydrogels in terms of absorption capacity both in water and in a Bovine Serum Albumin (BSA) solution. This is because the BSA ~~solution~~ can mimic blood plasma. The presence of possible differences in water absorption and hydrogels behavior in BSA solution was checked, too. To conclude the study, the hydrogels produced with wood-derived nanocellulose and the hydrogels from bacterial cellulose (already on the market and

used as a reference) were characterized by X-rays and thermogravimetric analysis. **Table 6.1** shows the grammage values of the nanofibrillated cellulose hydrogels produced by solvent casting and VF and the bacterial cellulose as reference.

	Grammage $\left(g/m^2\right)$
WOOD CNF SC	8.17 (0.11)
WOOD CNF VF	7.94 (-)
*BC**	7.39 (0.40)

*commercial reference

Table 6.1 Grammage values of hydrogels used in this chapter. Standard deviations are in parentheses.

6.2 X-ray diffraction

The XRD characterization was carried out by PAN analytical Empyrean X-ray diffractometer (Almelo, The Netherlands) with the sample in the dry state. The operation voltage and current were 40 kV and 35 mA, respectively. The range of diffraction intensity was recorded at $2\theta = 5° - 40°$. The wavelength radiation was $\lambda = 0.154\ nm$. The crystallinity index (CI) was measured by using a Segal's method (Segal *et al.* 1959). For the calculation of the CI, we refer to the **Equation 6.4**,

$$CI = \left[\frac{(I_{002} - I_{am})}{I_{002}}\right] \times 100 \tag{6.4}$$

where I_{002} is the intensity of the crystalline peak and I_{am} refers to the intensity of the amorphous peak. The crystalline content was calculated by Derby Scherer's equation (**Equation 6.5**)

$$D(nm) = \frac{k \cdot \lambda}{\beta \cdot \cos \vartheta}$$

where k is the form factor (0.89) and β is FWHM (*Full Width Half Maximum*) of maximum intensity (I_{002}) in radiant. The XRD patterns of hydrogels from nanofibrillated cellulose and bacterial cellulose are shown in **Figure 6.1**.

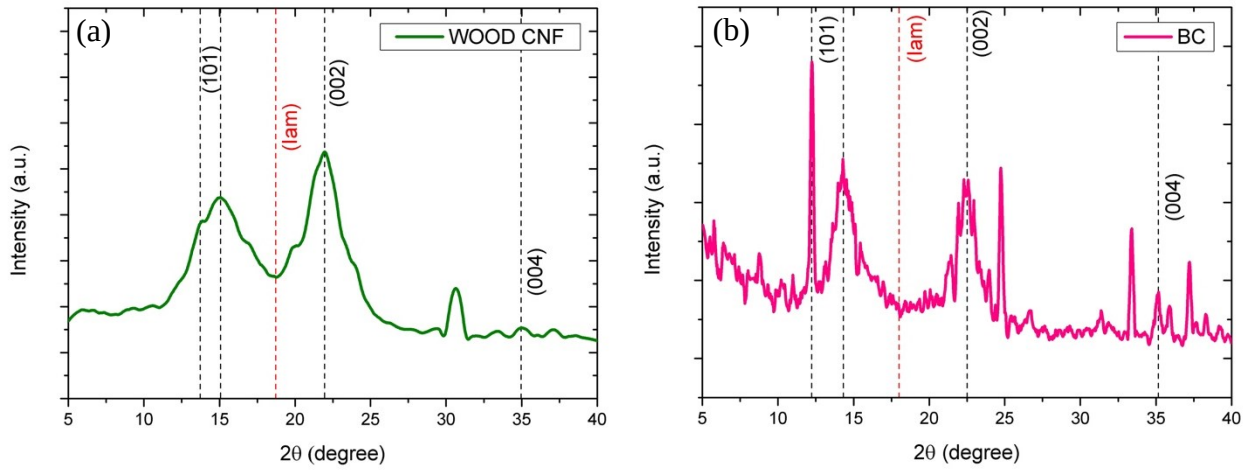

Figure 6.1 XRD patterns of WOOD CNF (a) and Bacterial Cellulose (b). Peaks are indicated by vertical dashed lines.

In both patterns the peaks corresponding to I_{002} are outlined and evident.

For *WOOD CNF* the cellulose, XRD diffraction patterns were recorded at $2\theta = 14.99°, 21.94°\ and\ 35.09°$, which are the characteristic peaks for the cellulose corresponding to the lattice planes 101, 002 and 004 (**Figure 6.1 a**) (Bano *et al.* 2017). The major crystalline peak was observed at 21.94°, and it confirms the presence of crystalline cellulose.

For bacterial cellulose, there are two peaks at $2\theta = 22.6°\ and\ 14.3°$, which indicate the crystal structure of cellulose type I. This result is due to the presence of intra and inter-molecular hydrogen bonds occurring in the cellulose through hydroxyl group that can trigger the formation of crystal order in the cellulose as reported by Sunil (Sunil *et al.* 2000). The results in terms of CI and D are reported in **Table 6.2.**

	CI (%)	*D* (nm)
WOOD CNF	59.83	2.63
BC	76.21	5.12

Table 6.1 Crystallinity index (CI) and crystalline size (D) from XRD analyses.

Bacterial cellulose has crystallinity higher than that of the nanocellulose from wood. The mechanical and thermal properties of nanocellulose depend on the crystalline characteristics. The influence of the difference in crystallinity between the hydrogels will be presented in the following paragraphs and its effects on the mechanical and thermal properties will be presented.

6.3 Thermogravimetric analysis

Thermogravimetric Analysis (TGA) is used to characterize materials intended for various environmental, biomedical, pharmaceutical, and petrochemical applications. In TGA, the mass (weight increases or decreases) of a substance is monitored as a function of temperature or time. Changes in physical and chemical properties of the material are measured as a function of increasing temperature (with constant heating rate) or as a function of time (with constant temperature and / or constant mass loss). Thermal stability of wood nanocellulose and bacterial cellulose hydrogels were investigated using the TA Instruments TGA-Q500 (New Castle, USA) (**Figure 6.2**). The analyses were performed at a heating rate of 10 °C/min from room temperature to 900 °C in a nitrogen atmosphere.

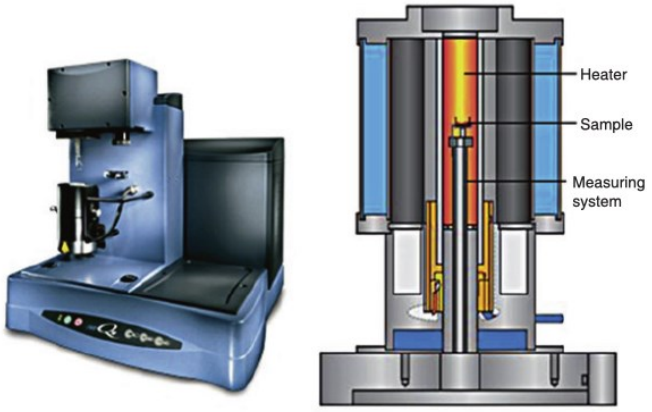

Figure 6.2 Thermogravimetric analyzer and its schematic diagram.

Typical TG and DTG curves for *WOOD CNF* and *BC* are shown in **Figures 6.3** and **6.4**.

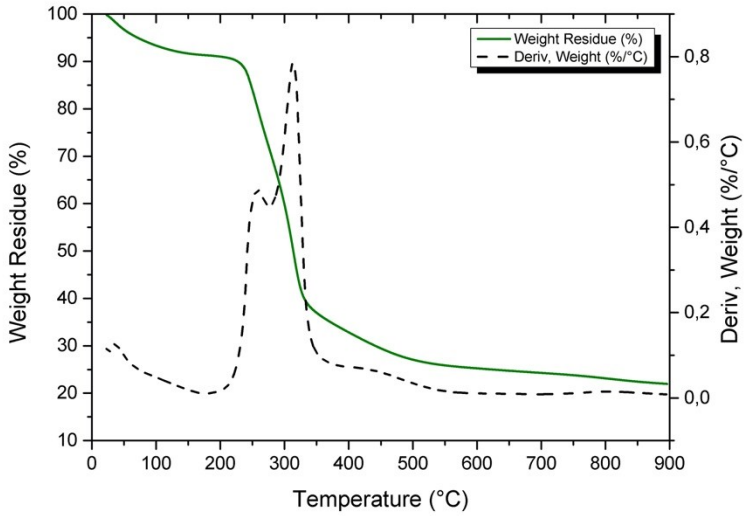

Figure 6.3 TG and DTG curves for WOOD CNF.

For the *WOOD CNF* sample, three stages of thermal degradation in the form of weight loss were observed. An initial steady-state decrease in weight till 150 °C is due to the evaporation of water. A sudden weight loss in the second stage between 200 and 380 °C is due to cellulose depolymerization. The final stage of rapid depolymerization of carbon residues occurred after 380 °C. In the central area, one can observe the appearance of a peak in the DTG curve: this peak-shoulder may be in principle assigned to the cellulose-hemicellulose, partially overlapping with lignin. As reported in a study (Li *et al.* 2004), under ordinary heating rate the hemicellulose pyrolysis is complete under 350 °C, cellulose pyrolysis between 250 °C and 500 °C, and lignin pyrolysis slowly spreads almost all the pyrolysis temperature range even over 500 °C and no sharp weight loss peak appears. The lignin is relatively more thermally stable than hemicellulose and cellulose. This confirms that, even if pre-treatments and mechanical and chemical treatments were carried out to extract and isolate cellulose nanofibers, completely pure cellulose was not achieved.

An initial weight loss of 10% was observed below 100 °C, and after that, no decomposition was recorded till 200 °C. Thus, TGA confirms the thermal stability of isolated cellulose and the presence of hemicellulose and extractives. Approximately 56% of the weight was lost by drying at 220-350 °C. A linear region of weight loss arose from 328-350 °C, which is the major characteristic thermal property of cellulose (Li *et al.* 2004).

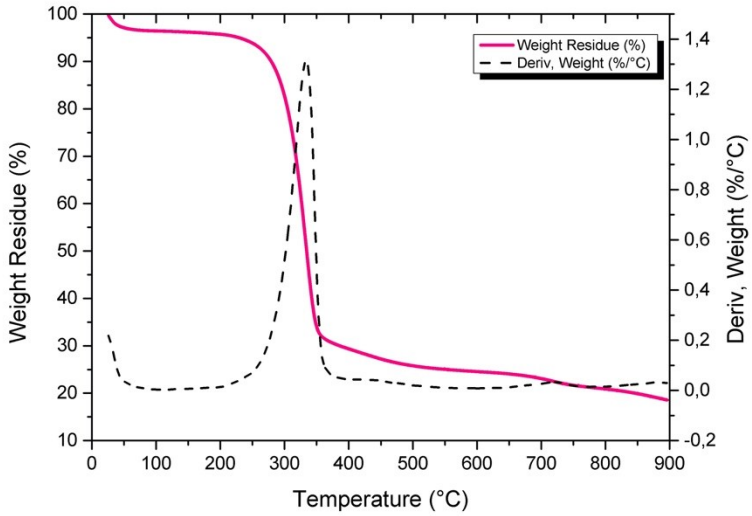

Figure 6.4 TG and DTG curves for BC.

For the BC sample, the change in weight loss can be classified into two different regions. From room temperature to 230 ° C, the weight loss was due to water evaporation. From 230 ° C to 400 ° C, the change in weight loss was due to organic decomposition. Physically adsorbed and hydrogen bond linked water molecules can be lost in the first stage. Initially, in the first phase, a weight loss of 5% was found due to water evaporation. During the next phase, a high weight loss was found with an approximate level of around 66%. It is worthy noticing that the substantial difference with respect to the main sample is the presence of a peak only in the DTG. This is due to the fact that there are no other polysaccharides present, such as hemicellulose or lignin, but cellulose.

6.4 Tensile test

Tensile tests were performed on two hydrogels: *WOOD CNF VF* and *BC*. The low grammage hydrogel produced with the solvent casting method is not included in this characterization because it broke during the pre-tensioning step performed to calibrate the sample. This, once again low grammage hydrogels produced by this method have poor mechanical properties. On the other hand, the mechanical properties are still good for hydrogels produced with this method when the quantity of fibers is greater than 10 g per square meter.

The tensile curves obtained from the commercial bacterial cellulose (reference) and the nanocellulose hydrogel from wood are shown in **Figure 6.5**.

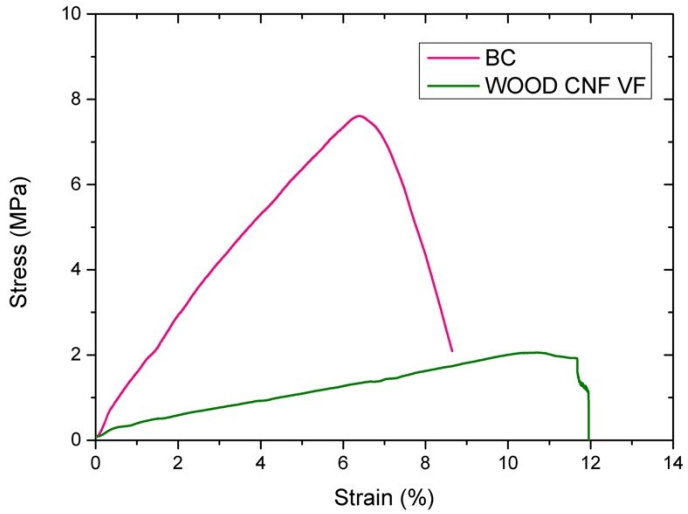

Figure 6.4 Stress vs. strain curves for BC and WOOD CNF VF hydrogels.

The best two curves obtained from the uniaxial tensile test are shown. **Table 6.2** shows the values of the most significant mechanical parameters calculated from the curves.

	Young's modulus (MPa)	*Max elongation* $(\%)$	*Ultimate tensile strength* (MPa)
WOOD CNF VF	16.46 (2.10)	9.65 (1.07)	2.28 (0.43)
BC	116.64 (11.06)	6.57 (0.22)	9.59 (0.31)

Table 6.2 Values of the mechanical parameters measured by tensile tests on the investigated hydrogels. Standard deviations are in parentheses.

Bacterial cellulose has excellent properties: its elastic modulus is five folds higher than that of the hydrogel produced by VF. Furthermore, the UTS of cellulose produced by bacteria is significantly larger than the nanocellulose hydrogel from wood. The elongation at break is less than 10% for both hydrogels, although the elongation of *WOOD CNF VF* is slightly better. Mechanical properties are influenced by the crystallinity of the considered material. In this case, the bacterial cellulose has a higher value than the cellulose extracted from wood. However, the mechanical superiority of BC cannot be attributed solely to differences in crystallinity. The structure of the network of the two hydrogels is extremely different: the BC is formed by the intertwining of

nanofibers secreted by bacteria (**Figure 6.5**), while the nanocellulose extracted from wood is the result of the superposition of layers formed by nanofibers and linked together by physical cross-linking. The microfibrillar structure of BC is responsible for most of its properties such as high tensile strength and high crystallinity index (Mohite *et al.* 2018).

Finally, the two samples showed that there is a non-linear stress vs. strain relation, indicating that some breakage occurs within the fiber network upon loading (e.g., bond break, fiber pull).

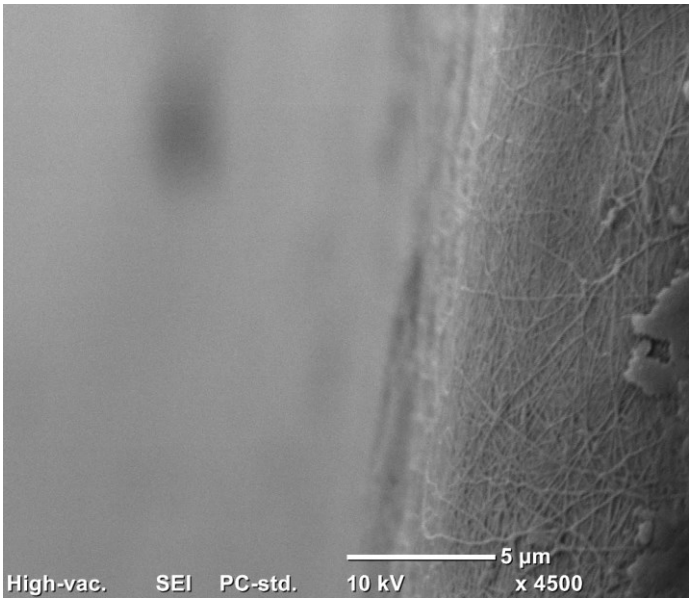

Figure 6.5 SEM of the section of the surface of the bacterial cellulose hydrogel used as reference (*S_2Medical AB*©).

Despite these considerations, the results obtained from the characterization of the bacterial cellulose substitute are satisfactory. Bacterial cellulose is known to have mechanical properties superior to plant-derived nanocellulose (Pogorelova *et al.* 2020). The hydrogels produced in this work are intended for wound dressing and their mechanical properties are sufficient to perform this function.

6.5 Swelling capacity

In this paragraph we compare the three hydrogels shown in **Table 6.1** in terms of liquid absorption capacity. The absorption of these hydrogels both in water and in BSA solution is evaluated.

6.5.1 Swelling at low grammage

In this section the water absorption of the hydrogels is evaluated and compared with that of the commercial bacterial cellulose product. Hydrogels have an extremely low grammage but they can absorb large quantities of water. **Figure 6.6** shows the absorption curves of the different hydrogels.

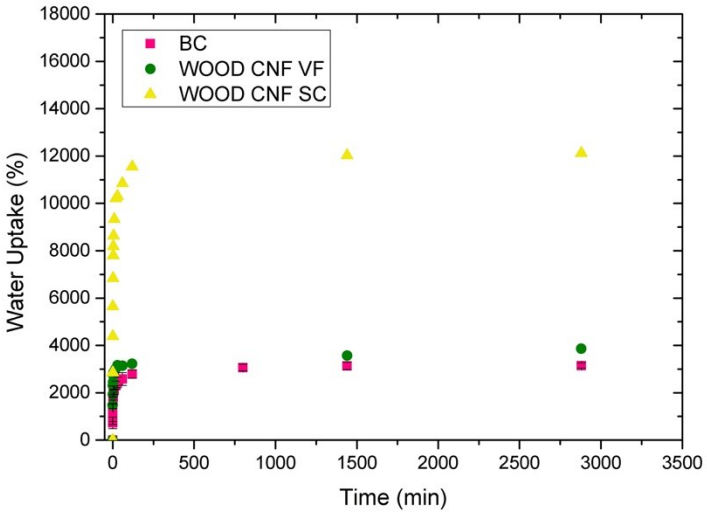

Figure 6.6 Water absorption curves for the WOOD CNF hydrogels and BC hydrogel with low grammages.

The solid content values from the absorption curves are shown in **Table 6.3**.

	Grammage $\left(g/m^2\right)$	*Solid content* $(\%\ wt.)$
BC	7.39 (0.40)	3.08 (0.10)
WOOD CNF VF	7.94 (-)	2.72 (-)
WOOD CNF SC	8.17 (0.11)	0.81 (0.15)

Table 6.3 Solid content reached during water absorption. Standard deviations are in parentheses.

In water, the hydrogels produced by solvent evaporation show exceptional absorption up to values of 12 000% of incorporated water by weight. It was also highlighted that, by slightly decreasing the grammage, it is possible to reach values of 18 000% of water uptake. However, these hydrogels can be easily broken due to the low resistance of the network. After 2 days of immersion in water, they reach a solid content of less than 1% proving to have a great affinity for water. With regard to the hydrogels produced with the VF method and the commercial reference (bacterial cellulose), an identical behavior is shown. The similar solid content values after 2880 minutes of immersion confirm that they have the same behavior when immersed in water. This result is of considerable importance as it has been possible to produce hydrogels capable of competing with commercial products. Furthermore, these hydrogels have a lower production cost and are more easily reproducible. Dehydration speed is another point in favor of our hydrogels. If compared with bacterial cellulose, it results that the WOOD CNF VF and WOOD CNF SC hydrogels take 36-48 hours for complete dehydration, while bacterial cellulose takes about 4-6 hours to reach the dry state.

6.5.2 Swelling on Bovine Serum Albumin

After testing all the hydrogels in water, it was decided to study the absorption behavior in a liquid that mimics the wound environment. It was decided to use a BSA solution with a concentration of 5% wt.

In the laboratory context, albumin is found under the name of serum albumin (SA, Serum albumin) and it is used as a reagent in various biochemical processes. SA is, in fact, albumin (i.e., a type of globular protein) that is found in the blood of vertebrates, or rather, more specifically, is found in the fraction of blood called serum. Albumin is a plasma protein produced by liver cells and commonly found in blood plasma. Albumin is the most abundant protein in the blood: moreover, SA is the main vehicle for other substances and biomolecules transported through the blood. Albumin, in fact, can function as a plasma carrier towards various hydrophobic steroid hormones to which it can bind due to a non-specific bond and, again, it can

act as a transport protein for fatty acids and even drugs. The absorption curves of the three different hydrogels in the BSA solution are shown in **Figure 6.6**.

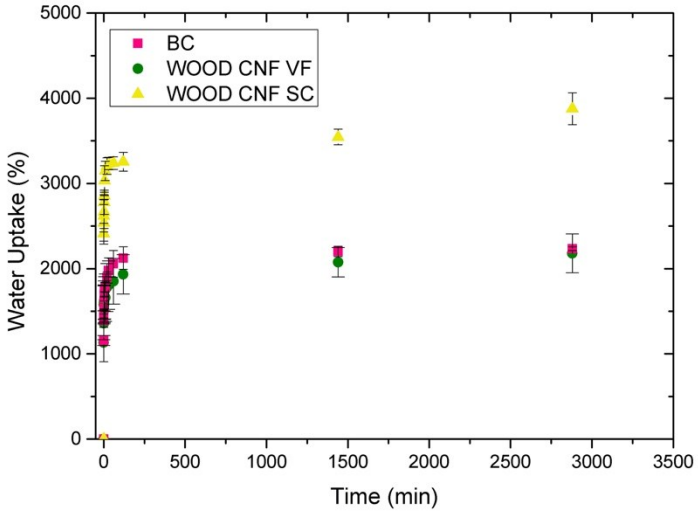

Figure 6.6 Absorption curves for the WOOD CNF hydrogels and BC hydrogel with low grammages in BSA solution.

The solid content values from the absorption curves are shown in **Table 6.4**.

	Grammage $\left(g/m^2\right)$	*Solid content* $(\%\ wt.)$
BC	7.39 (0.40)	4.28 (0.04)
WOOD CNF VF	7.94 (-)	4.41 (0.43)
WOOD CNF SC	8.17 (0.11)	3.55 (0.24)

Table 6.4 Solid content reached during BSA absorption. Standard deviations are in parentheses.

In this case, the absorption trend measured in water was maintained. In particular, the WOOD CNF SC has shown a greater absorption than the other two hydrogels even if the difference in the absorbed solution is much lower. Once again, bacterial cellulose and WOOD CNF VF have the same absorption curve, confirming previous absorption tests. Therefore, there is no change in the absorption behavior: changing the solvent, the trend remains the same with different values. In general, there is a good response from the hydrogels even if they are immersed in the

BSA solution that tries to mimic the wound environment as much as possible. **Figure 6.7** and **6.8** show the hydrogels during the absorption tests.

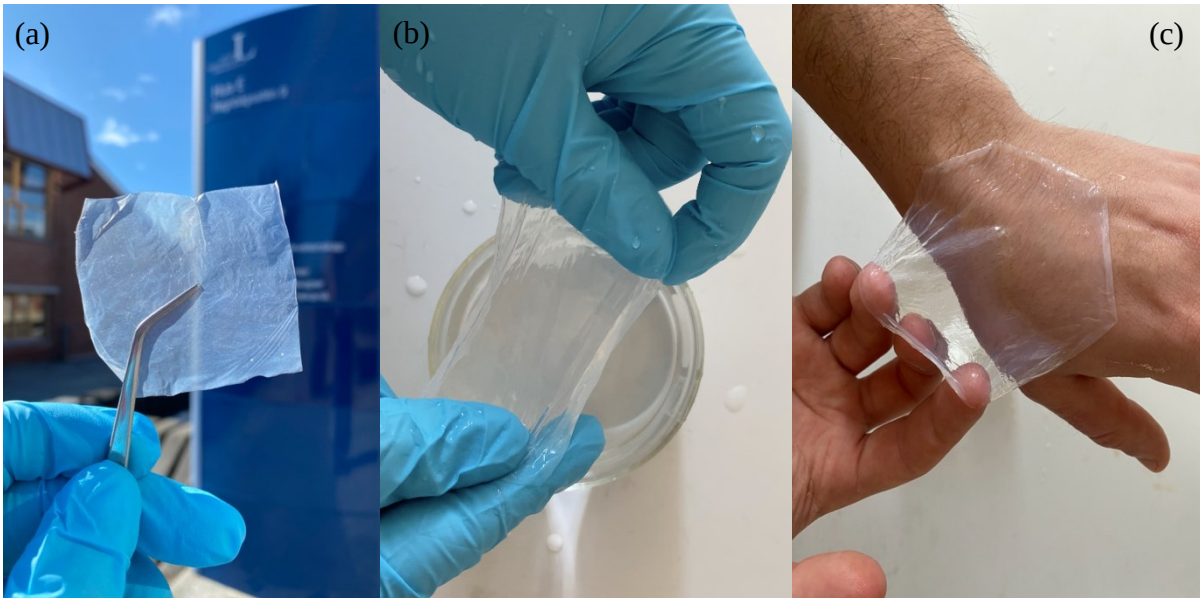

Figure 6.7 Bacterial cellulose hydrogel in dry state **(a)** and during swelling test **(b)(c)**.

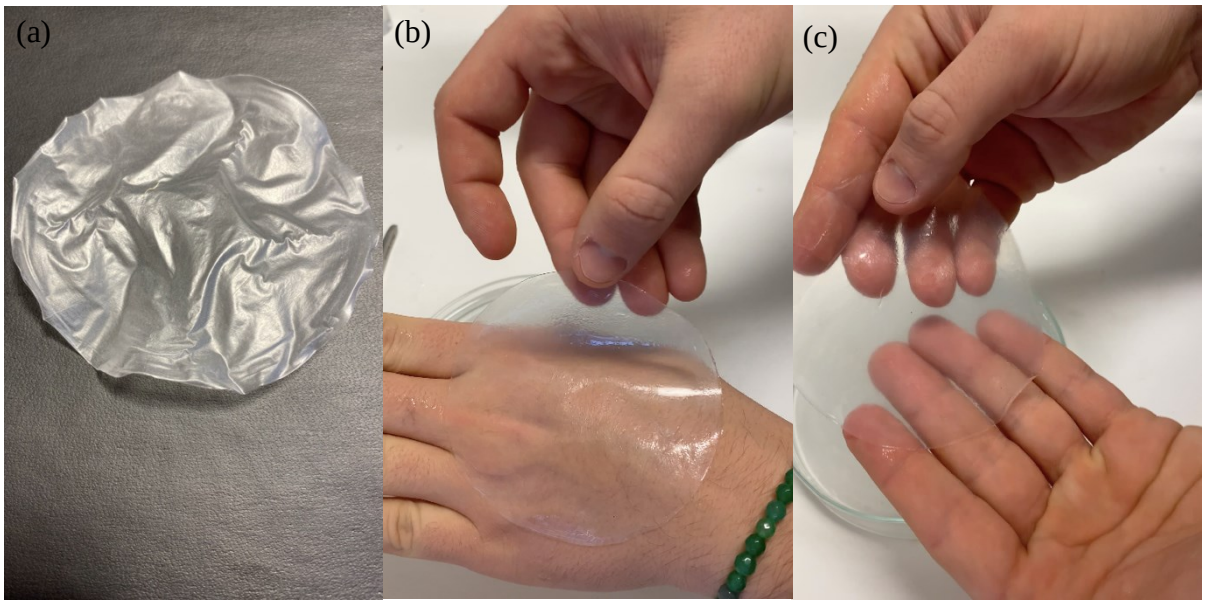

Figure 6.8 WOOD CNF VF hydrogel in dry state **(a)** and during swelling test (**b)(c).**

6.6 Conclusions

In this chapter, we compared the hydrogels produced by the solvent casting method and vacuum filtration with the bacterial cellulose hydrogel available on the market. To be comparable, hydrogels had to be produced with a grammage less than 10 $\left({}^{g}/_{m^2}\right)$ because the thickness of bacterial cellulose hydrogels can be controlled by process parameters. For the solvent casting method, there were no problems while it was slightly more difficult to produce hydrogels by VF. This is due to the filter used, which had to be removed with great care to not break the network.

Bacterial cellulose from wood and bacterial cellulose were initially compared. They were characterized by X-rays and by TGA. The XRD patterns provided data to analyze the crystallinity index and the size of the crystalline domains. Bacterial cellulose showed a higher index than the nanocellulose from wood. The sizes of both domains are small and comparable. TGA gave indications of the thermal properties of the two nanocelluloses: both degrade below 100 ° C due to dehydration. The biggest difference was seen when comparing DTG curves. The CNF showed two peaks, which indicated the presence of the nanocellulose but also of other polysaccharides such as hemicellulose and lignin. In contrast, bacterial cellulose showed only one peak. This means that it is composed exclusively of cellulose and there is no other polysaccharide. Both hydrogels showed a drastic decrease in weight in the temperature range between 200 ° C and 400 ° C. This interval corresponds to the depolymerization of cellulose.

At this point, the hydrogels produced with the methods indicated in Appendix A and Appendix B were compared with bacterial cellulose. The mechanical properties were assessed by uniaxial tensile test and the absorption properties were tested not only in water but also in a BSA solution.

Tensile tests highlighted the excellent mechanical properties of bacterial cellulose with a high Young's modulus and a high UTS value. As regards the hydrogels produced by VF, the results were good even if not at the level of the reference product. It should be noted that the elongation of hydrogels produced with cellulose from wood is higher, albeit slightly, than that of bacterial cellulose. It was not possible to test hydrogels produced by solvent evaporation due to the poor mechanical properties they possess when they do not have a high fiber content.

As previously mentioned, the absorption was tested in two liquids: water and BSA solution. This is because the absorption properties in water are important but do not give any complete indication of the behavior of these hydrogels when considering the application for which they are designed. The BSA solution was used to get closer to the real application: the wound environment. In both liquids, the hydrogels produced by solvent casting absorbed a large amount of water compared to *WOOD CNF VF* and *BC*. This was already known from previous chapters. However, a similar behavior was shown for bacterial cellulose and hydrogels made with cellulose from wood. In BSA solution, the trends were the same even if with lower absorption values. This is probably due to the affinity of the solution.

In conclusion, we achieved excellent results since the production of cellulose from wood is more convenient and reproducible than bacterial cellulose. The comparison confirmed the advantageous use of these hydrogels as dressing plasters. They are excellent candidate materials, but they need to be further characterized in terms of efficacy and safety before being approved for the market.

Chapter 7

Conclusions and future perspectives

Wound healing is a specific biological process related to tissue growth and regeneration; its compositional stages overlap but are clearly defined: hemostasis, inflammation, proliferation and maturation, in which various cells and endogenous factors are involved. To reduce the risk of wound infection and accelerate the healing process, the development of advanced wound dressings represents a promising approach. Among them, hydrogels are ideal dressing materials due to their excellent biocompatibility, high moisture retention and activation of immune cells.

The main goal of this thesis project was to replace bacterial cellulose hydrogels currently on the market with hydrogels composed of nanocellulose extracted from wood.

Cellulose is an abundant polymer in nature with excellent characteristics such as biodegradability, biocompatibility and renewability: for these reasons, this material has received great attention in recent years. Even if at first glance the two celluloses are the same, the physical and mechanical properties are not. The bacterial cellulose is obtained by a bottom-up process, while the wood-derived nanocellulose by a top-down process. This is the principal difference between the two kinds of cellulose. Bacterial cellulose is obtained by extrusion through the pores of bacterial cultures, while nanocellulose is obtained by extraction from vegetable fibers by means of chemical and mechanical treatments.

In this work, we started from the extraction and isolation of the nanocellulose from wood. Initially, we evaluated the physical and mechanical properties of the nanocellulose depending on the treatments performed on it. We have seen how a chemical whitening and alkali pre-treatment allowed obtaining the so-called "pulp". The pulp contains high amounts of polysaccharides such as hemicellulose and lignin. By a chemical treatment with TEMPO, combined with a mechanical treatment with high-pressure homogenization, the nanocellulose is derived from wood. This

nanocellulose still contains hemicellulose and lignin but in lesser extent. The fibrillation was initially evaluated by AFM analysis of the nanofibers and it was found that TEMPO and HPO treatments significantly increased nanofibers fibrillation by increasing their length and decreasing their size when compared to the pulp. This, it was possible to obtain hydrogels with significantly superior mechanical properties compared to hydrogels made with pulp. Furthermore, hemicellulose and lignin play a crucial role in the mechanical properties, which are negatively affected by these polysaccharides.

With regard to the absorption of liquids, these polysaccharides tend to increase the absorption capacity of these hydrogels. Chemical pre-treatment combined with TEMPO and mechanical treatments allowed obtaining nanocellulose with good mechanical properties and good adsorption properties. This nanocellulose was used to produce hydrogels through two alternative methods: solvent casting and vacuum filtration. These methods lead to the formation of hydrogel network through physical cross-linking. These hydrogels appear to be formed by multiple layers, which are superimposed on each other and joined by intermolecular bonds. The extent of the cross-linking is responsible for the mechanical and absorption properties of the hydrogels. The use of vacuum results in hydrogels that are characterized by excellent mechanical properties and good absorption capacity. Conversely, solvent evaporation produces a network with unsatisfactory mechanical properties and high-water absorption values. As to the elongation at break, it presents similar results for both hydrogels. This property is mainly due to the cellulose nanofibers and not to the cross-linking degree. The hydrogels produced by solvent casting have a high-water absorption capacity: having weaker cross-links, the porosity between the layers is higher allowing an easier water absorption. From a practical point of view, the vacuum filtration method is faster than the other. On average, 5-6 hours are needed to obtain a hydrogel in the dry state, while the solvent casting method takes about one week. To compete with a commercial bacterial cellulose product, in addition to excellent mechanical and liquid absorption properties, the hydrogel must also be reproducible and cheap. For these reasons, the vacuum filtration method is the optimal one also considering large-scale productivity. Therefore, the characteristics of the hydrogels produced with this method were assessed. From the mechanical point of view, there is no relation between the number of fibers and these properties. The elongation at break is the only property that seems to be dependent on the hydrogels grammage: increasing the number of fibers, increases the elongation at break. Despite the non-linearity, the mechanical property values are satisfactory because they

allow these hydrogels to be used as plasters for wound dressings without losing their structural integrity. Furthermore, the hydrogels obtained by filtration can recover their mechanical properties and characteristics by immersion in water for a short time. Therefore, if applied to a wound, they can keep it isolated from the external environment; by absorbing exudate, they are also able to maintain their physical and mechanical characteristics thanks to their recovery capacity. The hydrogels produced by vacuum filtration show a decrease in water absorption when subjected to absorption and desorption cycles at any grammages. The absorption, as well as the mechanical properties, is not related to the number of nanofibers present in the hydrogels. By SEM analysis of the hydrogels cross-section, it was shown that an increase in thickness appears as the immersion time increases. This confirms that water absorption occurs in a direction parallel to the surface and not in the orthogonal direction. These hydrogels can show a difference in absorption and a change in thickness when immersed in solutions of different pH. This result allows monitoring wound healing progression by inserting biosensors within the hydrogel. This prevents unnecessary and frequent removal of dressings. All these characteristics possessed by the hydrogels produced with wood derived nanocellulose constitute an excellent basis for their use as plasters for wound dressing. To evaluate their effectiveness, they were compared with a commercial bacterial cellulose product. A long time is required for the production of bacterial cellulose hydrogels and their properties depend on the parameters used in culturing bacteria. The characteristics of wood derived cellulose also depend on the treatments, but these are more easily controlled than those of bacterial cellulose. Furthermore, the production time of nanocellulose hydrogels by vacuum filtration are considerably shorter than those of bacterial cellulose. The mechanical properties of the bacterial cellulose, however, are superior: anyway, the overall features of the hydrogels produced in this work are good enough to be used as advanced dressings. This is also due to the high crystallinity of bacterial cellulose compared to the wood derived nanocellulose as evidenced by the XRD analysis. In terms of water absorption, it was shown that the hydrogels produced with wood derived cellulose and the commercial product based on bacterial cellulose have very similar behavior. This result is of great importance even if in any wound there is the production of other fluids, in addition to blood. To evaluate the behavior of these hydrogels in an environment more similar to a real wound, an absorption test was carried out in BSA solution. Also, in this case, the hydrogels produced and the reference product showed a similar behavior. This leads to the conclusion that the future commercialization of these hydrogels is possible as they possess characteristics similar

to those of the commercially available products with the advantage of a production and an effective reproducibility. Furthermore, from an economic point of view, wood is a resource of great abundance and easy accessibility, which contributes to make the nanocellulose also economical.

We predict that future research on hydrogels will move toward lower costs and more specificity. The effect on chronic wounds remains the focus of future research. To this purpose, bioactive hydrogel materials have to be discovered and exploited. In parallel, efforts have to be made to produce hydrogels for wound dressings by extracting nanocellulose from cocoa and ginger. Moreover, one of the main challenges of the future research will focus on the structural modification of natural polymers. In this work, a physical crosslinking was used but it is also possible to obtain a chemical crosslinking. Probably, increasing the extent of the crosslinking, mechanical properties will also increase.

The next step of the project, which involves different professional figures such as medical doctors, biomedical and material engineers, will aim at incorporating hydrophilic carbon quantum dots derived from wood hydrolysis to functionalize the hydrogel. Again, the rationale is that the hydrogels, which are characterized by high water absorption, can be enriched with antibiotics or other molecules capable of accelerating the healing process.

Appendix A

Hydrogel by vacuum filtration

This appendix briefly illustrates the procedure adopted for the preparation of hydrogels by vacuum filtration. After carrying out the pre-treatments for PULP CNF and fibrillation for WOOD CNF, the massive concentration of the nanofibers was evaluated. To this purpose, a portion of the material was dried in an oven at 30°C for 24 hours in order to evaporate water and evaluate ~~the~~ concentration. A statistically representative number of samples were tested in order to calculate the mean value and standard deviation. After obtaining the weight concentration of the nanofibers, a sample was prepared with a nominal concentration of 0.17%. The dilution was performed using the **Equation A.1** where C_i is the initial concentration, V_i is the initial volume, C_f is the final concentration and V_f the final volume.

$$C_i \cdot V_i = C_f \cdot V_f \tag{A.1}$$

In this work, circular samples with a diameter of 0.09 m and an area of $6.358 \times 10^{-2} m^2$ were prepared. After deciding the grammage ($^{g}/_{m^2}$) of the hydrogel to be prepared, it is necessary to calculate the amount of solution (**Equation A.2**, where *TG* it is the theoretical grammage):

$$ml\ of\ solution = \frac{TG\ {}^{g}/_{m^2}\ \cdot\ 6.358 \times 10^{-2} m^2}{0.0017\ {}^{g}/_{ml}} \tag{A.2}$$

After taking the desired amount of solution, it was diluted in a Teflon beaker until reaching a final volume of *300 ml*. Therefore, the solution was stirred using a magnetic stirrer for 2 hours in order to mix the solution and make it as homogeneous as possible. The stirring speed is moderate but not excessive to avoid the incorporation of air bubbles with consequent creation of porosity in the final hydrogel. Thus, after the stirring phase, the solution was placed for 24-48 hours in a degasser to eliminate air. At the beginning of degassing, it is likely to notice the formation of bubbles that slowly rise towards the surface. The procedure is considered completed when no more bubbles appeared. For hydrogels weighing more than 60 $^{g}/_{m^2}$ it can be necessary to alternate degassing

and sonication every 6 hours. Then, we moved on to the vacuum filtration phase. The experimental setup used is illustrated in **Figure A.1**.

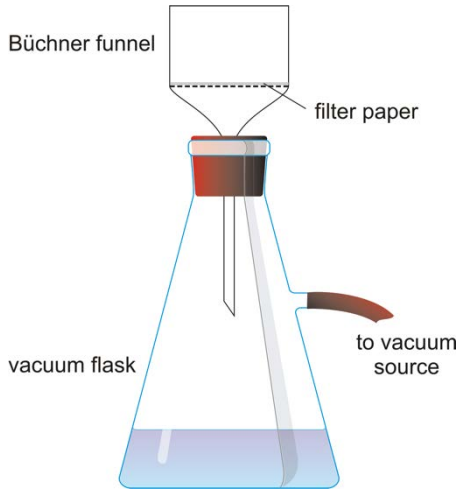

Figure A.1 Experimental setup for the vacuum-assisted preparation of hydrogel.

The filter was fixed by a circular disk of ultrafine metal mesh in order to avoid the formation of dots due to the escaping routes of liquid and air. For almost all the hydrogels a filter manufactured by *Whatman*™ with an identification code of 52 was used (with pores size of 7 micrometers). For hydrogels with a weight less than 20 $^{g}/_{m^2}$ a membrane (*Whatman*™, ME25 with a pores size of 0.45) was used as a filter in order to prevent the hydrogel from breaking during removal. For a hydrogel with a theoretical weight of 20 $^{g}/_{m^2}$ the complete filtration takes about 4 hours.

At the end of filtration, the paper filter and the hydrogel were placed in a container with distilled water for 24 hours in order to facilitate the removal of the filter. Tweezers were used to remove the filter taking care to gently remove any part from the hydrogel.

Appendix B

Hydrogel by solvent casting

This appendix briefly illustrates the procedure adopted for the preparation of hydrogels by solvent casting. After carrying out the various pre-treatments for PULP CNF and fibrillation for WOOD CNF, the massive concentration of the nanofibers was evaluated. To this purpose, a portion of the material was dried in an oven at 30°C for 24 hours in order to evaporate water and evaluate concentration. A statistically representative number of samples were tested in order to calculate the mean value and standard deviation. After obtaining the weight concentration of the nanofibers, a sample was prepared with a nominal concentration of 0.82%. The dilution was performed using the **Equation B.1** where C_i is the initial concentration, V_i is the initial volume, C_f is the final concentration and V_f the final volume.

$$C_i \cdot V_i = C_f \cdot V_f \tag{B.1}$$

In this work, circular samples with a diameter of 0.09 m and an area of $6.358 \times 10^{-2} m^2$ were prepared. After deciding the grammage $\left({}^{g}/_{m^2}\right)$ of the hydrogel to be prepared, it is necessary to calculate the amount of solution (**Equation B.2**, where *TG* it is the theoretical grammage):

$$ml\ of\ solution = \frac{TG\ {}^{g}/_{m^2}\ \cdot\ 6.358 \times 10^{-2} m^2}{0.0082\ {}^{g}/_{ml}} \tag{B.2}$$

In this case, a solution with a much higher concentration than that used in the method described in **Appendix A** was used. This is because the physical principle behind this method, that is the solvent evaporation, and the use of a *PTFE Petri dis*h with a diameter of 90 mm and a height of 15 mm, which limited the maximum volume available. By increasing the concentration of the starting solution, it is possible to obtain hydrogel with a high grammage. Furthermore, 0.82% wt. is the maximum allowable concentration that has been used. Above this value, there is a very viscous and gelatin-like aqueous solution, which does not allow the removal of bubbles by means of a vacuum pump and does not allow uniform distribution on the surface giving rise to a rather irregular surface.

Given the desired grammage and taken the solution necessary to obtain the intended hydrogel, the solution is transferred into a beaker and, if necessary, diluted with distilled water until the final volume of 95 ml is reached (maximum volume of the Petri dish considering an average density of $\left(1\,{}^{g}/_{cm^3}\right)$. Subsequently, using a magnetic stirrer, the solution is mixed at a speed that avoids the incorporation of air bubbles for 2 hours. The beaker is then placed for 12 hours under vacuum for removing bubbles. In this case, the hydrogels are of low grammage: this implies that the solution is not very viscous, and the removal of bubbles is facilitated: less than 24h are necessary. Afterwards, the solution is carefully poured into the *Petri dish* and placed on a flat surface. The evaporation of the water is thus awaited until a hydrogel in a dry state is obtained. The mean time for making a hydrogel depends on the grammage (the higher the grammage, the shorter the time) and varies from 6 to 8 days. The schematic process is illustrated in **Figure B.1**.

Figure B.1 Experimental setup for the preparation of hydrogel through solvent casting procedure.

Figure B.2 Solvent Casted hydrogel

Appendix C

Samples preparation for SEM analysis

Samples preparation of for SEM analysis is a critical issue. In the present work, several preliminary tests were carried out before obtaining satisfactory results that allowed the cross section of the samples to be analyzed by means of an electronic microscope. The most delicate part is cutting the samples to highlight the part of the section to be investigated. We tried to cut the samples using cutting tools such as scissors or cutters, but the results were not appropriate. First, the samples were cut using the dog bone cutter for the tensile test. The cutting was carried out with this tool using a manual press in order to guarantee the uniformity of the cut. Other tools have produced irregular cuts, compaction of layers or occlusion of porosities. **Figure C.1** illustrates the influence of the cutting tools on the cross section of the hydrogels samples.

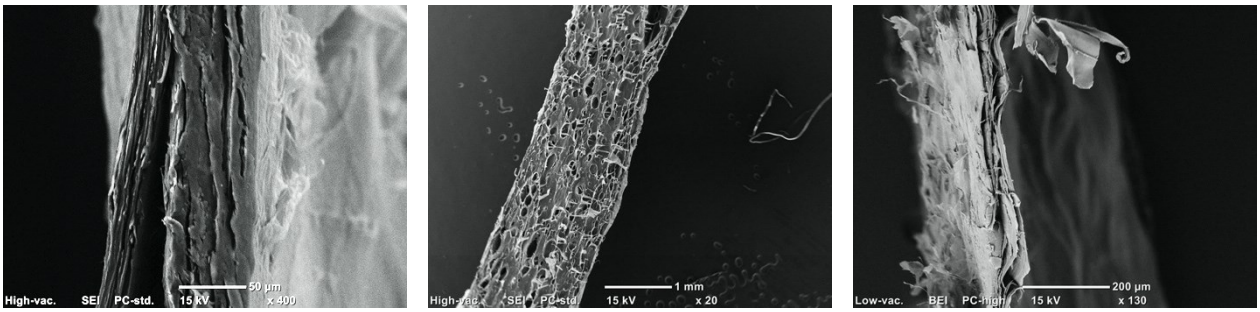

Figure C.1 Tool-related defects of the cross section: compaction of layers (left), occlusion of porosities (center) and irregularities of the section (right).

After cutting the sample in the wet state, the freeze-drying technique is used. This technique, also known as lyophilization or cryodrying, is a low temperature dehydration process that involves freezing the product, lowering the pressure and removing the ice by sublimation. With this method, high temperatures are not required to vaporize the water contained in the network, thus maintaining the original shape of the product. After cutting a portion of the sample, it is placed in the freezer at -20 °C in order to freeze the water present inside for 24 hours. Afterwards, the sample is placed in the apparatus that reaches the pressure of 1.0 mbar and keeps the temperature stable at -54°C for

48 hours. During this time the water is removed by sublimation, thus leaving the structure unaltered. A simple image of the sample after the treatment is shown in **Figure C.2**.

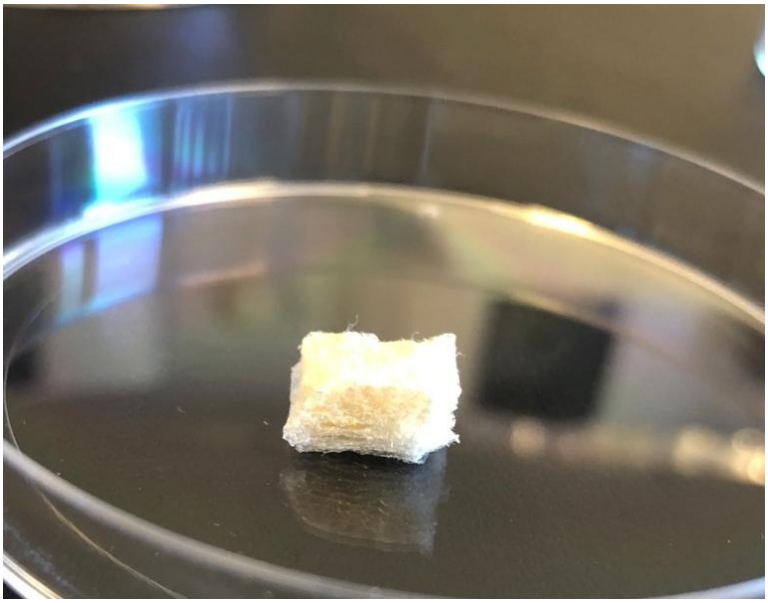

Figure C.2 CNF hydrogel with high grammage after freeze-drying treatment.

To get the sample for SEM analysis, it is necessary to cut it again to obtain a 5 mm high and 10 mm long specimen. The dog bone cutter is used with the help of the manual press. Finally, the samples are placed in the SEM holders and subjected to a gold sputtering process. During this last step, the cross section of the sample is covered with a golden layer of 15 nanometers. At this point, the sample is ready to be analyzed under an electrical microscope.

Appendix D

Zeta potential analysis

Zeta potential (ξ) of $(0.1\%\, wt.)$ aqueous CNF suspension was measured using a Zetasizer Nano S90 (Malvern Instrument) without adjusting the ionic strength. Three measurements were conducted for the suspension and mean values and standard deviations were reported in **Table D.1**.

	Temperature $(°C)$	*Zeta potential* (mV)	*Mobility* $(\mu m \cdot cm/Vs)$	*Conductivity* (mS/cm)
WOOD CNF	25	-59.8 (2.816)	-4.688 (0.224)	0.0285 (0.0007)

Table D.1 Zeta potential value of wood cellulose nanofibers.

The high value of ζ highlights how the nanofibers demonstrate excellent stability in the solvent in which they are dispersed. A high value of potential ζ gives greater stability to colloidal systems, as electrostatic repulsions are generated preventing the aggregation of dispersed particles

Appendix E

Optical microscope images

A Nikon Eclipse LV100 Pol (Kanagawa, Japan) polarized optical microscope with a 530 nm filter was used to characterize the surface of different hydrogels (supplementary information) in order to study nanofibers morphology. Polarized optical micrographs of the samples were recorded using a charge-coupled device camera. Figure E.1 shows the surface of the bacterial cellulose hydrogel.

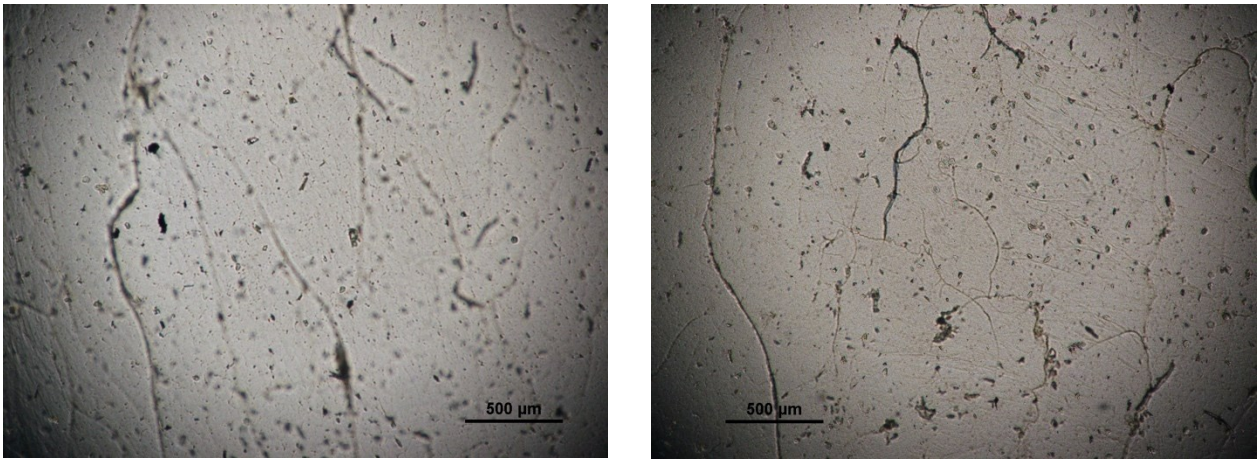

Figure E.1 Surface of BC in wet state.

The presence of nanofibers can be noted even if in small quantities. Furthermore, the nanofibers are very long. It is probably not possible to see only entanglements of nanofibers and no single nanofibers at this magnification.

The surface of the cellulose hydrogels coming from wood is different. As seen in **Figure E.2** and **E.3** tangles of nanofibers are visible. In these two images you can see the difference between the two production methods. In the vacuum filtration method, a high density of fiber entanglements is noted. This is due to the method that uses vacuum as a force to create cross-link bonds between the nanofibers. On the contrary, the solvent casting production method does not use any external force for the creation of bonds, and this results in a weaker network due to the absence of numerous

entanglements of fibers. The hydrogels used for this characterization have the same grammage. It is also noted that the length of the nanofibers between the two methods is the same.

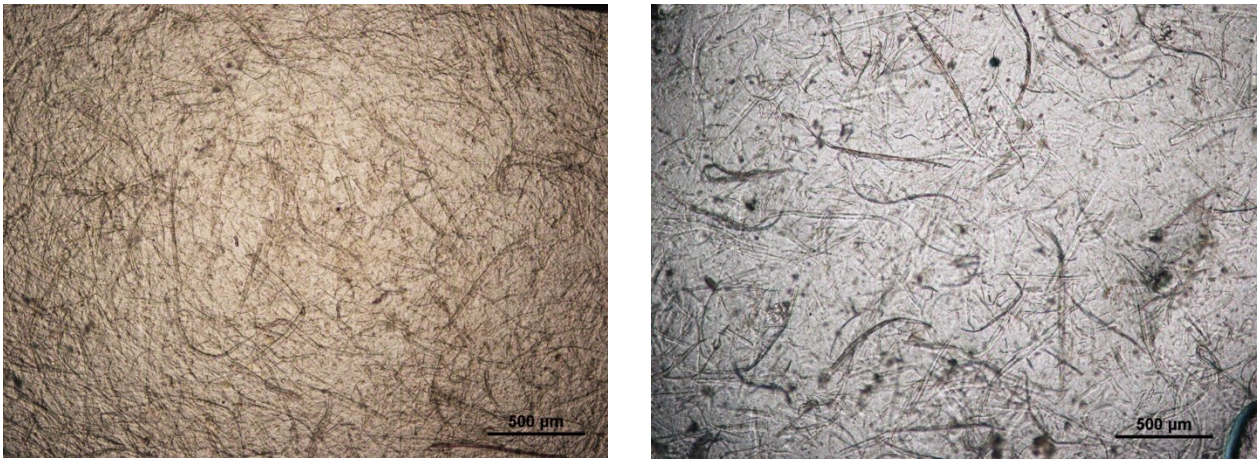

Figure E.2 Surface of WOOD CNF VF in wet state.

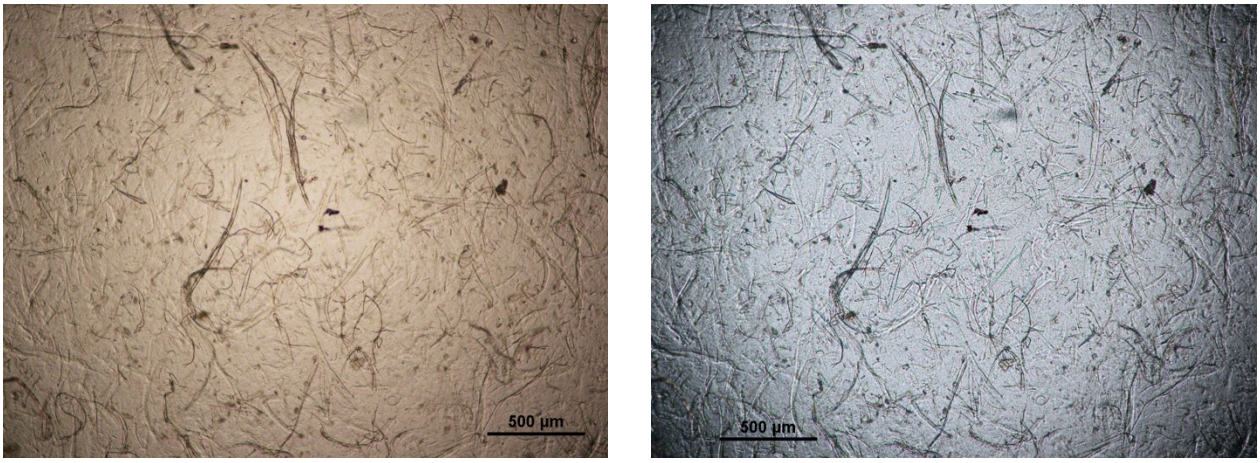

Figure E.3 Surface of WOOD CNF SC in wet state.

Finally, we also wanted to characterize the starting solution with which the hydrogels were made. More precisely, there are two solutions as the first (**Figure E.3 a)** was obtained from the High-Pressure Homogenization treatment while the second (**Figure E.3 b**) is the result of the dilution of the starting solution.

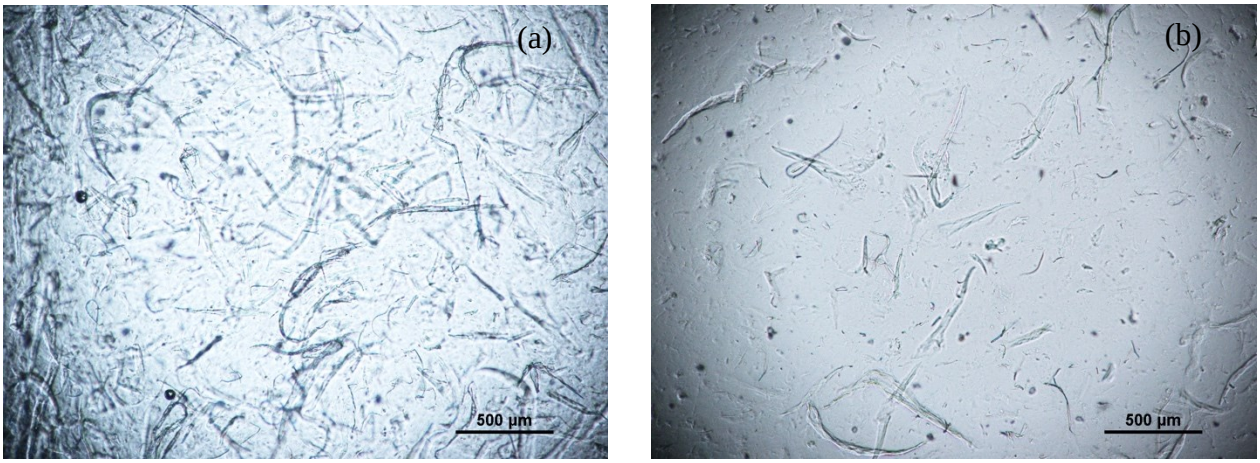

Figure E.3 WOOD CNF solution (a) 84% wt. (a) and at 17% wt.

In this case we see the difference in the concentration of nanofibers. The length of these nanofibers is the same as that seen in the hydrogels previously. This confirms that there is no structural modification of these nanofibers during the methods used to produce hydrogels. Since *WOOD CNF* hydrogel are constituted of long fibers, their size characterization with the granulometer was not possible. However, by means of microscopic observations, it was noticed that the fibers had a length greater than 500 μm.

Reference

Abdillahi H. et al. **2010**. High reinforcing capability cellulose nanocrystals extracted from Syngonanthus nitens (Capim Dourado). Cellulose, Volume 17, pp. 289-298.

Abrahama, E., Deepa, B.P., Pothen, L.A., Cintil, J., Thomas, S., John, M.J., Anandjiwala, R., and Narine, S.S. **2013**. Environmental friendly method for the extraction of coir fibre and isolation of nanofibre. Carbohydr. Polymers. Pages 1477-1483.

Alvarez V. A. et al. **2013**. Extraction of cellulose nanowhiskers from natural fibers and agricultural byproducts. Fibers and Polymers, 14(7), pp. 1118-1127.

Arcot J. et al. **2016**. Nanocellulose characteristics from the inner and outer layer of banana pseudo- stem prepared by TEMPO-mediated oxidation. Cellulose, Volume 23, pp 3023-3037.

Bano, S. & Negi, Y. S., **2017**.Studies on cellulose nanocrystals isolated from groundnut shells. Carbohydrate polymers 157, 1041–1049.

Belgacem M. N., Bras. J., Nechyporchuk O. **2016**. Production of cellulose nanofibrils: a review of recent advances. Industrial crops and products, Volume 93, Pages 2-25.

Belgacem N. et al. **2016**. Industrial and crop wastes: A new source for nanocellulose biorefinery. Industrial Crops and Products, Volume 93, p. 26–38.

Benini K. C. C. C. et al. **2015**. Vegetal Fibers in polymeric composites: a review. Polimeros, 22(1), Pages 9-22.

Bilek, E.M. (Ted); Cowie, John. **2014**. Market projections of cellulose nanomaterial-enabled products- Part 1: Applications. Tappi Journal, Volume 13, Number 5, 2014; pp. 9-16.

Björn Petri, M. Gabriele. **2006**. Bixel FEBS Journal, 273: 4399-4407.

Boateng JS, Matthews KH, Stevens HNE, Eccleston GM. **2008**. Wound healing dressings and drug delivery systems: a review. Journal of pharmaceutical sciences 97: 2892–923.

Boateng, Joshua & Matthews, Kerr & Stevens, Howard & Eccleston, Gillian. **2008**. Wound healing dressings and drug delivery systems: A review. Journal of Pharmaceutical Sciences. 97. Pages 2892 - 2923.

Brannon-Peppas L and Peppas N. **1991**. 'Equilibrium swelling behavior of pH-sensitive hydrogels', Chemical Engineering Science, 46, 715–22.

Bras J., Dufresne A., Siquiera G. **2010**. Cellulosic bionanocomposites: a review of preparation, properties and applications. Polymers, Volume 2, pp. 728-765.

Brigham C, B. Török, T. Dransfield (Eds.). **2018**. Biopolymers: Biodegradable alternatives to traditional plastics, Green chemistry, Pages 753-770.

Brown A. J., LXII. **1887**. Further notes on the chemical action of Bacterium aceti, Journal of the Chemical Society, Transactions, 51, 638.

Carrino L., D. M. **2011**. Realizzazione e caratterizzazione di laminati in composto polimerico termoplastico rinforzato con fibre naturali: ENEA, Agenzia Nazionale per le Nuove Tecnologie, l'Energia e lo Sviluppo Economico Sostenibile.

Czaja W., D. Romanovicz, R. m. Brown. **2004**. Structural investigations of microbial cellulose produced in stationary and agitated culture, Cellulose, 11, 403.

EC EUROPA. **2019**. Definition of a nanomaterial in European commission. https://ec.europa.eu/chemicals/nanotech/faq/definition_en.htm (Accessed November 2020).

Filson, P.B.; Dawson-Andoh, B.E.; Schwelgler-Berry. **2009**. Enzymatic-Mediated production of cellulose nanocrystals from recycled pulp, Green Chemistry, Volume 11, Pages 1808-1814.

Gurunathan T., Mohanty S., Nayak S. K. **2015**. A review of the recent developments in biocomposites based on natural fibers and their application perspectives. Composites part A: Applied Science and Manufacturing, Volume 77, pp. 1-25.

Hamid S. B. A., Lee H. V., Zain S. K. **2014**. Conversion of lignocellulosic biomass to nanocellulose: structure and chemical process. The Scientific World Journal, p. 20.

Hamid S. B. A., Lee H. V., Zain S. K. **2014**. Conversion ol lignocellulosic biomass to nanocellulose: structure and chemical process. The Scientific World Journal, p. 20.

Iguchi, M.; Yamanaka, S. & Budhiono, A. **2000**. Bacterial cellulose: a masterpiece of nature's arts. Journal of materials science 35, Pages 261-270.

Jorfi M., E. Johan Foster. **2015**. Recent advances in nanocellulose for biomedical applications, Journal of applied polymer science, Volume 132.

Junka, K., Filpponen, E., Lindstrom, T., & Laine, J. **2013**. Titrimetric methods for the determination of surface and total charge of functionalized nanofibrillated/microfibrillated cellulose (NFC/MFC). Cellulose, 20(6), Pages 2887-2895.

Kaith B. S., Kalia S., Kaur. I. **2011**. Cellulose fibers: bio- and nano-polymer composites. Green Chemistry and Technology. Springer.

Karaaslan, Muzaffer & Tshabalala, Mandla & Gisela, Buschle-Diller. **2010**. Wood hemicellulose/chitosan-based semi: Interpenetrating network hydrogels: Mechanical, swelling and controlled drug release properties. Bioresources, 5.

Klemm D., B. Heublein, H. P. Fink, A. Bohn. **2005**. Cellulose: fascinating biopolymer and sustainable raw material, Angewandte Chemie International Edition, 44, 3358.

Klemm D., Kramer F., Moritz S., Lindström T., Ankerfors M., Gray D., Dorris A. **2011**. Nanocelluloses: A New Family of Nature-Based Materials. Green nanomaterials.

Lahtinen, Panu & Liukkonen, Sari & Pere, Jaakko & Sneck, Asko & Kangas, Heli. **2014**. A Comparative Study of Fibrillated Fibers from Different Mechanical and Chemical Pulps. BioResources.

Lee S and Park K. **1996**. 'Synthesis and characterization of sol-gel phase-reversible hydrogels sensitive to glucose', Journal of Molecular Recognition, 9, 549–57.

Li, Shiguang & Xu, Shaoping & Liu, Shuqin & Yang, Chen & Lu, Qinghua. **2004**. Fast Pyrolysis of Biomass in Free-Fall Reactor for Hydrogen-Rich Gas. Fuel Processing Technology – fuel process technology. 85. 1201-1211.

Lin N, Dufresne A. **2014**. Nanocellulose in biomedicine: Current status and future prospect. European Polymer Journal 59: 302–325.

Martini A. **2011**. Cellulose nanomaterials review: structure, properties and nanocomposites. Chem. Soc. Rev., Volume 40, pp. 3941-3994.

Miao, Q., Chen, L., Huang, L., Tian, C., Zheng, L., and Ni, Y. **2014**. A process for enhancing the accessibility and reactivity of hardwood kraft-based dissolving pulp for viscose rayon production by cellulose treatment. Bioresour. Technol., Volume 154, Pages 109–113.

Mohite, Bhavana & Koli, Sunil & Patil, Satish. **2018**. Bacterial Cellulose-Based Hydrogels: Synthesis, Properties, and Applications.

Mondal S. **2017**. Preparation, properties and applications of nanocellulosic materials. Carbohydrate Polymers, Volume 163, pp. 301-316.

Mostafalu, P., Tamayol, A., Rahimi, R., Ochoa, M., Khalilpour, A., Kiaee, G., Khademhosseini, A. **2018**. Smart Bandage for Monitoring and Treatment of Chronic Wounds.

Mtibe, A., Linda, Z., Linganisoa, L.Z., Mathew, A.P., Oksman, K., John, M.J., and Anandjiwala, R.D. **2015**. A comparative study on properties of micro and nanopapers produced from cellulose and cellulose nanofibers. Carbohydr. Polym., 118, Pages 1–8.

Nečas D., Klapetek P. **2012**. Gwyddion: an open-source soft- ware for SPM data analysis. Cent Eur J Phys 10:181–188.

Nicolai E., Reginald Dawson Preston. **1997**. Cell-wall studies in the Chlorophyceae. I. A general survey of submicroscopic structure in filamentous species. Proc. R. Soc. Lond. B 140, Pages 244–274.

Ning Lin, Alain Dufresne. **2014**. Nanocellulose in biomedicine: Current status and future prospect, European Polymer Journal, Volume 59, Pages 302-325.

Pasche, Stéphanie & Angeloni, Silvia & Ischer, Réal & Liley, Martha & Luprano, Jean & Voirin, Guy. **2008**. Wearable Biosensors for Monitoring Wound Healing. Advances in Science and Technology.

Peppas N, Bures P, Leobandung W and Ichikawa H. **2000**. 'Hydrogels in pharmaceutical formulations', European Journal of Pharmaceutics and Biopharmaceutics, 50, 8 27–46.

Pogorelova, N., Rogachev, E., Digel, I., Chernigova, S., & Nardin, D. **2020**. Bacterial Cellulose Nanocomposites: Morphology and Mechanical Properties. Materials (Basel, Switzerland).

SAFENANO. **2020**.Nanotechnologies Standard terms and their definition for cellulose nanomaterial in Safenano. https://www.safenano.org/knowledgebase/resources/faqs/what-is-a-nanomaterial/ (Accessed November 2020).

Segal L, Creely JJ, Martin AE, Conrad CM. **1959**.An Empirical Method for Estimating the Degree of Crystallinity of Native Cellulose Using the X-Ray Diffractometer. Textile Research Journal.

Sunil J. C. C., N. George, and S. K. Narayanankutty. **2016**. Isolation and characterization of cellulose nanofibrils from arecanut husk fiber, Carbohydr. Polymers, Volume 142, pp. 158–166.

Terenzi C., Kasinee Prakobna, Lars A. Berglund. **2015**. Nanostructural Effects on Polymer and Water Dynamics in Cellulose Biocomposites. Biomacromolecules. Pages 1506-1515.

Thangaraju, Rajasekaran & Kannan, Gokul. **2016**. Evaluation of mechanical characteristics of treated and untreated sugarcane fiber composites. Journal of Chemical and Pharmaceutical Sciences. Volume 9. Pages 652-656.

Velnar T., T. Bailey, V. Smrkolj. **2009**. The Journal of International Medical Research, 37: 1528 – 1542.

Yuxin Liu, Bing Sun, Xuefan Zheng, Lingfang Yu, Jianguo Li. **2018**. Integrated microwave and alkaline treatment for the separation between hemicelluloses and cellulose from cellulosic fibers, Bioresource Technology, Volume 247, Pages 859-863.